

DETERMINATION OF SULPHUR CONTENT OF UN-ALLOYED AND LOW-ALLOYED STEEL BY ICP-AES SPECTROMETRY USING WET CHEMICAL SAMPLE PREPARATION

OLIVÉR BÁNHIDI

University of Miskolc, Institute of Chemistry
3515 Miskolc Egyetemváros, Hungary
akmbo@uni-miskolc.hu

Sulphur has a great influence on the properties of steel. Therefore its determination has always been very important. Normally it is measured using optical emission spectrometry with spark excitation or non-dispersive infrared absorption, thermal conductivity detection, or iodometric titration after combustion in oxygen. It might cause problems when none of these methods is at one's disposal, as most other methods require wet chemical sample preparation. In this paper a wet chemical sample preparation method is presented, which seems to be able to meet the requirements of a reliable method when ICP-AES spectrometry is used for the determination of sulphur.

Keywords: determination of sulphur in steel, ICP-AES spectrometry, wet chemical sample preparation.

Introduction

Sulphur has always been a very important constituent of steel, as it has a great influence on the properties. That is why its determination has always been very important both in the course of manufacturing and in the quality control of steel and steel products. At first its determination based upon the combustion of the material to be tested in oxygen. The gases formed during the test were absorbed in an aqueous solution and the sulphur was determined by a volumetric method [1]. The advent of the so-called direct reading optical emission spectrometers offered a new possibility, a rapid method using solid samples [2]. Nevertheless the new method has some drawbacks regarding its accuracy therefore the old combustion method was developed, and instead of the volumetric method, the use of non-dispersive infrared absorption spectrometry became generally accepted [3]. These techniques require solid samples and are able to provide results in a short time. Their disadvantage is that a special analytical instrument or a rather expensive spark optical emission spectrometer is necessary for the determination.

Principally other optical emission methods using wet chemical sample preparation, such as ICP-AES spectrometry may also be suitable for sulphur analysis [4], but the sample preparation could cause problems. It is because most wet chemical sample preparation procedures of steel involve dissolution in hydrochloric acid. Sulphur, which can be found in steel mainly in form of sulphides, forms hydrogen-sulphide and will leave the solution, i.e. analyte-losses must be encountered in these conditions. These losses can only be avoided if it is ensured that the sulphur content of the steel is not only dissolved but it is oxidized during dissolution.

Using nitric acid, sulphuric acid or phosphoric acid is not very common in the analysis of steel, because their use may lead to the passivity of the metal to be dissolved, which

would prevent the dissolution. Lack of a suitable acid is the main problem of developing of suitable methods.

Studying the effect of nitric acid it turned out that dilute nitric acid is able to dissolve most un-alloyed and low-alloyed steels, and it can be used in a wet chemical sample preparation method, provided sufficient care is taken to prevent passivity of the sample.

1. Experimental

1.1. Chemicals and materials used in the experiments

High purity acids and chemicals of analytical grade were used in the course of the experiments. For calibration certified reference materials prepared exactly in the same way as the samples were applied. In the course of their selection not only their sulphur content was taken into account but their general chemical composition too, so that it could cover the concentration range typical for most low-alloyed steel qualities. Their composition is presented in Table 1.

Identifier	C	S	Si	P	Mn	Cr	Ni	Cu	Mo	Al	V
ASMW Nr 177	0.036	0.003	0.223	0.0141	0.18	0.116	0.167	0.058	0.068	0.135	0.061
ASMW Nr 59/2	0.40	0.033	1.61	0.039	0.65			0.14			
ASMW Nr 162	0.37	0.020	1.40	0.031	1.27						
ASMW Nr 174	0.43	0.024	0.39	0.032	1.78	0.143					0.075
ASMW Nr 103	0.176	0.0095	0.50	0.013	0.46	1.29	0.11		1.08		0.300
ASMW Nr 159	0.127	0.042	0.30	0.086	0.521	0.76	0.13	0.36			0.047
ASMW Nr 98/1	0.16	0.016	0.32	0.011	0.40	1.36	3.53				

Table 1. Chemical composition of the standards used for calibration

All the concentration values presented in Table 1 are given in m/m %.

1.2. The wet chemical sample preparation procedure

As not only the sulphur content but also phosphorous and silicon were also to be determined the sample preparation procedure contains steps and chemicals necessary only for the latter two elements.

0.4 g sample was into a glass beaker, which was covered with a watch-glass and 10 cm³ dilute nitric acid (dilution 1:3) was added to the sample. The dissolution was carried out by gently heating. Overheating should be avoided by all means as it may lead to sulphur loss. Depending on the chemical composition of the sample the complete dissolution may take even 2 or 3 hours. Following that the sample was oxidised with 2 cm³ 20 g/dm³ KMnO₄. The excess of the oxidizing agent was decomposed by the addition of 2 cm³ 20 g/dm³

NaNO_2 . As a result of the oxidization sulphur will be in the form of sulphate, while phosphorous will be in the form of phosphate. When the solution cooled down to room-temperature it was taken to a plastic baker and 0.5 cm^3 concentrated HF was added. This transformed silicon to SiF_4 . The excess HF attacks the sample introduction equipment, which is made of glass and silica. Therefore 5 cm^3 4 m/m % boric acid was added to the sample solutions. Finally the solutions were made up to a volume of 100 cm^3 . Beside sulphur the procedure makes possible to determine both phosphorous and silicon content of the steel samples. In the present form, the concentration range in that the method is suitable for the determination of sulphur is 0.005%–0.070%. If higher sulphur content is to be measured, the sample mass can be reduced so that the concentration range could be extended upward. When e.g. the sample mass is around 0.1 g, the uncertainty caused by weighing is about 0.1%, which is negligible, and as high as 0.28% sulphur content can be determined in this way.

1.3. Measurement conditions

1.3.1. Line selection

Almost all lines of sulphur can be found in the vacuum-ultraviolet range, except for a couple lines lying in the visible range. Because of the low concentration to be measured, only the most sensitive lines can be applied. Eventually three lines can be taken into account: 182.562 nm S I. atom line, 181.971 nm S I. atom line and 180.669 nm S I. atom line. The spectral background of the lines can be seen in Figure 1. The data presented in this figure were obtained by measuring a steel sample with sulphur content of 0.042%, prepared using the procedure written in section of 1.2.

Looking at the figure it can be seen that there is a serious spectral interference on the 182.562 nm line, therefore it is not suitable for measuring sulphur in steels and it was excluded from the further experiments. The two other lines both seems to be fit for the determination, therefore both of them were used in the course of the measurements.

1.3.2. The spectrometer and the measurement conditions

In the course of the measurements 720 OE ICP spectrometer, manufactured by the Varian Inc. (at present belongs to Agilent) was used. Its main features can be found in Table 2.

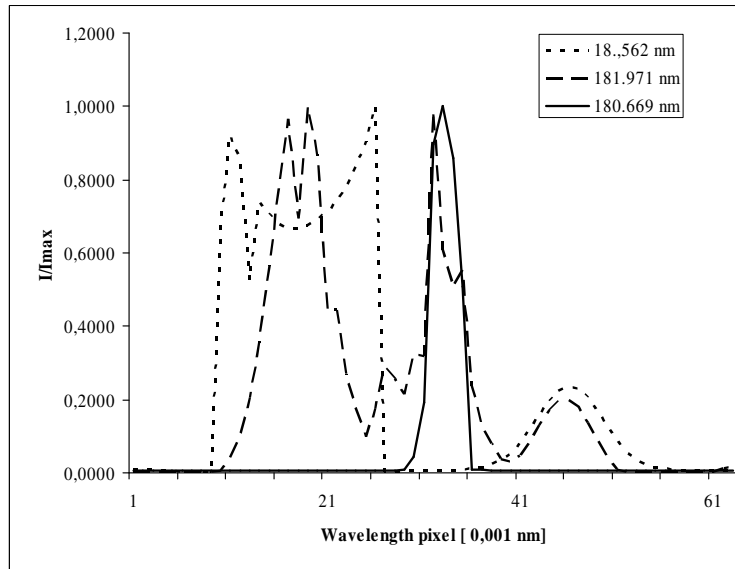


Figure 1. The spectral environment of the selected sulphur lines

Type of viewing the plasma:	Axial
The frequency of the generator:	40 MHz
The RF performance applied on the torch:	900 – 1500 W, adjustable by the software
Type of the optical system:	Double monochromator with Echelle gratings
Type of detector:	Two-dimension CCD
Wavelength range:	160 – 780 nm
Primary sample introduction system:	Pneumatic (K-type) nebulizer
Secondary sample introduction system:	Ultrasonic nebulizer
Controlling software:	ICP Expert II (under Microsoft Windows XP OS)

Table 2. Features of the ICP spectrometer used in the course of experiments

The radio-frequency power applied to the torch was 1050 W. Pneumatic sample introduction was used. The measured intensities were averaged from 3 subsequent readings each of them has an integration time of 8 s.

2. Results

2.1. Determination of the detection limits (DL)

In the course of the determination of the detection limit values, the measurement conditions were the same as those written above, except for the number of the subsequent

readings, which was 10 in that case. A blank solution prepared in the same way as the samples were, was used to determine the background standard deviation. Nr 159 ASMW reference material was used as a sample with known sulphur content (0.042%). The results are presented in Table 3.

Line [nm]	SD _{IBL} (net)	C _{Std} [m/m %]	C _{Std} [mg/dm ³]	I _{Std} (net)	DL [mg/dm ³]	DL [m/m %]
181.971	4.9	0.042	1.68	1360	0.018	0.0005
180.669	1.9	0.042	1.68	807	0.011	0.0003

Table 3. The detailed data of DL of sulphur determination

The detection limit values were calculated by the following formula:

$$DL = \frac{3 * SD_{IBL} * C_{Std}}{I_{Std}}$$

where: DL the detection limit [mg/dm³]
 SD_{IBL} standard deviation of the intensity of the blank solution [a.u.]
 I_{Std} background corrected net intensity of the standard [a.u.]
 C_{Std} the concentration of the analyte in the standard solution [mg/dm³].

Based upon the results, it can be stated that as low as 0.005 % S content can be measured with sufficient accuracy. (This value is one order of magnitude higher than the detection limit.)

2.2. Calibration

The calibration was carried out by applying the same conditions as for the measurement of the samples. The transfer function was established by using the linear regression procedure. The calibration curves obtained are presented in Figure 2 and 3. As it can be seen, linear calibration curves could be obtained on both lines.

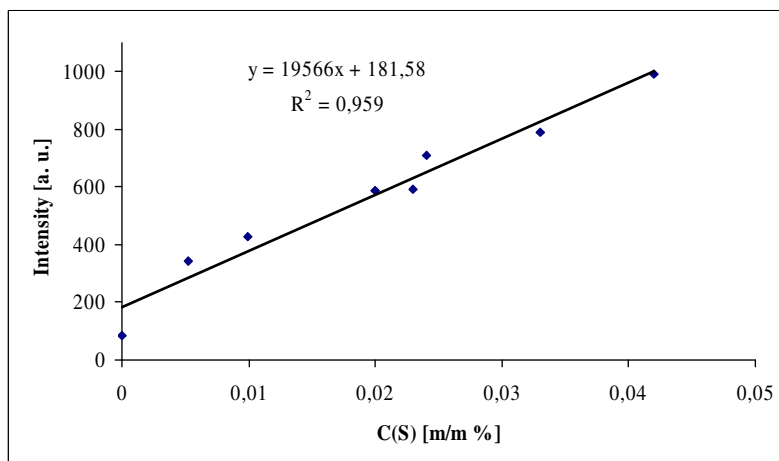


Figure 2. Calibration curve on the 180.669 nm S I. line

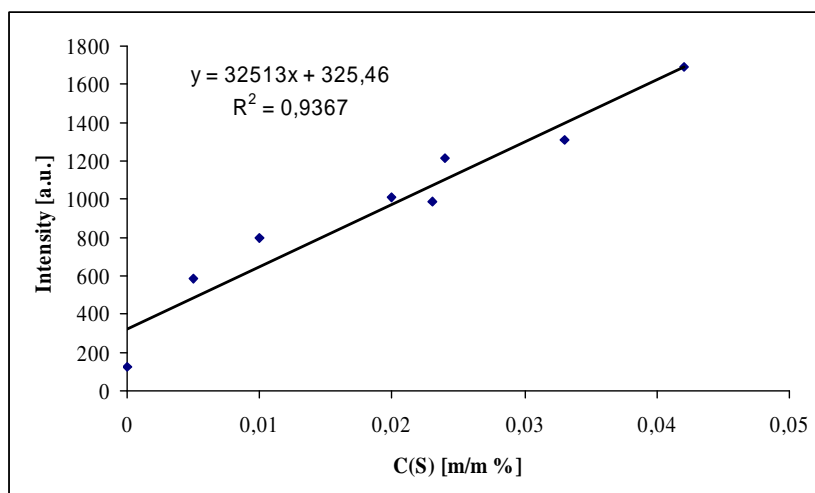


Figure 3. Calibration curve on the 181.971 nm S I. line

Neither of the curves produces 0 intensity value in the blank solution. The reason for this background intensity is partly the scattered light in the vacuum ultraviolet range and partly the sulphur content of the chemicals used in the course of sample preparation. The uncertainty of the calibration is calculated from the differences among the certified values of the standards and those of calculated using the equation of the calibration curves. It is 0.00242 m/m % for the curve recorded on the 180.669 nm line and 0.00248 m/m % for the 181.971 nm line respectively. Comparing the two sulphur lines, only little differences can be observed. Although, based upon this fact either of the 2 lines could be used for analysis,

we chose the 180.669 nm line for further experiments because of the slightly better detection power.

2.3. Obtaining the repeatability of the determination

To get a real repeatability for the method 5 samples – including certified reference materials – were chosen so that wide concentration range could be tested. Five parallel samples from each selected standard and in-house standard were prepared using the method presented in this paper. Following the calibration the samples were measured, and the repeatability values were calculated. The results are presented in Table 4. All the data in the table are in m/m % units.

Identifier	Nominal conc.	Measured average	SD	RSD
A 12 (Ferroetalon)	0.065	0.0661	0.0046	6.97
A 16 (Ferroetalon)	0.023	0.0260	0.0013	5.00
A 17 (Ferroetalon)	0.029	0.0306	0.0008	2.69
C 12X (MBH An.)	0.024	0.0237	0.0008	3.32
C 14X (MBH An)	0.647	0.671	0.0576	8.59

Table 4. Data for the repeatability

Looking at Table 4 it can be seen that the method is suitable to measure the sulphur content of the steel in a wide concentration range. The repeatability values also include the uncertainties of the sample preparation procedure and inhomogenities of the samples. The later has significant effect especially at higher concentration level, where great part of the sulphur content can be found in different inclusions.

3. Discussion of the results

Steel can be regarded as a difficult matrix from the viewpoint of the chemical analysis. It is because this material often contains elements with different chemical properties and chemical behaviour. As for as the atom-spectroscopy iron, the main constituent of steel is very rich in spectral lines, therefore the possible spectral interferences always have to be encountered in the course of method development. If wet chemical sample preparation has to be applied, further difficulties may emerge. In case of sulphur, the main difficulty is that the usual method, i.e. dissolution of the sample in hydrochloric acid cannot be used, as hydrogen-sulphide can form, which may lead to analyte losses. Using nitric acid as a dissolving agent, care must be taken to avoid metal passivity. That is why dilute nitric acid is used in our method. From the chemical composition data is obvious that this procedure is suitable for most unalloyed and low-alloyed steels. For highly-alloyed steels, e.g. stainless steels it is not suitable, as the occurrence of the passive state cannot be avoided because of the high chromium content.

Although there is about a substantial dilution because of the dissolution, the detection power is suitable for the determination, even in case of low (0.005%) sulphur concentration. The calibration resulted in linear curves on both lines, and the uncertainty

values (0.00242% and 0.00248% respectively) are sufficiently low, therefore they can be used down to the concentration of 0.005%.

The repeatability values were determined by preparing and measuring 5 standard samples, and the data obtained prove that the method is suitable to determine the sulphur-content in a wide concentration range. Looking at Table 4, it can be seen that it can be used even in case of resulphurised steel. Comparing the values to those obtained by using combustion methods with non-dispersive IR detection, it can be stated that the values produced by applying our method have the same accuracy or quality.

Finally a question could be raised, when this method is worth using by the analyst. Regarding the fact that much time is necessary for the wet chemical preparation, this method cannot compete with fast methods, when there is only little time at the analyst's disposal. On the other hand if the analysis time is not a key-importance demand, this method may be applied especially when the special equipment necessary for the combustion methods is not available.

Acknowledgement

The described work was carried out as part of the TÁMOP-4.2.1.B-10/2/KONV-2010-0001 project in the framework of the New Hungarian Development Plan. The realization of this project is supported by the European Union, co-financed by the European Social Fund.

References

- [1] Bagshave, B., Pill, A. L.: *Analyst*, **80**, 796–802, (1955)
- [2] Mika J., Török T.: *Emissziós színképelemzés*, Akadémiai Kiadó, Budapest, 1968.
- [3] ISO 4935:1989 standard: Steel and iron – Determination of sulfur content – Infrared absorption method after combustion in an induction furnace.
- [4] Zárny, Gy. (Editor): *Az elemanalitika korszerű módszerei*, Akadémiai Kiadó, Budapest, 2006.

ANTHROPOLOGICAL ANALYSIS ON THE SOCIOCULTURAL CONDITIONS OF A TECHNICAL INNOVATION MODEL: THE CSERNELY BIOMASS PROJECT CASE

GÁBOR BICZÓ

Miskolc University,
Institute of Cultural and Visual Anthropology
bolbiczo@uni-miskolc.hu

The paper analyses a large scale interdisciplinary research that is carried out at Miskolc University. In its applied anthropological approach the analyses takes into consideration the social scientific background of a basically technical innovation model. On the basis of research results so far the multicultural local society in Csernely (Borsod County, North Hungary) treats the project with ambivalence. It is clear if the aversion of the sub-communities towards the realization of the project continues to exist the development plan will suffer.

Keywords: applied anthropology, Roma minority, social conflict analysis, local community, biomass-based community energy system.

1. The conception of an interdisciplinary social-scientific research

A large scale interdisciplinary research is carried out within the TAMOP research project at the University of Miskolc that is rather unusual to national practices.

The basic idea is that Csernely, an isolated and economically disadvantaged peripheral community is subject to a complex set of tasks through an experiment of development with the introduction of the biomass-based heating system in the region. The preparation and analysis of conditions is more than just an analysis of technical, environmental economical and legal aspects. Contrary to Hungarian practices an unusual aspect is also taken into consideration: the Applied Anthropological and Sociological background of the project¹ [1].

It is unusual because while in the majority of developed societies a successful innovation is always considered to be a result of an overall analysis of conditions, in Eastern Central European practices a detailed research of social consequences is not part of the innovation. All over the World is a typical phenomenon, fields of knowledge, which contribute to the realization of the goals of the political and economic élites by “producing” social-science knowledge of practical value, are highly appreciated.

The project entitled “The Development of a Biomass-Based Community Energy System” is carried out at Csernely, South of Ózd, surrounded by hills and basins, covered by large forests. The history of the settlement goes back to the 13th century. In the late 20th century the majority of the inhabitants were agricultural or forestry workers or worked in the industrial plants of Ózd. Following the political changes of the 1990s, with the closing down of industry in the region, there was a dramatic increase in the number of unemployed

¹ The so called applied anthropology is an important subfield of modern sociocultural anthropology. Applied anthropology refers to the practical application of socio-scientific information. Foster, George M. (1968) 38-55.

workforce resulting in the migration of younger generations and the impoverishment of the population.

The population of Csernely is a little over 800 today constituting around 400 households. The majority of the inhabitants are old people living alone. This requires the sustenance of a pensioner care network, and also serves as a last tie of the emigrated to their place of origin.

Another important sociocultural element of the region is the increasing Roma minority population consisting of large families of different generations, contrary to the Hungarian majority. The Romas, however, do not constitute a homogeneous ethnical community, there is an opposition between those having lived there for generations and recently settled families. If we want to understand the sociocultural complexity of Csernely we should grasp it as a multicultural community. The cultural conception of multiculturalism² [2] is basically pluralistic³ [3]. According to this, in a community several cultural scales of values, religious and moral beliefs can be valid simultaneously, and their acceptance is necessary. Plural communities' basic experience is that the self-assertion of different groups is reconcilable with the local identity. Therefore in a plural community the support and maintenance of multiplicity is a clearly evident goal. The interdependence and equality of groups – which are different from each other but live together – is considered to be an essential part of local democracy. The main characteristic of multicultural communities is that power is owned not only by the majority, but is shared with the other groups as well.

The present survey aims at presenting the different attitudes towards plans for the development of the biomass-based heating center within different segments of the Csernely society. Since all technological innovation developments are realized within a given sociocultural environment a very important element of success the acceptance of the project by the local communities. Different segments of this community have different “acceptance” strategies towards the project, reasons of which need to be examined. The analysis will provide us with sociological information serving as a basis for a communication strategy helping us increase the acceptance of the project.

2. Elements of the Csernely Society

“The Development of a Biomass-Based Community Energy System” project initiated a questionnaire-based research within the households of the settlement. Besides basic questions concerning ways of disposing of litter, and means of heating in the household as well as whether the inhabitants had any information on biomass-based heating other aspects were brought to light. As it turns out the community consists of sub-communities existing next to, and partially overlapping each other. These sub-communities have an ambivalent, often opposing attitude towards each other. This ambivalence is characteristic of their attitude towards the biomass project as well; acceptance is very much in coherence with the sympathy or opposition of the sub-communities towards each other.

² The notion of multiculturalism is generally used to describe and characterize complex societies, which are either connected with contemporary global processes – that is, as the result of the migration which accompanies globalization they cause permanent relations between cultures and the individuals and groups representing them –, or they reflect a historically formed cultural situation of co-existence as a stable characteristic.

³ Pluralism is a concept that acknowledges the multiplicity of interests, ideologies, values and views.

A very interesting situation prompted us to examine this aspect; we asked for directions from a middle-aged man in the village once time. Since the lists of households were already divided among the questioners the man was informed during the conversation that he will also be given the questions at a later occasion. The middle aged man was very helpful and promised to support the research if it proves to serve the modernization of the community and provides possibilities for opening jobs in the region. To the surprise of the questioners the same man later refused to provide any information at all. Later research showed the opposition between the sub-communities to be the reason for this first helpful and later refusing attitude towards the question.

2.1. Elderly inhabitants

A major sub-community of the settlement consists of inactive old pensioners. On the basis of the questionnaires we can see that these people feel responsible for their environment but their existential vulnerability and their fear of impoverishment as a result of the loss of the value of money makes them unstable. They feel they have no say in the community's life anymore. They definitely believe the future of their community is predestined by the increasing number of Roma settlers. Their attitude towards the biomass project is largely influenced by their everyday experiences of physical threat. Most of these people support the project but the main obstacle of development in their view is the Roma population's lack of interest, passivity and criminalized life. This standpoint is created on the base of physical experiences and long-standing stereotypes. Theories on social relations between groups defy the notion of stereotypical functionality. This means that each stereotype bears practical significance in expressing its attitude "towards the other"⁴ [4]. In most cases stereotypes help maintain the ethnic and cultural dividing lines; furthermore, they justify the behaviour towards the given group. There are two types of stereotypes depending on the direction of social classification: auto- and hetero stereotypes.

Auto stereotypes are images referring to one's "own" group. Generally they are simplifications marking positive characteristics, and their goals are to strengthen the group's inner cohesion and mobilize common active power⁵ [5]. Hetero stereotypes are categories used to name and characterize "strange" groups and their members. Their content is more often negative; they serve to create a hierarchy between groups and to draw the symbolic line between them⁶ [6]. The system of mutual stereotypes in Csernely is functioning as a complex system.

⁴ The phrase stereotype first was used by Walter Lippmann in 1922. By this phrase he understands simplified, one-sided and schematic images ("prejudices"), which show each social group as a homogeneous, organic formation based on some typical characteristic features. Stereotypes are the sum of impressions and images, with the help of which experience referring to the social environment can be classified and ranked.

⁵ Auto stereotypes may have inner or outer sources. The Hungarians typical inner auto stereotypes referring to themselves are hospitality and resourcefulness (the number of Nobel prize winners). Good examples of auto stereotypes originating from outer sources are that Hungarians have a good temperament, are pessimistic, prone to complain and cunning.

⁶ Hetero stereotypes are used to identify and rank "other" socio-cultural communities. In the opinion of the Hungarians the German are hard working, disciplined, precise and "without personality".

2.2. Roma minority inhabitants

The second important sub-community is the Roma minority inhabitants consisting of two opposition groups. We have to make difference between the Roma families having lived in Cserney for generations and those having moved out of Ózd because of unemployment problems. The relationship of the Hungarians and the old Roma families was characterized by mutual recognition and respect in the past decades, but this changed with the appearance of the new settlers, the stigma of crimes attributed to them casting a shadow on the Hungarian-Roma relationship. Our research and the qualitative analyzes of data shows that both Roma communities and the Hungarians consider the main reason for the tensions to be unemployment.

30% of the total population is of active age and 40% of this is unemployed. In the case of the Roma population that constituted 10% of the total population of 802 in 2010, the unemployment rate is 80%.

2.3. Employees

A third group of the Cserney population consists of those employed at local institutions or small businesses (tailoring company, local store). These families of at least one member having a regular income are of a better financial situation and have a more varied attitude towards the project. They seem to be interested in a more economical family energy utilization practice but only consider the possible employment opportunities to be an option if it comes with a better income than their present jobs.

3. The Biomass Project a Possible Means of Sociopolitical Adaptation and its Communication

It is often said that technological innovation and the resulting employment projects have an advantageous influence on the whole of the society. The research also deals with the attitude of the Cserney inhabitants towards the question of potential employment possibilities as a result of the development project. Most of the answers were characteristic of the general attitude of the given group while reflecting the general evaluation of the whole community. The pensioners for example expressed their positive expectations towards the developments, their interest being, as a result of their age reasons, in the bettering of living conditions rather than in the possibility of new employment. At the same time the general view is that the infrastructure employed in the new technology would not last long because of thefts and damages made, these opinions expressing explicit generalizations of experiences with the Roma population.

The positive attitude of the local municipality towards the project is exemplary.

The potential sociopolitical advantages in coherence with the general development plan of the village are clear for everyone concerned: improving living conditions, employment opportunities and a fight against impoverishment.

At the same time we have to see that the opinion of the local municipality towards the project has a positive influence on the opinion of one group and a negative influence on the attitude of another. The older population for example has a positive view of the project as a result of the municipality's support. Some segments of the Roma population on the con-

trary, the lifestyle of which had been strongly criticized by the municipality, are prompted to reject the developments as something automatically connected to the work of the local authorities.

The biomass project is intended to be a complex development plan influencing not only economical-energetical and employment aspects of the local society but also their existing relationship with each other. Thus one future aspect of the project will be the analysis of its influences to the life of the Cserney population from emic viewpoint⁷ [7]. Also, on the other way around, a precondition for the project's successful realization is its acceptance by the local population and a positive attitude towards its preparation and development.

On the basis of results so far the Cserney society treats the project with ambivalence, as a result of a number of clearly outlined reasons:

- a) The majority population of the village is aging and in their case the potential aims and advantages of the biomass project are irrelevant. Single people households with lonely old people have no interest and neutrally accept the plan.
- b) People in opposition with the local municipalities reject all attempts connected to the authorities.
- c) The increase of the Roma population generates an ethnic confrontation between the majority and minority groups of the population. A visible obstacle of the plan being accepted by the Romas is that the initiative is connected to the majority population.
- d) The division of the Roma population into those having lived in the village for generations and the new settlers increase their ambivalent view towards any kind of development.

The above four aspects are generally hindering the realization of the project. A possible solution may be an effective and well aimed communication strategy towards the groups affected. If the aversion of the sub-communities towards the realization of the project continues to exist the authenticity of the development plan will suffer.

Acknowledgement

The described work was carried out as part of the TÁMOP-4.2.1.B-10/2/KONV-2010-0001 project. The realization of this project is supported by the European Union, co-financed by the European Social Fund.

References

- [1] Dobosy Iászló: Ózdi kistérség. Ózd. Inka, 2007.
- [2] Foster, George M.: Applied Anthropology. Boston. Little, Brown and Company, 1968.
- [3] Geertz, Clifford: The Available Light. Princeton. Princeton University Press, 2000.

⁷ The emic account is an attempt at understanding from the point of view of the "natives", which has been worked out in detail by modern cultural anthropology as the frame condition for genuine cognition both in the methodological and the theoretical sense. (Seymour-Smith, Charlotte 92.)

- [4] Glazer, Nathan: *We Are All Multiculturalist Now*. Cambridge (Ma). Harvard University Press, 1997.
- [5] Seymour-Smith, Charlotte: *Macmillan Dictionary of Anthropology*. London. Macmillan, 1986.
- [6] Spickard, Paul: *Mixed Blood: Intermarriage and Ethnic Identity in Twentieth Century America*. (Tucson, AZ: U of Arizona Press, 1989)
- [7] Young, Robert: *Colonial Desire: Hybridity in Theory, Culture and Race*. (N.Y.: Routledge, 1995)

ELECTROREFINING OF TIN IN PURE ACID SOLUTIONS BY MECHANICALLY CONTROLLED CATHODE DEPOSITION AND SOLAR POWER UTILIZATION

ZSOLT DOBÓ¹, TIBOR KULCSÁR², TAMÁS KÉKESI³

¹ University of Miskolc, Department of Combustion Technology and Thermal Energy,

^{2,3} University of Miskolc, Department of Chemical Metallurgy and Surface Techniques,
3515 Miskolc-Egyetemváros
kekesi@uni-miskolc.hu

Electrorefining, producing pure tin from waste materials in cheap acid electrolytes can be effectively operated with parameters set to provide for the stability of the solution and high current efficiencies and the use of the periodical current reversal (PCR) technique. However, the cathodic deposit is roughly dendritic, requiring regular interventions. For the long term automatic operation, we have devised an electromechanical system that regularly compresses the metal deposited with a loose structure, applying pre-set force and time intervals, thereby eliminating the dangerous outgrowths. Thus the operation of the cell can be stabilized for longer runs. As a free alternative of electrical supply, the system was detached from the mains supply by applying a solar input. The long term electrolysis experiments have proved the stable and efficient work and the high – close to 99.99% – purity of the product.

Keywords: tin refining, HCl solution, cathodic deposition, dendrites, cathode compression.

1. Introduction

Conventional pyrometallurgical refining is not efficient in producing high purity tin, therefore electrorefining has become a convenient way to eliminate most of the impurities in a single operation [1, 2]. As alkaline solutions require higher temperatures and double as much specific charge of the tin ions as in acid solutions, the use of sulfuric acid based electrolytes is usually applied [3]. However, the stabilizing the Sn(II) ions require high amounts of cresylic phenylic sulfonic acid, an expensive and hardly available component. Controlling the growth of the rough tin crystals at the cathode surface is usually carried out by the application of special organic additive agents. Application of PCR technology has also been introduced [4] in sulfuric acid electrolytes with moderate success. In order to make this technology inexpensive and available for smaller scale applications, simple hydrochloric acid – tin chloride electrolyte solutions have been suggested, which offer the natural inhibiting effect by chloride complex formation, and the added advantage of high solubility and the possibility to apply high current densities [5]. The beneficial effect of PCR current on the morphology of the cathode [4, 6] can be utilized also in this system. However, the simple acidic solutions of tin may lose their stability because of the gradual oxidation and $\text{SnO}_2 \cdot x\text{H}_2\text{O}$ precipitation, and the reaction of the deposited tin with the Sn(IV) species – in addition to the danger of hydrogen evolution – may spoil the current efficiency. All these difficulties can be counteracted by an optimizing the process of PCR electrorefining in HCl – SnCl_2 solutions, however the formation of a rough and loosely dendritic cathode deposit is hard to be avoided [5]. Diverting from the optimized conditions

offering solution stability and high current efficiency is not recommendable and the use of simple organic inhibitors could neither be justified [5]. If controlling the growth of whiskers and long dendrites is not convenient in the possible ranges of electrolytic parameters, a mechanical method can still be considered to avoid the difficulties caused by the strong tendency of isotropic electrocrystallization. The main purpose was to devise such an electro-mechanical cathode compacting system which prevents the outgrowth of long crystals, thereby helps avoiding the short-circuits and the contamination by the anode slime, and requires no continual cell inspection.

The production of metals by electrolytic procedures converts the value of the used electric energy into the value of the produced metals, readily stockpiled. This is a reliable constant use of the generated electric charge, which allows the utilization of a green and inexhaustible source of energy to the highest efficiency. As the electrolysis requires longer times of operation than the normal daylight hours, a battery based storage facility needs also to be incorporated to span the night periods. Thus the possibility of a long-term uninterrupted operation can be offered from the current supply side, but with the automated control of deposit structure, also from the current consumption side.

2. The experimental equipment and procedure

The system consists of three groups of units. As shown on the left side in Figure 1, the energy supply section consists of the solar panel, the charge controller and the acid lead battery. The other side consists of the electrolysis cell equipped with the mechanism of cathode compression. The current for the electrochemical process and the rotation of the electric motor is controlled by the electronic circuit, based on a programmable microcontroller, between the electric energy supply and consumption sides (Figure 2). In order to provide for the periodically reversed current, a suitable switching unit is also incorporated in the power supply section. The microcontroller receives digital input from a connected keyboard and sends information to a liquid crystal display. The cell can be operated under galvanostatic or potentiostatic conditions, by setting either the required intensity of the current or the cell voltage. The microcontroller operates also the programmed cathode pressing functionality. The pressure is exerted on the deposited crystals by a pressing plate parallel to the cathode surface. It is driven by an electric motor and a transmission mechanism. The position and the exerted force are sensed and the program uses this information for controlling the movement.

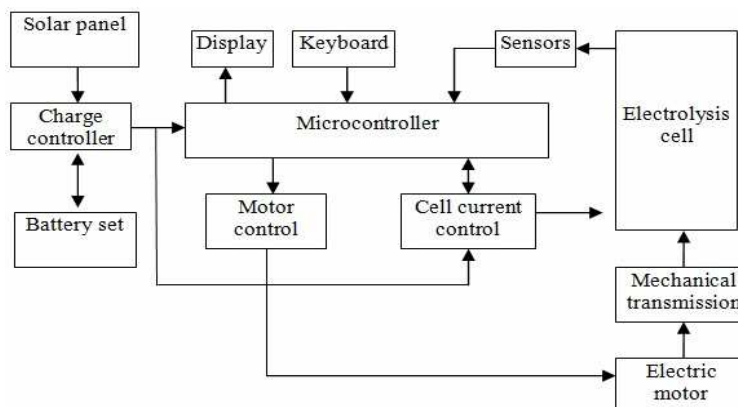


Figure 1. The lay-out of the electro-mechanical electrolysis system equipped with solar energy supply

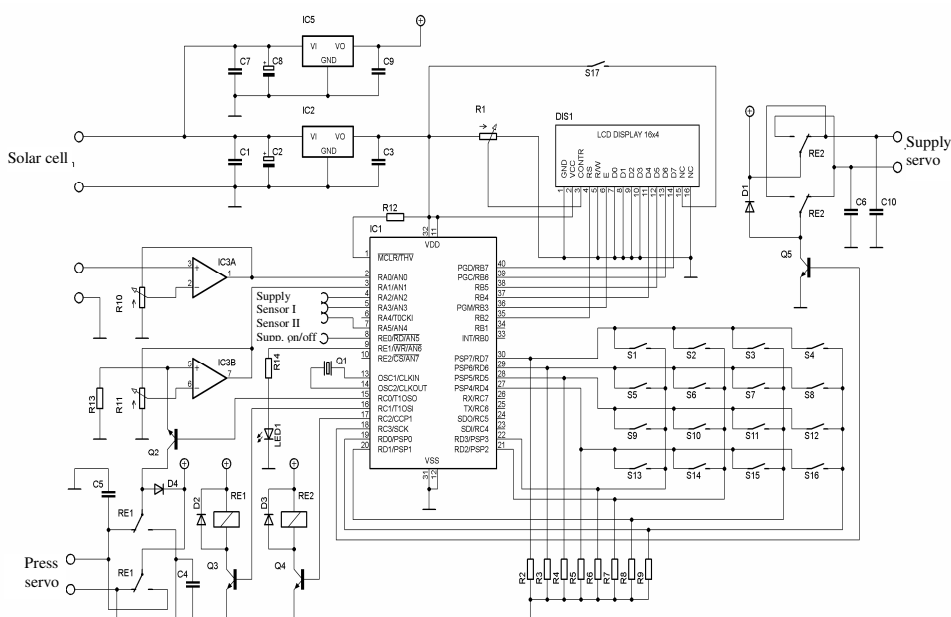


Figure 2. The main electronic devices and the electric circuitry of the controlling unit

The structure of the electrolysis cell is shown in Figure 2. The rotation of the electric motor is transmitted through a suitably designed gear and threaded spindle-nut mechanism to a perforated pressing plate. Its movement is limited by magnetic sensors, sending signals to the microcontroller. As the cathodic deposit grows thicker, the pressing movement must be stopped earlier. Therefore, the pressing plate is returned to the standby position if the

current uptake of the electric motor reaches a preset value. In order to eliminate the danger of short circuits, the pressing plate covers the complete cross section of the electrolyte bath. Thus no crystals are allowed to grow in the gaps between the edges and the walls.

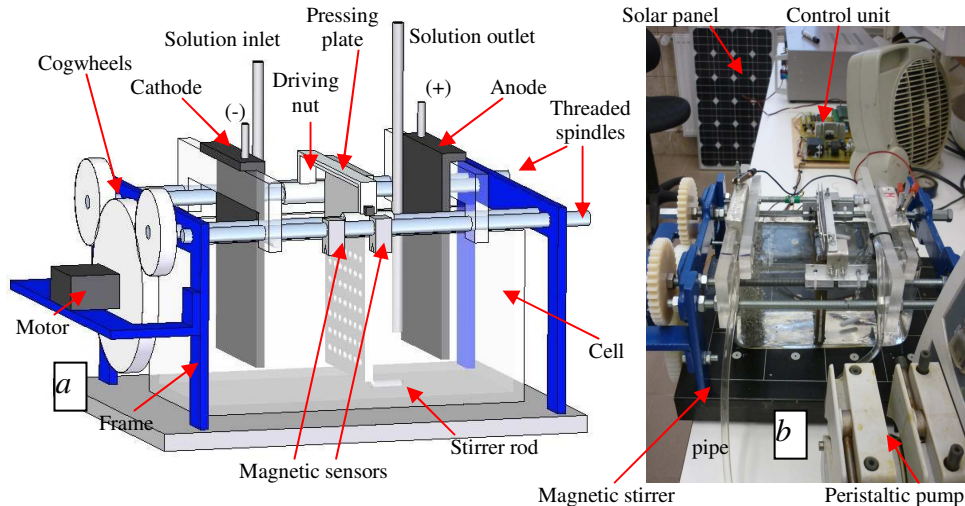


Figure 3. Structure (a) and picture (b) of the electromechanical electrolysis cell

The electrolyte solution is circulated from the lower edge of the anode to the top of the cathode through a peristaltic pump. This helps compensate for the differences in the tin concentration, thereby suppressing diffusion polarization. This purpose is assisted also by a magnetic stirrer rod placed in the anodic compartment.

The anode was cast after melting the soldering waste material and removing the dross. The cathode plate was cast of purified tin and the reverse side was covered by an acid resistant lacquer layer. The immersed surface was 8 cm x 8 cm. The un-dissolved impurity elements of higher electrode potential than that of tin are collected in the sludge layer on the surface of the anode. Dissolved impurity elements of more negative electrode potential than that of tin remain in the electrolyte solution, therefore some of the circulated solution should be removed for purification and replaced by pure raw solution of equal volume as the concentration of the impurities require it. The inadvertent changes in the tin concentration can also be compensated by this procedure. The electrolysis is terminated when the thickness of the deposited layer reaches the position of the magnetic sensor set closer to the cathode. When the cathode is removed from the cell to detach the produced deposit, the anode is also removed to wash the collected sludge off its surface. It may be a valuable raw material for the extraction of silver – and also copper – by selective hydrometallurgical processing.

3. Experimental results

In order to test the efficiency of the cathode compression system under the extreme conditions, the experimental electrolysis was carried out by applying DC current, which allows longer outgrowing crystals than the PCR current. The progress of the operation is

demonstrated by the series of pictures in Figure 4. The dark sludge layer is obvious at the surface of the used anode in Figure 4. *b*) The initial conditions of crystal growth are illustrated by Figure 4. *c*) This crystals quickly develop into large whiskers and needles shown in Figure 4. *d*) which can be compressed into a relatively dense layer, shown from the side in Figure 4. *e*) The compressed deposit becomes gradually denser as several (10–15 min long) cycles of compression take place. After multiple cycles, a virtually compact deposit is produced, as demonstrated in Figure 4. *f*) Optionally, the movement of the pressing plate can be activated by the sensed decrease in the resistivity of the cell, caused by the outgrowing masses of dendritic crystals.

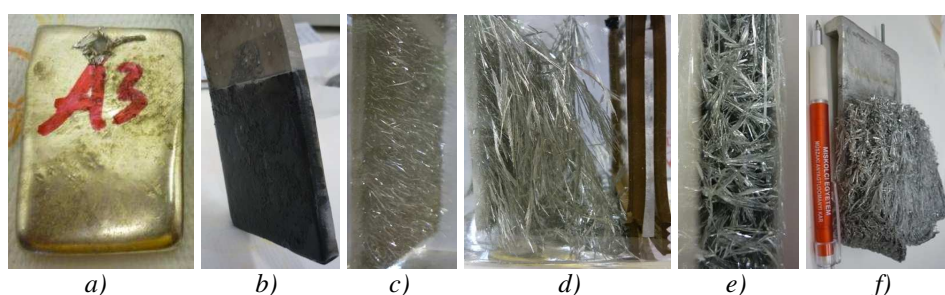


Figure 4. Pictures of the (*a*) cast anode, (*b*) used anode, (*c*) initial crystals, (*d*) loose crystals, (*e*) the compressed crystals, (*f*) the cathode deposit after multiple compressions

We have observed that the current distribution becomes more and more even as a result of the increasing number of compression cycles during a long electrolysis run. It is caused by the multiplication of deposition sites among the main dendrite branches when the outgrowing crystals are pressed back to a relatively uniform surface. As a result, the electrocrystallization of tin becomes denser and the layer more compact. This mechanism is demonstrated by the series of macro photographs in Figure 5.



Figure 5. The increasing thickness of the secondary dendrite arms after multiple compression

The relatively even surface of the deposit is beneficial also for the current efficiency. We have measured stable net current efficiencies continuously close to 95% during the entire length of the electrolysis run. The change in the tin concentration is shown by Figure

6, when as high as 1000 A/m^2 current density was applied in the 1 M HCl tin chloride solution. This experiment was run with PCR current of 20:1 forward: reverse cycle time ratio. The theoretical net current efficiency is calculated from the measured weight increments of the cathode and the amount of the effective charge causing cathodic deposition:

$$H_{\text{net}} = \frac{\frac{zF}{118,71} \Delta m_{\text{Sn}}}{\int_{t_s}^{t_c} \left(\frac{t_+}{t_+ + t_-} I_+ - \frac{t_-}{t_+ + t_-} I_- \right) dt} \quad (1)$$

where Δm_{Sn} is the mass increment of the cathode in the $(t_c - t_s)$ interval, I_+ and I_- are the absolute forward and reverse currents in the t_+ and t_- corresponding periods, F is the Faraday constant $z = 2$ is the valence of the electro-active ions. In this case the forward and reverse currents were set equal. A virtual value of the determined current efficiency was expressed assuming the deposition of the predominant Sn(II) species. The practical gross current efficiency – referring to the total charge consumed - could be expressed with a similar formula where the second term in the integral argument is added to the first one.

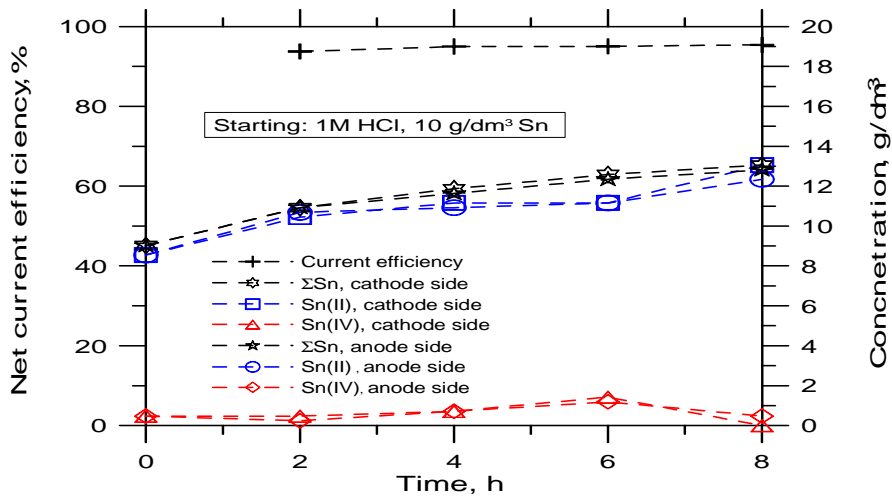
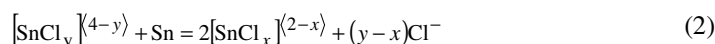


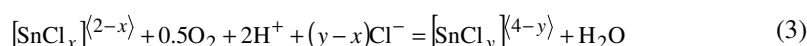
Figure 6. Changes in the virtual net current efficiency and the tin concentrations in the cathode and anode compartments during electrolysis (1 M HCl , 1000 A/m^2 , PCR 20:1)

When the electrolysis was interrupted for removing and weighing the cathode – after washing and drying – samples were also taken from the homogenized solution and examined by iodometric analysis for Sn(II) . The total tin concentration was determined by a complete cementation of the sample with aluminium powder and re-dissolution in boiling HCl and finally analyzing the total tin as Sn(II) . This value was slowly, but continually increasing in both compartments of the electrolysis cell. At the same time the Sn(IV)

concentration remained low. The set HCl concentration was also found stable or negligibly increasing. This corresponds to the assumed mechanism of cathode corrosion by



reducing Sn(IV) by re-dissolving some of the deposited metal. This could be the major cause of any current loss. The generation of the Sn(IV) species can be attributed to the oxidizing effect of air



in the first place, as the cell was operated open to the atmosphere. This effect may have been enhanced by the stirring of the solution before taking the multiple samples. Another source of oxidation may be attributed to the anode, especially at elevated current densities. The rise in the total tin concentration can be counteracted by treating a portion of the circulated electrolyte solution through a conditioning cell, where the anode is made of insoluble material. The accumulation of impurities dissolved from the anode endangers purity on the long run; therefore they have to be removed from the necessary portion of the circulated electrolyte solution by further techniques. This is a general feature of any electrorefining procedure, but in this case these impurities are at a relatively low level.

The purity of the metal deposited and periodically compressed at the surface of cathode is reliably high. As a result of the periodic compression, no outgrowing crystals may touch the sludge layer on the anode, and the sites of electron transfer are distributed over a large and relatively uniform cathode surface. The former feature eliminates entrapped impurities, and the latter condition does not allow the formation of sharply preferential deposition sites causing a severe depletion of tin ions in their vicinity and harmful diffusion polarization. Thus the application of the periodic cathode compression technology may finally enhance the purity of the cathodic product. The main impurity, copper and the most valuable alloying element, silver are practically and safely retained in the anode slime. The rest of the impurities, are also separated. The efficiency of purification can be assessed by comparing the compositions of the anode made of the raw material and the produced cathodic deposit after detaching it from the base plate, melting and sampling. Table 1 shows the efficiency of purification for the most important impurities.

	Concentration, %						
	Ag	Bi	Cu	Fe	Ni	Pb	Total
Anode	0,4903	0,0600	0,2006	0,0051	0,0075	0,0153	0,7798
Cathode	0,0063	0,0023	0,0077	0,0005	0,0003	0,0022	0,0249

Table 1. Impurity concentrations in the raw anode and the refined cathode materials

Due to the dissolution of copper from the contacts of the electronic devices by the tin bath during the wave soldering process, the copper concentration tends to surpass the set limits in the soldering material. Therefore, the most important target of purifying waste soldering materials is copper. A comparison of the starting concentration in the anode and

the final one in the cathode shows, that the removal of copper is highly efficient. The purity of the produced tin is ~ 99.98%, which is above the standard level offered in metal exchange stocks. The cathodic product can be easily detached and melted, although this step also requires the exclusion of oxidation. Because of the high specific surface of the crystals, the product is best melted by quick submersion into an existing tin bath.

Conclusions

Due to the high market price of tin, secondary raw materials generated in the soldering technology carry great value. Earlier experimental work has established the optimum conditions for achieving high current efficiencies and stability in the inexpensive dilute HCl – SnCl₂ electrolyte solutions without the application of any special additives. These conditions proved favorable also to producing pure tin at the cathode. The essentially rough structure of the cathodic deposit, tending to form long outgrowing crystals, still required further development. This difficulty could be solved by incorporating an automated electromechanical system in the cell, which periodically compresses the loose cathode, thereby allows long-term operation without the need of inspection. The compressing mechanism and the cell current are both controlled by a programmable central electronic unit developed for this specific purpose. The cathodic deposit becomes gradually denser and more uniform as the operation progresses. The current required for the whole system can be supplied by an integrated photovoltaic source and a buffer storage facility. The purity of the product and the utilization of the electric charge is enhanced by the compressing mechanism, thus superior quality metal can be produced efficiently

Acknowledgement

This research was supported by the program TÁMOP 4.2.1.B-10/2/KONV-2010-0001.

References

- [1] Wright, P.: Extractive Metallurgy of Tin, Elsevier Press, 1967.
- [2] Halsall, P.: The Refining of Tin, Metall, 43 (1989) 131-136.
- [3] Mackey, T.: The Electrolytic Tin Refining Plant at Texas City, J. Met., June 1969, 32-43.
- [4] Behmer, J, Krajewski, W., Krüger, J.: Untersuchungen zur elektrolytischen Raffination von Zinn unter Anwendung periodischer Stromumkehr, Raffinationsverfahren in der Metallurgie, GDMB - Verlag Chemie, Weinheim, 1983.
- [5] Rimaszéki, G., Kulcsár, T., Kékesi, T.: The characteristics of electrolytic refining of tin soldering scrap in hydrochloric acid solutions, Proc. 50th Ann. Conf. of Metallurgists, COM2011, – Waste Processing and Recycling –VI, Ed. Rao, S.R., et.al., Montreal, QC, Canada. 2-5. October, 2011. 137-145.
- [6] Szepessy, A., Kékesi, T.: Investigation of the Specific Energy Consumption of PCR Copper Refining. Acta Techn. Acad. Sci. Hung., 105,3 (1993), 197-209.

EXAMINATION OF PRECIPITATION HARDENING OF AlSi10MgCu0,5 ALLOYED AUTOMOTIVE CASTINGS

MELINDA GODZSÁK¹, JENŐ SÓLYOM², ÁRPÁD KOVÁCS³,
PÉTER PEKKER⁴, ZOLTÁN GÁCSI⁵

University of Miskolc
Faculty of Materials Science and Engineering, Institute of Physical Metallurgy,
Metalforming and Nanotechnology
3515 Miskolc, Egyetemváros
¹godzsak.melinda@gmail.com
²femsj@uni-miskolc.hu
³femkov@uni-miskolc.hu
⁴pekkerpeter@gmail.com
⁵femtangz@uni-miskolc.hu

Automotive castings have to meet more and more versatile requirements these days. There is a constant need for production engineering developments ranging from purity degree – that is producing molten metal with high cleanness – to grain refinement and alloy improving including heat treatment technologies. In our research we investigated the opportunities of production development in an automotive company producing aluminium based castings.

Keywords: heat treatment, AlSi alloy, aluminium-silicon alloy, automotive casting, casting alloy, AlSi10MgCu0,5, precipitation, precipitation hardening, solid solution treatment, quenching, ageing, T5, T6, Guinier-Preston zones, segregation.

Introduction

We dealt with the correlation of the so called T6 heat treatment and mechanical properties and changes in microstructure. Several publications helped us in our research [2, 3, 4]. We also examined optimisation of heat treatment parameters and reducing the heat treatment time. Our aim was to find ways of cost reduction of age hardening, as economic factors are also very important for an engineer besides technical parameters and feasibility.

1. Presentation of the experiments and results

The alloy we experimented with is AlSi10MgCu0,5, which the automotive parts are made of. The exact places of examinations and required stress limits are defined by the buyers' demands. The castings provided by the factory were cut and mechanised to these demands. This way we had the necessary specimens for our experiments. They were separated into two groups. Some samples are from the upper- part of the casting which was cooled down in a normal way.

The other group of workpieces are from the lower- part of the casting which were cooled down in a controlled way. In the following we will refer to these samples as upper-part and lower- part samples for the sake of simplicity.

2. The heat treatment plan

In case of the casting made of AlSi10MgCu0,5 alloy the heat treatment applied in the foundry lasts for 9 hours. In the first stage there is a 6-hour solid solution treatment at 530 °C temperature and then the castings are intensively cooled down in water of 60-80 °C temperature. In the second stage after the fast cooling there is a 3-hour ageing process at 210 °C temperatures. In the experimental part of our examination we worked out a heat treatment plan based on the heat treatment parameters in the foundry. The aim was to find out whether the stress limits required by the buyer could be met despite the reduction of heat treatment time.

1.	Cast product, 2 days after casting	
2.	Cast product, 14 days after casting	
3.	530 °C - 3 h - 210 °C - 2 h	Group 1
4.	530 °C - 3 h - 210 °C - 3 h	
5.	530 °C - 3 h - 210 °C - 4 h	
6.	530 °C - 4 h - 210 °C - 2 h	Group 2
7.	530 °C - 4 h - 210 °C - 3 h	
8.	530 °C - 4 h - 210 °C - 4 h	
8.	530 °C - 5 h - 210 °C - 2 h	Group 3
10.	530 °C - 5 h - 210 °C - 3 h	
11.	530 °C - 5 h - 210 °C - 4 h	
12.	530 °C - 6 h - 210 °C - 3 h	
13.	Casted and measured in the Foundry	

Table 1. The plan of the heat treatment

The parameters of age hardening were defined in accordance with this aim (the temperatures were not changed). We set up 3 groups (Table 1). The heat treatment described in line N° 12 we carried out just for curiosity to see how big the difference might be in the results if we apply heat treatment to a whole casting in a special charge basket in the foundry or we apply the heat treatment to mechanised specimen of smaller sizes in a furnace of the university laboratory. The results show that there are differences but not significant.

3. The results of the hardness test

In Brinell hardness measurement tests the diameter of the steel bullet was 5 mm, the load force was 250 kp (2452,5 N) and the time period was twelve seconds. The hardness features of upper-part and lower-part test samples were composed of the average of 7 measurements.

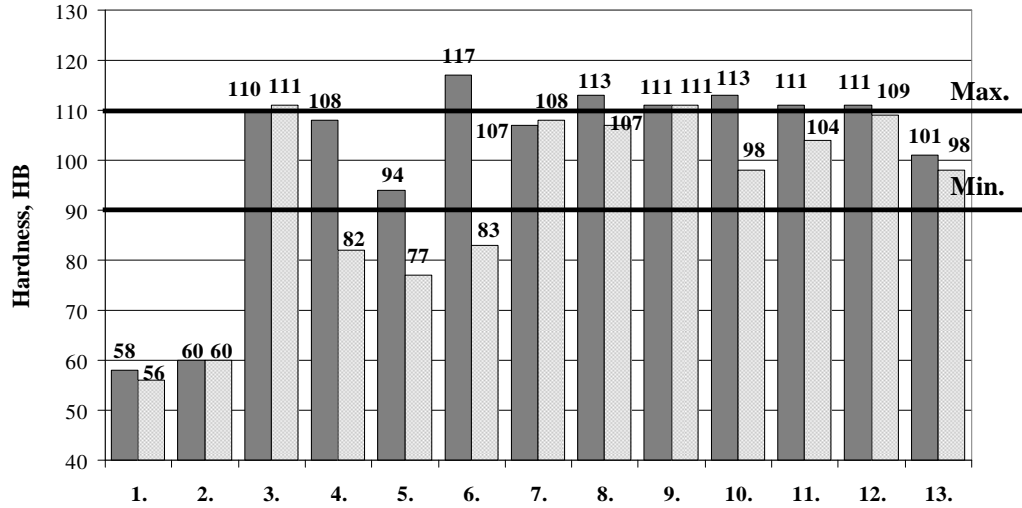


Figure 1. Hardness depending on different heat treatment parameters

Figure 1 shows Brinell hardness depending on different ageing times with the same solid solution treatment time. The darker colour shows the hardness measured on the lower-part samples (cooled down in a controlled way). The requirements prescribe 90-110 HB for both the upper and the lower-part of the sample castings. Apart from measuring inaccuracies we strictly insist on the HB interval and we can see that both the specimen treated in the foundry and the specimen we treated (530 °C temperature – 4 hours solid solution treatment and 210 °C temperature – 3 hours ageing) fell into this interval.

The Guinier-Preston zones responsible for the increase in hardness are formed in large quantities in the α solid solution, so we have done Vickers hardness tests inside of the dendrit arms to determine the effect of the Guinier-Preston zones on hardness. In this case the test samples were completely prepared, the loading force was 10 g, and loading took 10 seconds. This type of measurement is not used in the Foundry, so I could not mark any expected values. The results can be seen in Figure 2.

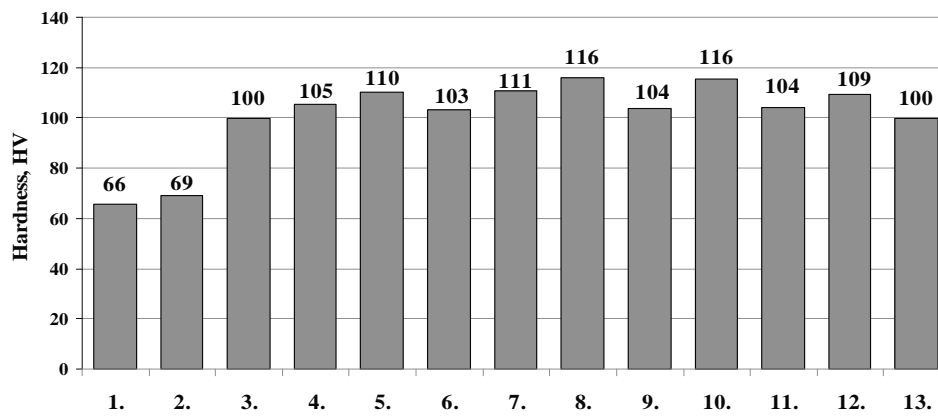


Figure 2. Microvickers hardness depending on different heat treatment parameters

Figure 2 shows that the hardness values of the heat treatments 4+4 h and 5+3 h are the largest (115,6 HV and 116 HV), they are over the hardness value the reproduction of the heat treatment in the Foundry (109,3 HV). Besides we can also see, that the hardness values are increasing with the raising of the heat treatment times, because more dissolved alloying content will be in the later increasing amount of tempering to able to form GP zones.

4. The results of the mechanical measurements

The most important mechanical properties were defined by the tensile test. Figure 3 shows that all the heat treated workpieces reached the required minimal tensile strength value (220 MPa). The most constantly high tensile strength can be attributed to 4-hour solid solution treatment and the highest figures are with 4+3 – hour precipitation hardening. This value is higher than tensile strength of the foundry piece treated for 9 hours.

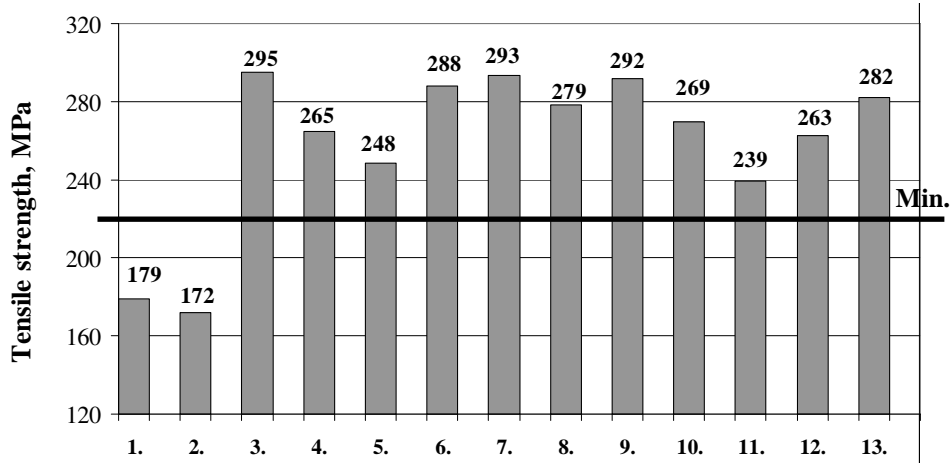


Figure 3. Tensile strength depending on different heat treatment parameters

Figure 4 shows that both the heat treated pieces and the non-heat treated castings reached the required minimum of 0,5% elongation. If elongation value is too low the castings become too rigid. Similarly too high elongation is also harmful to tensile properties.

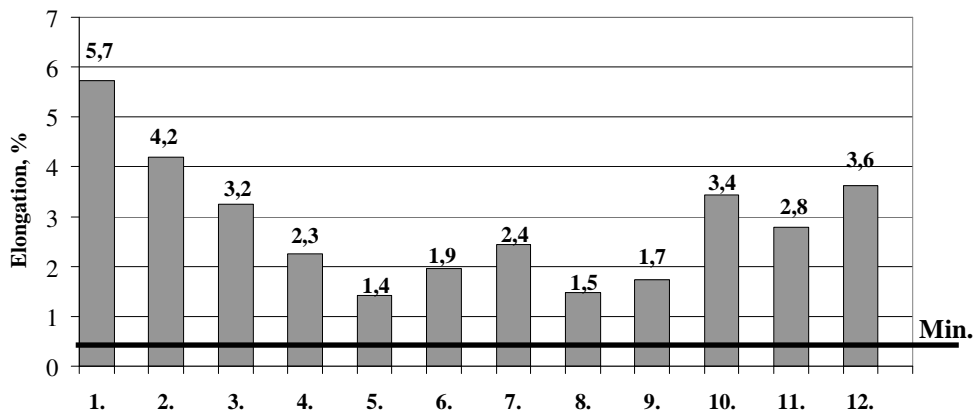


Figure 4 Elongation depending on different heat treatment parameters

5. The results of the XRD measurements

The X-Ray diffraction measurements were carried out on the {311} lattice plan. The values of the lattice parameters indicate the dissolved component content. According to the professional literature [1] if the magnesium content of the alloy is solved it increases the value of lattice parameter. If the copper, manganese or silicon content of the alloy is solved it causes reduction in the lattice parameters.

The ability of silicon to cause changes in lattice parameter is very low. As the process is advancing the silicon, copper and manganese atoms getting into the solution might moderate the effect of magnesium regarding the lattice parameters. The 4-hour solid solution treated workpiece has the highest lattice parameter.

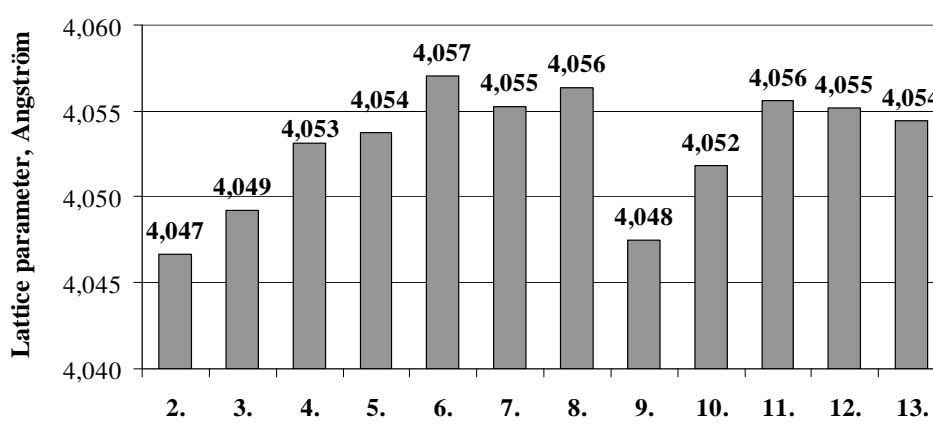


Figure 5. Lattice parameter depending on different heat treatment parameters

It can be seen in Figure 5 that lattice parameters of all heat treated samples have increased compared to the non-heat treated workpiece. The most even lattice parameter changes can be seen in 4-hour solid solution heat treatments, probably the alloying components are solved in the biggest amount in this case and later during the ageing process may cause precipitations.

Half value width can be increased by lattice defects, lattice stress, uneven component content distribution, precipitations and Guinier-Preston zones might also change the interplanar crystal spacing in their environment as they have coherent surface, so they can increase lattice potential. Figure 6 shows that half value width figures (except two of them) decreased. We might conclude that probably Guinier-Preston zones do not cause as much widening as the microconcentrations of dendrit in the non-heat treated casting. G-P zones might result in further decrease in lattice potential if they coarsen and their lattices are not coherent in aluminium matrix.

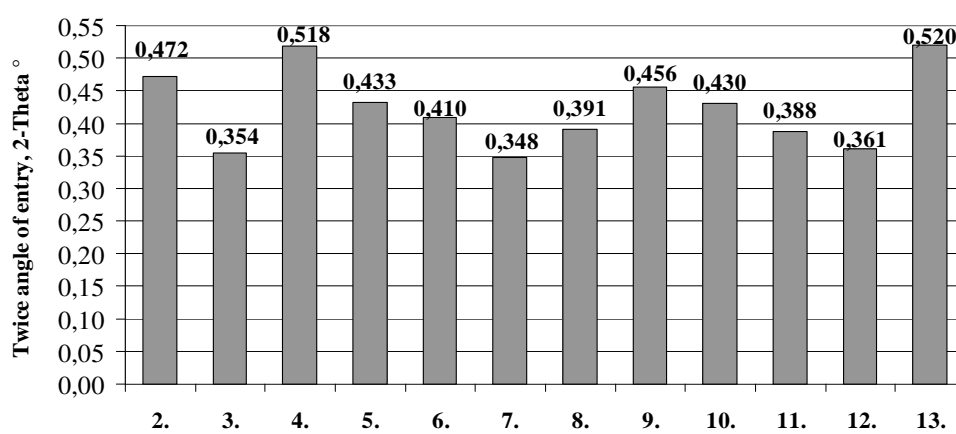


Figure 6. Half value width depending on different heat treatment parameters

6. The results of the TEM measurements

Nano-size Guinier-Preston zones which are responsible for the increase in hardness and tensility in aluminium alloys can be examined directly only by transmission electron microscope. In our research we had the opportunity to examine a single specimen so we chose a sample with suitable hardness and tensility properties (530 °C temperature – 4 hours and 210 °C temperatures – 3 hours). Figure 7 shows very characteristic „fishbone” or „Chinese character” formation the so called α -type iron-manganese precipitation.

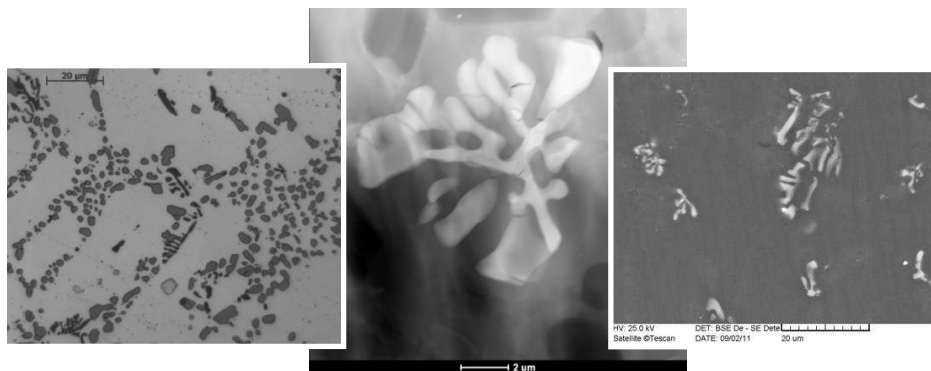


Figure 7. Photos of the Fe-Mn phase (α -type) like “Chinese character”; light microscope – (left side), TEM – (middle) and SEM – (right side)

Figure 8 illustrates G-P zones in different magnification rates. Reading the professional literature we found photos where G-P zones can be seen more sharply [2] [3] [4] but in these photos it is more difficult to see them in the matrix and their composition cannot be identified either.

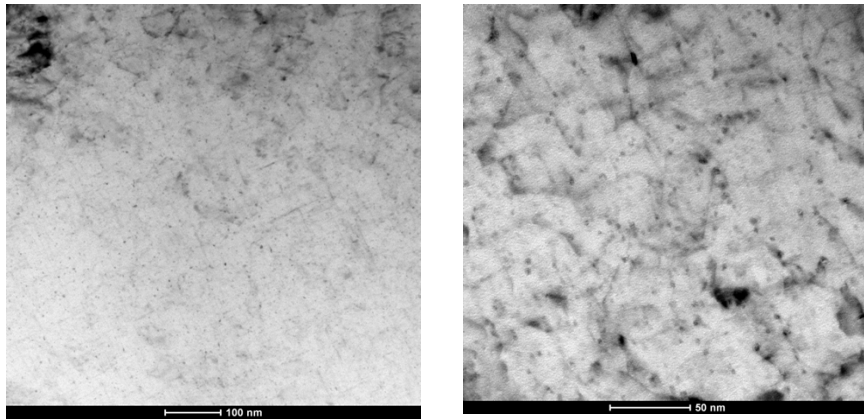


Figure 8. Photos of the Guinier-Preston zones

7. The results of the SEM measurements

Figure 9 illustrates the discontinuity surface on one of the tensile test specimens in 500 x magnification rate.

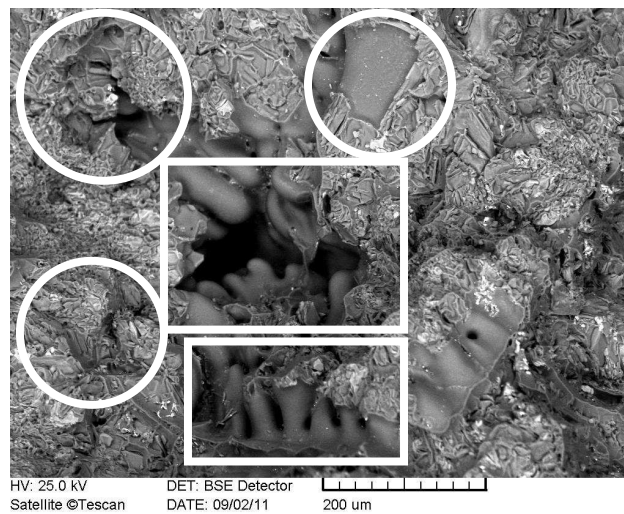


Figure 9. Discontinuity surface

We can see all of the discontinuity surfaces, a lot of coarse compound phases marked with a white circle and a lot of interdendritic porosity marked with a white rectangle. As a whole, a lot of coarse compound phases, interdendritic porosity and microcracks can be

found on the discontinuity surface. These material defects may cause the low yield strength and elongations.

Summary

Our task was to find other heat treatment parameters to reduce the treatment periods and power consumption (530 °C temperature – 6 hours and 210 °C temperature – 3 hours). The most important aim was to reduce the heat treatment time but at the same time meet the mechanical requirements expected by the customers. Therefore we experimented with 9 different T6 heat treatment parameters lasting for different time periods without changing the temperature of the treatment. When analysing the data we examined the changes in hardness and tensility values together with the lattice parameters and half value width. Based on the test results we found that the most suitable precipitation hardening is with the following parameters: 530 °C temperature – 4 hours and 210 °C temperature – 3 hours. This heat treatment process is 2 hours shorter than the same process in the foundry. Consequently, it would mean reduction in the costs for the company. In addition to mechanical properties we also studied the microstructure and its changes with transmission electron microscope and indirectly with X-Ray diffraction tests as well. In our research we found that the mechanism of strength increasing in various aluminium alloys is a complicated and complex process, it is determined by a lot of factors. We think examination of electrical conductivity and thermoelectric power would provide more exact information about precipitation processes, these areas are definitely worth doing further research in.

Acknowledgments

This work has been carried out as part of the TÁMOP-4.2.1.B-10/2/KONV-2010-0001 project within the framework of the New Hungarian Development Plan. The realization of this project is supported by the European Union, co-financed by the European Social Fund.

References

- [1] W. B. Pearson: A handbook of lattice spacings and structures of metals and alloys, Pergamon Press, 1956
- [2] Tavitas – Mohamed – Gruzleski – Samuel – Doty: Precipitation-hardening in cast Al-Si-CuMg alloys, Springer S+B Media, LLC, 2009.
- [3] E. Sjölander, S. Seifeddine: The heat treatment of Al-S-Cu-Mg casting alloys, School of Engineering, Jönköping University, Sweden, 2010.
- [4] R. X. Li, R. D. Li, Y. H. Zhaob, L. Z. He, C. X. Li, H. R. Guanc, Z. Q. Huc: Age-hardening behavior of cast Al–Si base alloy, China, 2004.

THE ESSENCE OF EQUILIBRIUM OF MATERIALS IN 17 SHORT STATEMENTS

GEORGE KAPTAY

University of Miskolc, Department of Nanotechnology
3515 Miskolc-Egyetemváros
kaptay@hotmail.com

The paper summarizes the essential thesis of the equilibrium of materials in 17 statements, with the following subjects: 1. semantics, 2. the five base units of nature, 3. the 84 stable elements and their non-constant atomic masses, 4. systems and phases, 5. phases and components, 6. characterization of the equilibrium state, 7. state parameters, 8. extended phase rule, 9. the requested size of the data-bank on materials equilibria, 10. the four laws, 11. the Gibbs energy, 12. the Gibbs energy of solutions and mixtures, 13. the conditions of equilibrium, 14. the Calphad system, 15. the Gibbs energy of nanophases and the size dependence of equilibrium, 16. the Estphad system, 17. the electrochemical synthesis diagrams.

Keywords: materials equilibria, thermodynamics, Gibbs, nano-equilibria.

This paper describes the essence of equilibrium of materials. There is nothing new here compared to what is already known. The novelty is the size of this paper. There are lengthy books, in which the ordinary reader can be easily lost. This short paper helps to keep our mind on the essence of the subject. The 17 statements are as follows [1]:

1. The origin of the word “matter” (= materia in Latin) is word “mother” (“mater” in Latin), proving that materials sciences is the mother of all sciences. This semantic unity found in indo-European languages was transported even into the Hungarian language in the 19th century by creating an artificial word “anyag” (= matter) from the ancient Hungarian word “anya” (= mother) [2].
2. Nature can be described by 5 base quantities and units [3]: length (m), mass (kg), time (s), temperature (K), electric charge (C). Additionally there is an infinite number of derived quantities and units, such as force (N), or electric current (A), or even intensity of light (cd), the later being a combination of derived units of W, sr, Hz. Additional arbitrary quantities and units can be created based on arbitrary definitions, as the amount of matter (mole) is created together with the Avogadro number by declaring that in an arbitrary way that the mass of 1 mole of C-12 is taken exactly as 12 g/mol [4]. The difference between the system of Planck and the current SI system of units [5] is hard to understand and is due only to incorrectly treated scientific diplomacy. Let us ask the current officials of science to correct this situation.
3. There are 84 stable elements in Nature [6]. All other elements are unstable, i.e. they cannot be stabilized and utilized to create useful materials without a danger for workers and users. The majority of the elements consist of some isotopes. However, the distribution of different isotopes is found different even along the surface of the Earth, and thus the atomic mass of the elements cannot be considered any more as constants of nature [6].

4. Nature can be divided in an arbitrary way into an infinite number of systems upon our convenience to ease our analysis. Systems are made of at least one phase, or several phases (P = the number of phases), divided from each other by interfaces. Phases (Φ) in a system are characterized by phase ratios ($y_\Phi \equiv n_\Phi / \sum_\Phi n_\Phi$, where n_Φ = amount of phase Φ in the system, mole). Their sum equals unity ($\sum_\Phi y_\Phi = 1$).
5. Phases are made of components (i), which are usually selected from the 84 stable elements (C = the number of components). Upon convenience, stable compounds can also be considered as components. Phases are characterized by their structure and composition, expressed in mole fraction of component i in phase Φ ($x_{i(\Phi)} \equiv n_{i(\Phi)} / \sum_i n_{i(\Phi)}$, where $n_{i(\Phi)}$ is the amount of component i in phase Φ , mole). Their sum equals unity ($\sum_i x_{i(\Phi)} = 1$). The system is characterized by the average mole fraction of components: $x_i \equiv n_i / \sum_i n_i$ (where n_i is the total amount of component i in the system, mole). Their sum equals unity ($\sum_i x_i = 1$).
6. The state of any system is characterized by four types of information: the number of co-existing phases (P), their nature (Φ), their phase ratios (y_Φ) and their compositions ($x_{i(\Phi)}$).
7. The equilibrium state of the system (i.e. the equilibrium values for P , Φ , y_Φ and $x_{i(\Phi)}$) depends on state variables (their number = VAR). In a most abundant situation there are $VAR = C + 1$ independent state variables: pressure (p), temperature (T) and the average mole fractions (x_i) of ($C-1$) components in the system. For nano-systems (i.e. systems with at least one phase having at least one dimension below 100 nm) the total number of atoms in the system is an additional state variable. Additionally, gravitational, electrical and magnetic fields might have an influence on the equilibrium state of the system. Thus, the actual number of state variables: $VAR = C - 1 + K$, where K is the number of active state variables not connected to composition, i.e. K is the number of actual state variables from the list of pressure, temperature, number of atoms, gravitational, electrical and magnetic fields. If all of them are active, then $K = 6$ and $VAR = C + 5$. If only p and T are active, then $K = 2$ and $VAR = C + 1$. The maximum number of state variables for $K = 6$ and $C = 84$: $VAR_{\max} = 89$.
8. The maximum number of phases, which can co-exist with each other in a given system is written as: $P_{\max} = C + K$. State variables are divided into those having free (VAR_{free}) and fixed (VAR_{fixed}) values, with a relationship between them: $VAR = VAR_{free} + VAR_{fixed}$. The number of freedom (the number of state variables

with free values) is the difference between the maximum number of co-existing phases and the actual number of phases: $VAR_{free} = C + K - P$. Then: $VAR_{fixed} = P - 1$. Thus, VAR_{fixed} is independent on both C and K . For 1 phase to exist in the system ($P = 1$), none of the state variables should be fixed ($VAR_{fixed} = 0$) and the number of freedom equals the number of state variables. The above equations simplify to the Gibbs phase rule at $K = 2$ [7].

9. The relationship between state variables and the equilibrium state of the system (i.e. the equilibrium values for P , Φ , y_{Φ} and $x_{i(\Phi)}$) can be found empirically, in an experimental way. If each of the maximum 89 state variables have only 1,000 quantified values, then the number of different situations in nature equals $1000^{89} = 10^{267}$. If each of the 10^{10} homo sapiens species to be alive at the same time on the Earth by 2050 can perform one such accurate experiment every day (what is a largely over-optimistic estimate), it would take 10^{257} days, i.e. more than 10^{253} years. This is much more than passed since the Big Bang (10^{10} years). Even if we consider only 5-component systems with temperature as the only additional state variable, there are 5 independent state variables, calling for $1000^5 = 10^{15}$ combinations, so it would take 1,000 years for this full databank to measure for the whole mankind. Thus, although the empirical establishment of the relationship between the state variables and the equilibrium state is possible in principle, this task will never be actually realized in an empirical way.
10. The above situation calls for another solution. The relationship between state variables and the equilibrium state of the system should be established theoretically, using super-computers. The theoretical basis of this task was published by Gibbs in 1876 [7] and it is based on the first two laws of materials equilibrium (= chemical thermodynamics): i. the energy in Nature is constant (different forms of energy can be transformed into each other) [8–9], ii. The entropy in Nature constantly increases [10–11]. A third law was introduced by Nernst in 1906 to make possible to calculate the Gibbs energies of systems: iii. The entropy of pure and perfect crystals at zero Kelvin is zero [12–13]. The recent 4th law guides the calculations at high temperatures: iv. Real solutions tend towards ideal solutions when temperature is increased [14–15].
11. All systems, phases and components can be described by their so-called Gibbs energies, which determine their behavior and equilibrium. When $K = 2$ (pressure and temperature), the Gibbs energy of a system is written in 3 parts: $G = U + p \cdot V - T \cdot S$, where the symbols are in order of their appearance: the molar Gibbs energy (J/mol), the molar inner energy (J/mol), pressure (Pa), molar volume (m^3/mol), temperature (K) and molar entropy (J/molK). Also, molar enthalpy (J/mol) can be introduced as: $H = U + p \cdot V$. The same equations for phase Φ : $G_{\Phi} = U_{\Phi} + p \cdot V_{\Phi} - T \cdot S_{\Phi}$ and $H_{\Phi} = U_{\Phi} + p \cdot V_{\Phi}$ where quantities with subscript Φ are: molar integral Gibbs energy, internal energy, volume, entropy and enthalpy of phase Φ . The same equations for component i in phase Φ : $G_{i(\Phi)} = U_{i(\Phi)} + p \cdot V_{i(\Phi)} - T \cdot S_{i(\Phi)}$ and $H_{i(\Phi)} = U_{i(\Phi)} + p \cdot V_{i(\Phi)}$ where quantities with subscript $i(\Phi)$ are: molar partial Gibbs energy, internal energy, volume, entropy and enthalpy of component i in phase

Φ . The hierarchy of system – phases – components is preserved: the total Gibbs energy of the system is composed from the integral Gibbs energies of the phases of the given system ($G = \sum_{\Phi} y_{\Phi} \cdot G_{\Phi}$), while the integral Gibbs energy of a phase is composed

of the partial Gibbs energies of the components of a given phase: $G_{\Phi} = \sum_i x_{i(\Phi)} \cdot G_{i(\Phi)}$. Similar equations are valid for all other state functions (U, H, V, S).

12. The partial Gibbs energy component i in a solution phase Φ is written as a sum of 3 terms [16]: $G_{i(\Phi)} = G_{i(\Phi)}^o + \Delta G_{i(\Phi)}^{id} + \Delta G_{i(\Phi)}^E$. The first term is the standard Gibbs energy for a pure 1-component phase $i(\Phi)$. The second term is due to the formation of an ideal solution: $\Delta G_{i(\Phi)}^{id} = R \cdot T \cdot \ln x_{i(\Phi)}$, where $R = 8.3145$ J/molK, the universal gas constant. The third term is due to the difference between ideal and real solutions, written in the first approximation for a binary solution as [17]:

$$\Delta G_{i(\Phi)}^E = \Omega_{\Phi} \cdot (1 - x_{i(\Phi)})^2 \cdot \exp\left(-\frac{T}{\tau_{\Phi}}\right),$$

where Ω_{Φ} (J/mol) and τ_{Φ} (K) characterize the binary Φ solution. When $\Omega_{\Phi} < 0$, the components attract each other, while at $\Omega_{\Phi} > 0$ the components repulse each other at low temperatures. This special interaction between the components gradually weakens at high temperatures, in accordance with the 4th law. The characteristic value of τ_{Φ} has a magnitude 2,000 ... 4,000 K for alloys [14]. The average Gibbs energy of a mixture of several phases is written as: $G = \sum_{\Phi} y_{\Phi} \cdot G_{\Phi}$.

13. If the G_{Φ} functions for all possible phases are known (as function of pressure, temperature and composition), the equilibrium phase can be selected from a simple principle: $G \rightarrow \min$ [7]. Sometimes instead of one phase, a mixture of several phases (α and β , for example) provide the equilibrium state, i.e. the most negative G-value. In this case an additional condition of the heterogeneous equilibrium should be satisfied: $G_{i(\alpha)} = G_{i(\beta)}$ [7].

14. The principles, outlined by Gibbs were transformed into the first computer programs by Kauffmann and others [18–20]. Since then, a large number of binary and higher orders systems have been successfully optimized (see [21] and other Calphad-calculations) and many phase diagrams were measured and calculated.

15. Phases which are smaller in any of their dimensions than 100 nm, have an additional term of their Gibbs energy: $G_{\Phi} = H_{\Phi} - T \cdot S_{\Phi} + A_{\Phi} \cdot V_{\Phi} \cdot \sigma_{\Phi/x}$, where A_{Φ} is the specific surface area of the phase ($\text{m}^2/\text{m}^3 = \text{m}^{-1}$), $\sigma_{\Phi/x}$ is the interfacial energy between the phase and its surrounding (J/m^2). This equation means that all size-dependent thermodynamic properties (vapor pressure, melting point, other equilibrium

temperatures, solubility, decomposition potential, etc.) are due to the specific surface area and not due to curvature, as incorrectly stated in the Kelvin, Gibbs-Thomson, Ostwald-Freundlich, etc. equations [22–23].

16. Phase diagrams contain a huge number of measured, interpolated and extrapolated equilibrium information. In more complex codes (such as to calculate the crystallization during casting) the data calculated by the Calphad method are needed. However, for this type of applications calculations by actual Calphad software is too time-consuming. To overcome this problem, a simplified version called Estphad was developed by Roosz et al, in which equilibrium values are stored in the form of polynomials [24–25].
17. The Gibbs energy data, optimized by the Calphad community can be used not only for the calculation of phase diagrams, but also to calculate chemical equilibria and even to calculate the equilibrium composition of a cathodic product obtained by electrochemical synthesis [26].

Acknowledgement

This work was carried out as part of the TAMOP-4.2.1.B-10/2/KONV-2010-0001 project with support by the European Union and the European Social Fund.

References

- [1] Kaptay, G.: Anyagegyensúlyok makro-, mikro- és nanorendszerekben (Equilibrium of Materials in macro, micro and nano systems). University of Miskolc, 2011.
- [2] Grétsy, L., Kemény, G. (szerk.): Nyelvművelő kézikönyvtár. Tinta Könyvkiadó, Budapest, 2005.
- [3] Planck, M.: "Über irreversible Strahlungsvorgänge. in: Proceedings of the Royal Prussian Academy of Sciences in Berlin, 5 (1899) 440-480.
- [4] Kaptay, G.: On the five base quantities of nature and SI (The International system of Units). JMM B, 47 (2011) p. 241-246.
- [5] The International System of Units (SI), 8th edition, 2006.http://www.bipm.org/utis/common/pdf/si_brochure_8_en.pdf.
- [6] Wieser, W. B., Coplen, T. B.: Atomic weights of the elements 2009 (IUPAC Technical Report). Pure Appl. Chem., 83 (2011) 359.
- [7] Gibbs, J. W.: On the Equilibrium of Heterogenous Substances. Trans. Conn. Acad. Arts Sci. 3, (1876-1878), p. 108-248 and 343-524.
- [8] Joule, J. P.: On the heat evolved by metallic conductors of electricity. Phil. Mag. 19 (1841) 160.
- [9] von Mayer, J. R.: Remarks on the forces of inorganic nature. Ann. Chem. Pharmac., 43 (1842) p. 233 (translated by Foster, G.C.: Phil Mag 24 (1862) p. 371)
- [10] Clausius, R.: Über die bewegende Kraft der Wärme und die Gesetze, welche sich daraus für die Wärmelehre selbst ableiten lassen. Ann. Phys. 79 (1850) 368.
- [11] Clausius, R.: Über die bewegende Kraft der Wärme und die Gesetze, welche sich daraus für die Wärmelehre selbst ableiten lassen II. Ann. Phys. 79 (1850) 500-525.
- [12] Nernst, W.: Über die Berechnung chemischer Gleichgewichte aus thermischen Messungen. Nachr. König. Gesellsch. Wissensch. Göttingen, Mat-Phys. Klasse I (1906) 1.
- [13] Planck, M.: Über neuere thermodynamische Theorien (Nernstsches Wärmetheorem und Quantenhypothese). Ber. Deutsch. Chem. Gesellsch. 45 (1912) 5.
- [14] Lupis, C. H. P., Elliott, J. F.: Correlation between excess entropy and enthalpy functions. Trans Met Soc AIME, 236 (1966) 130.

-
- [15] Kaptay, G.: On the tendency of solutions to tend toward ideal solutions at high temperatures. *Metall Mater Trans A*, 43 (2012) p. 531-543.
- [16] Lewis, G. N.: The osmotic pressure of concentrated solutions and the laws of the perfect solution. *J. Amer. Chem. Soc.* 30 (1908) p. 668-683.
- [17] Kaptay, G.: A new equation for the temperature dependence of the excess Gibbs energy of solution phases. *Calphad* 28 (2004) p. 115-124.
- [18] Kaufman, L., Bernstein, H.: *Computer Calculation of phase diagrams (with special reference to refractory metals)* - Academic Press, NY, USA, 1970.
- [19] Saunders, N., Miodownik, A. P.: *CALPHAD, a Comprehensive Guide*, Pergamon, 1998.
- [20] Lukas, H. L., Fries, S. G., Sundman, B.: *Computational Thermodynamics. The Calphad method*. Cambridge University Press, 2007, Cambridge, UK.
- [21] Yuan, X., Sun, W., Du, Y., Zhao, D., Yang, H.: Thermodynamic modelling of Mg-Si system with the Kaptay equation for the excess Gibbs energy of the liquid phase. *Calphad* 33 (2009) p. 673-678.
- [22] Kaptay, G.: On the size and shape dependence of the solubility of nano-particles in solutions. *Int. J. Pharmaceutics*, 430 (2012) p. 253-257.
- [23] Kaptay, G.: The Gibbs equation versus the Kelvin and the Gibbs-Thomson equations to describe nucleation and equilibrium of nano-materials. *J. Nanosci. Nanotechnol.*, 12 (2012) p. 2625-2633.
- [24] Roósz, A., Farkas, J., Kaptay, G.: Thermodynamics-based semi-empirical description of the liquidus surface and partition coefficients in ternary Al-Mg-Si alloy. *Mater Sci Forum*, 414-415 (2003) p. 323-328.
- [25] Mende, T., Roósz, A.: Calculation of the miscibility gap by Estphad method. *Mater Sci Forum*, 659 (2010) p. 423-428.
- [26] Kaptay, G.: The conversion of phase diagrams of solid solution type into electrochemical synthesis diagrams for binary metallic systems on inert cathodes. *Electrochimica Acta*, 60 (2012) p. 401-409.

EFFECTS OF STRONTIUM ON THE MICROSTRUCTURE OF AL-Si CASTING ALLOYS

ANETT KÓSA¹, ZOLTÁN GÁCSI², JENŐ DÚL³

^{1,2}University of Miskolc, Institute of Materials Science, 3515 Miskolc-Egyetemváros

³University of Miskolc, Department of Metallurgical and Foundry Engineering,
3515 Miskolc-Egyetemváros,

femanett@uni-miskolc.hu, femtangz@uni-miskolc.hu, ontdul@uni-miskolc.hu

The modification effect of Sr addition on the microstructure of Al-Si casting alloys (AlSi9Cu1 and AlSi9Cu3Fe) was investigated. The modification of eutectic in Al-Si casting alloys is a generally accepted process used primarily to improve mechanical properties by promoting the refinement of the inherently coarse and plate-like eutectic silicon phase. Furthermore, the combined effect of Sr addition and cooling rate was also studied in this paper because the microstructure of the eutectic is significantly affected by the cooling rate. The following measurements were used in this research: optical microscopy, measurement of secondary dendrite arm spacing, computer image analysis, scanning electron microscopy and electron microprobe analysis.

Keywords: Al-Si alloys, strontium, eutectic modification, cooling rate.

Introduction

Al-Si alloys are an important class of aluminum die casting alloys having wide ranging applications especially in the automotive industry, but even in the aerospace industry. The application area of an alloy is specified by the physical and mechanical properties of the casting, which are influenced by the chemical composition and microstructure. The two major microstructural components of the hypoeutectic Al-Si casting alloys are the primary α -Al solid solution dendrites and the Al-Si eutectic, therefore the mechanical properties mostly depend on the properties of these structural constituents [1–4].

The eutectic silicon crystallizes into a coarse, plate-like morphology during the formation of the eutectic, which is mechanically disadvantageous for the casting, because sharp corners concentrate stress, which can cause fracture during the use of the casting. The most commonly used modifier element is strontium because even a few hundred ppm of Sr can result a very fine, fibrous structure, furthermore it has a longer decay time than sodium. Strontium as a modifier element is added to Al-Si casting alloys to change this morphology, which causes a well-refined fibrous structure of the eutectic Si, thereby improving the mechanical properties of the casting [3–8].

The fine, fibrous eutectic structure can be achieved in two ways: either by the addition of modifying elements, such as Na, Sr or Sb; or by increasing the cooling rate, but in this case complete modification cannot be produced, thus the addition of modifier elements are essential [3–6].

1. Method

AlSi9Cu1 and AlSi9Cu3Fe low Sr containing alloys were used in the experiments. The alloys were melted in an electric furnace at 750 °C, as in industrial practice. Different amounts of Sr were added to the Al-Si alloys (Table 1) in the form of AlSr10 master alloy. After strontium addition an incubation time of 10 min was allowed. The alloys were poured into a thin cylindrical steel cup with a diameter of 30 mm (thermal analysis) and into a pre-heated (to 200 °C) permanent mould of tensile test rods with a diameter of 16 mm. Therefore the effect of the cooling rate was also investigated. The contents of Sr in testing samples were analysed by Spark Optical Emission Spectrometer and are listed in Table 1.

Casting series	Alloy	Samples	Calculated Sr, ppm	Analysed Sr, ppm
1.	AlSi9Cu1	1/1	20	11
		1/2	50	41
		1/3	100	115
		1/4	150	152
2.	AlSi9Cu3Fe	2/1	20	17
		2/2	50	45
		2/3	100	105
		2/4	150	171
		2/5	200	222
		2/6	250	326

Table 1. Concentration of strontium in test samples

2. Results and discussion

2.1. Effects of strontium and cooling rate on the microstructure

Figure 1 shows the effect of cooling rate on the microstructure, which is made much finer by applying rapid cooling. Secondary dendrite arm spacing (SDAS) was measured to define the cooling conditions with computer image analysis developed by the Department of Physical Metallurgy.

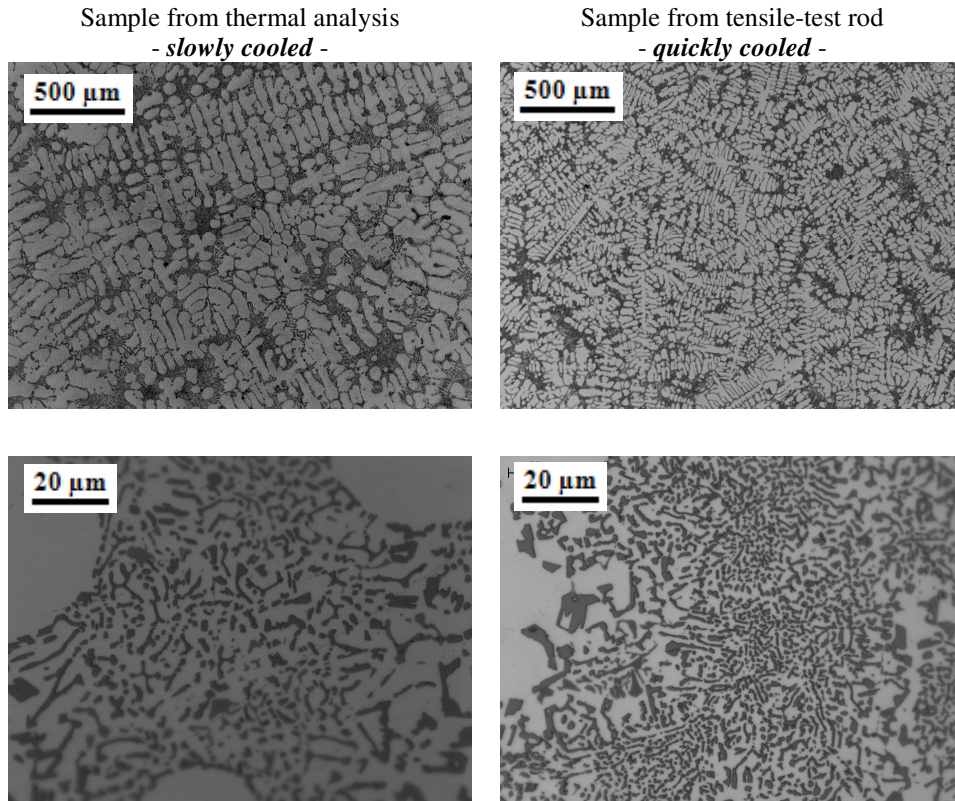


Figure 1. Effects of cooling rate on the microstructure of AlSi9Cu1 alloy containing 152 ppm Sr

The results (Table 2) show that there is an approximately two-fold difference between the SDAS of the samples from thermal analysis and from the tensile test rods, therefore this deviation works out to an eight-fold cooling rate difference by equation 1.

	SDAS, μm
Samples from thermal analysis (slowly cooled)	47
Samples from tensile test rods (quickly cooled)	23

Table 2. Average secondary dendrite arm spacing of the samples

$$SDAS = konst \left(\frac{dT}{dt} \right)^{\frac{1}{3}} \quad (1)$$

The micrographs of the quickly cooled samples (from the tensile test rods) and the slowly cooled samples (from the thermal analysis) of AlSi9Cu3Fe alloys are compared in Fig 2. In both cases the refinement of eutectic silicon induced by the strontium is clearly visible, and in the case of tensile test rods it can also be observed that the faster cooling rate results in an even finer eutectic microstructure at the same Sr level.

The microstructure of the additional samples was also examined, but significant differences in the extent of the modification cannot be observed in the samples containing more than 105 ppm Sr.

2.2. Quantitative metallographic characterization of eutectic Si particles by computer image analysis

The extent of the modification of the samples was quantified by three parameters – area, roundness and number of particles – which were measured with Leica computer image analysis. Figure 3 shows the change in these parameters depending on the strontium content. Solid lines show the change in the value of the slowly cooled samples from the thermal analysis and dashed lines show the quickly cooled samples from the tensile test rods.

It can be clearly seen that the average value of area (Figure 3a) and roundness (Figure 3b) of Si particles decreases, while the number of Si particles (Figure 3c) increases with increasing strontium content, so the eutectic becomes finer. Furthermore, it was observed that the modification effect is significant even at very low Sr content, and then it stabilizes at a specific value.

Due to the differences between the cooling conditions (thermal analysis and tensile test rods) the curves of the average area and number of Si particles are well separated from each other. The modification effect is more intensive for the quickly cooled samples. The deviation of the cooling conditions does not cause such large differences in the values of the roundness. The curves of the slowly cooled samples show that there is no change in the values of the average area of the Si particles above ~100 ppm Sr, where the area of the Si particles stabilizes at ~10 μm^2 , while the area of the Si particles stabilizes even at ~50 ppm Sr at the value of ~10 μm^2 for the quickly cooled samples. The value of the roundness stabilizes at ~2.5 for both Sr contents (50 and 100 ppm Sr).

The area of the Si particles decreases precipitously to ~50 ppm Sr content, which is made even steeper by the increase of the cooling rate, as can be seen from the shape of the curves. (Figure 3a)

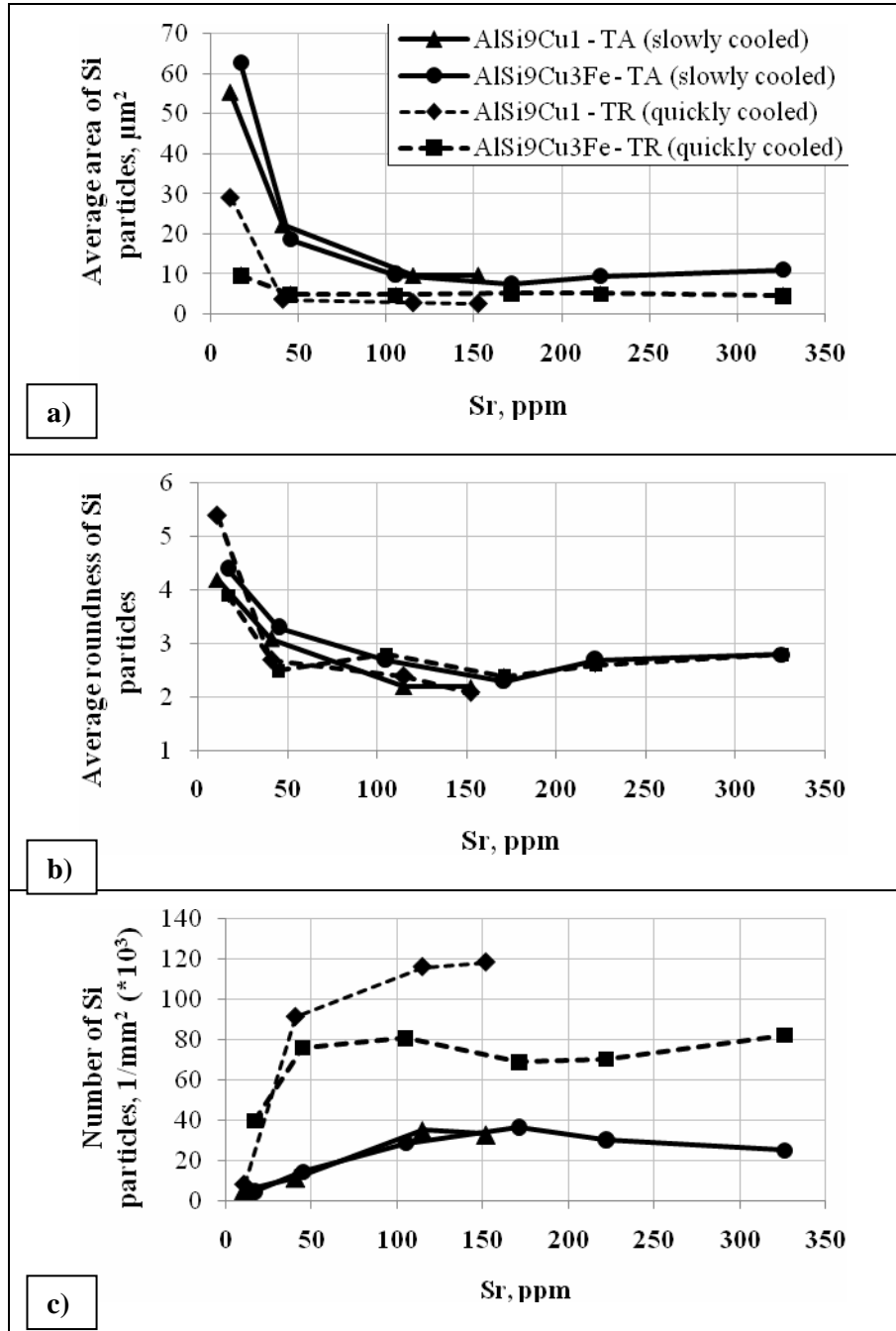


Figure 3. Effects of Sr on the parameters of the eutectic Si particles

2.3. Scanning electron microscopy and EDS analysis

A strontium-containing compound phase – probably $Al_xSi_ySr_z$ – was identified in sample 1/4 from AlSi9Cu1 alloy containing 152 ppm Sr (Figure 4), which is significant, because Sr bounded in compound does not expound the modification effect on the eutectic silicon. [9, 10] Oxygen was also measured in the sample, so the compound phase probably appeared in oxide form.

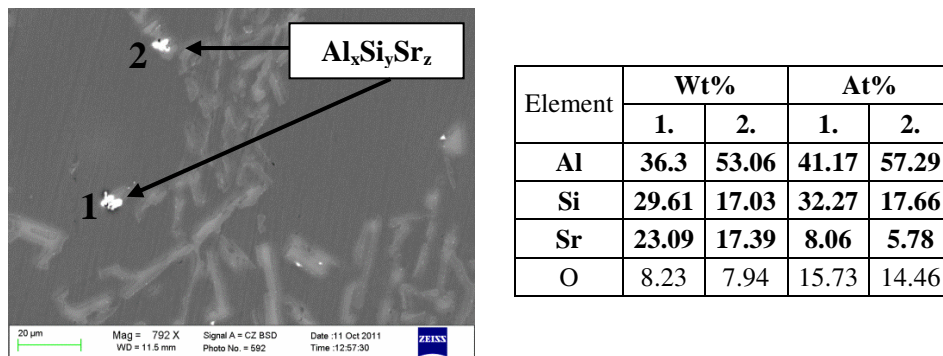


Figure 4. SEM image of the $Al_xSi_ySr_z$ IMC phases and their chemical composition

The sample containing 326 ppm Sr from AlSi9Cu3Fe alloy was also observed by SEM, but the strontium-containing compound could not be identified despite the higher concentration of Sr. The reason is that the AlSi9Cu3Fe alloy contains much more impurity elements, such as lead, which also appear white on the SEM images, so this makes it difficult to find the Sr-containing compound phases.

Conclusions

AlSi9Cu1 and AlSi9Cu3Fe casting alloys with different amounts of strontium addition were examined in this study. The combined effects of strontium and cooling rate were also investigated. The following conclusions can be drawn from the experimental results:

1. The increase of the cooling rate has a significant effect on the eutectic microstructure; the quicker the cooling, the finer the eutectic at the same strontium concentrations.
2. The modification effect of Sr is very intensive up to a certain value then stabilizes after reaching it. This value is 100 ppm in the case of the slowly cooled samples (from the thermal analysis), while it is 50 ppm for the quickly cooled samples (from the tensile test rod). Above these values further strontium addition does not cause further refinement of the Al-Si eutectic.
3. An $Al_xSi_ySr_z$ intermetallic compound phase was detected in the microstructure of the test sample containing 152 ppm Sr. The amount of strontium bounded in this compound is unable to participate in the modification process.

Acknowledgement

This research was carried out as part of the TÁMOP-4.2.1.B-10/2/KONV-2010-0001 project in the framework of the New Hungarian Development Plan. The realization of this project is supported by the European Union, co-financed by the European Social Fund.

References

- [1] Warmuzek, M.: Aluminum-Silicon Casting Alloys; Atlas of Microfractographs, ASM International, 2004.
- [2] Kaufman, J. G.; Rooy, E. L.: Aluminum Alloy Castings; Properties, Processes, and Applications; ASM International, 2004.
- [3] Dahle, A. K.; Nogita, K.; McDonald, S. D.; Dinnis C.; Lu L.: Eutectic modification and microstructure development in Al-Si Alloys, *Materials Science and Engineering A* 413-414, (2005), p. 243-248.
- [4] Chen, X.; Geng, H.; Li, Y.: Study on the eutectic modification level of Al-7Si Alloy by computer aided recognition of thermal analysis cooling curves, *Materials Science and Engineering A* 419, (2006), p. 283-289.
- [5] Shin, S-S.; Kim, E-S.; Yeom, G-Y; Lee, J-C.: Modification effect of Sr on the microstructures and mechanical properties of Al-10.5Si-2.0Cu recycled alloy for die casting, *Materials Science and Engineering A* 532, (2012), p. 151-157.
- [6] Sun, Y.; Pang, S-P.; Liu, X-R.; Yang Z-R., Sun G-X.: Nucleation and growth of eutectic cell in hypoeutectic Al-Si alloys, *Transactions of Nonferrous Metals Society of China* 21, (2011), p. 2186-2191.
- [7] Liu, L.; Samuel, A. M.; Samuel, F. H.; Doty, H. W.; Valtierra, S.: Characteristics of α -dendritic and eutectic structures in Sr-treated Al-Si casting alloys, *Journal of Materials Science* 39, (2004), p 215–224.
- [8] Zafir, M.; Mckay, B.; Schumacher, P.: Study of Heterogeneous Nucleation of Eutectic Si in High-Purity Al-Si Alloys with Sr Addition, *Metallurgical and Materials Transactions*, (2011), p. 1684-1688.
- [9] Gergely, G.; Gácsi, Z.: Characterization of the morphology of Si in the modified Al-Si alloys, *Materials Science Forum*, Vol. 649 (2010), p. 177-182.
- [10] Garay-Tapia, A. M.; Romero, A. H.; Trapaga, G.; Arróyave, R.: First-principles investigation of the Al-Si-Sr ternary system: Ground state determination and mechanical properties, *Intermetallics* 21, (2012), p. 31-44.

LOCAL SOCIETY AND THE BIOMASS PROJECT IN CSERNELY – THE IMPACT OF CONFLICTS BETWEEN ROMA AND NON- ROMA HUNGARIANS ON THE REALIZATION OF THE PROJECT

JÓZSEF KOTICS

Institute of Cultural and Visual Anthropology at University of Miskolc
3515 Miskolc-Egyetemváros
kotics.j@gmail.com

In my paper I focus on the patterns of living together from a historical point of view. By using Fredrik Barth's concept on ethnicity the focal point of my analysis are the situations in which the different ethnic groups associate. A special focus is given to the inner configuration of the Roma community of Csernely and also to the specific system of values and norms. The complex analysis of the narrative structures of Roma and Non-Roma living together is carried out in order to describe the different points of views, behavioral patterns and images of the other that exist in the village.

Keywords: Biomass project, patterns of living together, conflicts of the local society, the impact of conflicts on the project.

Introduction

In order to develop a model of biomass-based energy provision sufficient for completely or partially satisfy the heating energy needs of a given locality a multidisciplinary research team was formed at the University of Miskolc (engineers, sociologists, anthropologists, economists and jurists). The settlement chosen as the locality of the pilot project is situated halfway between Ózd and Szilvásvárad. The aim of the project in Csernely is to replace the heating energy system using natural gas with a system using renewable sources. The project also aims to create workplaces, to utilize currently not used lands and to create a settlement that is not only an energy user but also an energy provider [1]. The social scientific research focuses on risk management and conflict potential.

The applied anthropological research is based on the hypothesis that the simple description of the relations between the different groups of citizens at Csernely does not cover all the social and cultural aspects to be known for the success of the project. The biomass project includes a complex development plan the impact of which shall not only be understood in terms of economy, energy or labor market but also in terms of the relations between the citizens of the settlement. The impact of the project on the life of the local society is predictable.

In order to successfully realize the "Biomass Project" it is an absolute necessity to ensure that the local citizens are cooperative and accepting. The complex survey carried out at Csernely showed us that one of the strongest conflicts of the local society arise from the different lifestyles, values and norms of the Non-Roma and the Roma citizens the later being relatively new settler at the village. In my paper I focus on the patterns of living together from a historical point of view. By using Fredrik Barth's concept on ethnicity the

focal point of my analysis are the situations in which the different ethnic groups associate [2].

The patterns of living together in Csernely are developed by using the results of the survey and the qualitative interviews that were made. A special focus is given to the inner configuration of the Roma community of Csernely and also to the specific system of values and norms. The complex analysis of the narrative structures of Roma and Non-Roma living together is carried out in order to describe the different points of views, behavioral patterns and images of the other that exist in the village.

Based on the methodological findings of existing researches we claimed that there is a huge discrepancy between attitudes and actual behaviors. Therefore the quantitative data gained by the survey had to be completed by using qualitative methods (life interview, narrative biography).

In order to conceptualize the research question it is essential to describe the most important social aspects of the local society. In 1900 the village was inhabited by 1227 person. The number of citizens increased between the wars reaching 1474 by 1940. After the World War II the rate of increase slows down reaching its highest point at 1496 in 1960. From that time the village experiences a constant decline in number of citizens. In 1980 the number of inhabitants is 1292, while at the time of the collapse of the regime in 1989 it is only 1091. The decrease continues up to our times. According to the data given by the local government 800 people lived in the village in 2010, which means that, compared to the data of 1960, the number of inhabitants lessened by 50%.

The most important factor of decrease is the higher migration potential arising from the closing down of nearby mines, factories and plants. We can also observe a different reason for migration: the inhabitants with better education or higher degrees move to the urban areas. This process started during the time of the socialist modernization and continues today. Although it cannot balance the deficit, from the time of the collapse of the regime a inward migration can also be experienced in the village. This later is process is characterized by the arrival of settlers of different ethnic origin. Roma people from the neighboring village move in Csernely. At the beginning they used the state given social aid to purchase empty houses. Nowadays it is more and more common that they move in the empty houses arbitrary. After 1989 Dutch and Belgian families also bought properties in the village, but with the increasing number of Roma settlers, this process slowed down.

As a result of the migration three specific segments formed within the local society: mostly elderly non-Roma Hungarians living in single or two-person households, Roma people living in Csernely for generations and Roma newcomers arriving to the village in the last 10 years. The 50 Roma families make up 40 per cent of the total population. In the kindergarten there are only Roma children. The children of the non-Roma inhabitants attend elementary school in the nearby settlements. As a result the elementary school of Csernely had to be closed down two years ago.

According to the data on employment currently more than half of the inhabitants are inactive pensioners, most of the people in active age are unemployed only a few families have regular income. Since the first two decades of the 20th century the inhabitants of Csernely have been employed by the mining corporations or by the Iron Work Factory of Ózd. Beside a few families living from agriculture most of the families were employed by the heavy industry. Up to the 1980's the village experienced successful modernization with outstanding work opportunities, chances of gaining wealth and better social status. This era

is characterized by wealth and success in the reminiscences. The formerly prosperous village faces several problems now: aging population conflicts with the newcomers, outward migration of the younger generation and the local government being constantly in debt.

1. Narratives of the Roma and non-Roma Hungarian living together

In terms of time the narratives of the Roma and non-Roma Hungarian living together can be described as follows:

- The past in which the living together was absolutely ideal
- The present with all its conflicts
- The future that is lost for the local Hungarians

This narrative is characterized by the notions of decline, of devastation. According to the locals the formerly existing values got contested in the last 10-15 years. The reasons are obvious: in their point of view the closing down of mines and factories together with the arrival of Roma are causing the decline of the village. The most important attributes of the decline-narrative are: aging, rapid decay of living standards, future beyond recovery, disintegration of the local order, fear of everyday crimes, danger. The reason for all of these is the process of Gypsies moving in the village – the locals say. The social, existential problems of the village are understood as of ethnic conflicts.

Many times the narratives on Gypsies distinguish between Gypsies living in the village for generations and Roma newcomers. It is also true though that negative attitudes are expressed toward the Roma as a whole.

Beside the narrative of deprivation also the narrative of revival exists. The most important characteristic of the later is that it considers the recovery of the village as a possibility. The process is reversible; if certain circumstances and requirements are met the decline of the village becomes avoidable. In this view the natural environment of Csernely is a potential based on which a new future is possible. We have to add though that this new future excludes Gypsies. Mounted tourism, renovation of the Strumann mansion and the utilization of it, establishment of a local museum and the usage of alternative/renewable energy sources are the main elements of this new future. These suppose to help the village. According to this concept the “troublemaker” Gypsy families “who don’t like living in a village where there is order” will voluntarily move out. Others believe that the outward migration of the Gypsies would only speed up with the help of non-local financial resources.

The actual practical aspect of the narrative of revival is preventive and pro-active. Firstly, the further moving in of “troublemaker” Gypsy families should be prevented, together with the purchase or arbitrary occupation of empty houses. Some say that to prevent this the empty houses should be demolished. The pro-active dimension seeks to change the situation by making reasonable decisions. These include the creation of workplaces for the younger generation, the re-opening of the school, touristic developments, renovation of the mansion, and modernization of energy supply, to name just the most important ones.

2. The changing image of Gypsies

The locals of Csernely distinguish between two types of Gypsies living in the village. All the narratives formed around Gypsies are characterized by the categories of Gypsies living in the village for generations and newcomers. These categories have their own values added to them: the “normal” or “decent” Gypsies are old settlers, while the newcomers a “troublemakers”.

In terms of newcomers the mostly cited attributes are: their living conditions are frugal, they live on stealing and social aid, they are untrustworthy in terms of work, they are aggressive and lazy, they only accept a job when there is nothing else they can do. The devaluation of newcomer Gypsies legitimizes the negative attitude toward them [3]. Many times serious accusations are made against them. One for example is that they consciously provoke other locals or that incest is common among them. Such narratives obviously strengthen the stigmatization of the newcomers. The old settlers, e.g. Gypsies living in the village of generations, regard the newcomers with the same hostile attitude. The attributed stigmas are exactly the same and they distance themselves from the newcomers. According to the interviews they cannot even imagine having any relationship or contact with them.

In terms of the Gypsies living in the village for generations, the locals of Csernely formulate quite a different opinion. They believe that a different behavioral pattern is characteristic of this group. The words used to describe the old settlers are the total opposites of words describing the newcomers. Accordingly, the old settlers are decent, hard-working, clean, trustworthy, honest, etc. Ad hoc working relations are common with them. The locals were and are giving smaller loans to the old settlers, because they always give it back in time. These Gypsies are part of the local religious congregation, they are baptized and they participate at the funerals honoring the deceased.

Even among the old settlers there is one Roma family, let's call them the Z. family, with which the locals have more and more conflicts. They say that there were no problems with the grandparents, who accepted the norms and values of the major society and lived accordingly. Some of the children and most of the grandchildren though live a life that is unacceptable for the local society. The Z. family is regarded as the newcomers. This fact makes the image of local, old settlers a bit more complicated, because, as we've seen, one family falls into the category of “troublemakers”.

Some aspects of the ideally described Roma-Hungarian relationship of the past suggest asymmetries. The establishment and intensity of fictional kinship shall be interpreted by considering this. It was a common practice that the Roma families chose Hungarian godparents for their children. The collective memory does not preserve any case though in which a Hungarian family would have chosen Roma godparents.

One of the most obvious signs of the taboo of crossing certain social borders can be observed by looking at the question of mixed marriages [4]. Not a single case of mixed marriage existed before the last ten years. Both groups tend to insist on choosing a partner from his/her own group. Although the Gypsies regard mixed marriages as unfortunate but it is the reputation of the Hungarian family that is really harmed by such event. The rejection of mixed marriages shall be understood as a tool of preserving ethnic identities. It is interesting to take a look at the only mixed marriage of the village. One of the male members of an old settler Gypsy family married a Hungarian woman from a nearby village. Both families were against the marriage, the Hungarian parents expressively forbade it. The

bride's family didn't even participate the wedding, only time brought some acceptance. The Hungarian brother-in-law works with the Gypsy husband now and the later was really furious when telling us that his brother-in-law does not admit that they are relatives. The Hungarian bride was not welcomed in the Roma family either. They expected her to adapt to their customs, cultural traditions. Although the local non-Roma society is completely aware of the fact that the bride is a Hungarian from a neighboring village she is regarded as Roma because of her husband. Her husband coming from an integrated Roma family she has good and intensive relationship with the non-Roma locals but still the woman with two children is identified as Roma. The husband himself has an expressively Roma identity. For years he was an active member of the Roma Minority Council. On the contrary his family seeks assimilation. It is also proved by the fact that the sister of the husband chose a Hungarian man to marry, just like their cousins who live in the capital.

Their older son is seeing a Hungarian girl. For him the identification as Roma is offensive. Notwithstanding, the locals regard all members of the family as Gypsy. The Hungarian woman told us that when she applied for a job at the local school the headmaster turned her down because of being Roma. The stigmatization was made because of her being part of a Roma family. The obvious ethnic discrimination is contrary to the behavioral patterns applied in the interactions with Roma families living in the village for generations. Theoretically the locals accept the old settlers but in practice the behavior toward them is different.

The locals of the village still cannot forget the stealing of three bells from the local cemetery in 2008. One week prior to the theft there was the funeral of a local Gypsy man on which several Roma from the neighborhood were participating. One of the local Hungarians who has an intensive relationship with his Roma godchild now living in Budapest and also with the local old settler Roma people see a direct connection between the funeral and the theft. He supposes that the thieves were present at the funeral and that the plan of stealing the bells was actually formed when attending the event. It is out of question that the thieves were Gypsies, although the investigation was closed without any result. This example shows us that even the formerly positive experiences cannot prevent the emerging of a negative image of Gypsies. This image though is characterized mostly by attributes connected to the newcomers.

Earlier the image of Gypsies at the settlement was formed along the positive experiences of everyday living. Economic relations were not based on a patron and client type of relationship. During the socialism the local Gypsies worked as agricultural day laborers, but not in Csernely. Therefore the common pattern of patron and client relationship could not be formed here. The most important connection between the local Roma and non-Roma inhabitants was formed by fictional kinship.

Most of the local Roma were able to successfully adapt to the norms and values of the majority. During the socialist modernization their employment rate and their living conditions were similar to that of the non-Roma Hungarians in the village. Because of this successful integration the relationship between the two ethnic groups was characterized along social and not ethnic lines. The ethnic discrimination against newcomers, the interethnic tension and the general attitude toward the Gypsies show that things have changed nowadays. Today the living together of Roma and non-Roma Hungarians is mainly characterized by asymmetry. The most important aspect of the attitude toward the newcomer Gypsies is defined by devaluation, by the over-valuation of one's own ethnic

groups and by the common degradation of the others. The Hungarian majority adopted a model-like behavior toward Gypsies, which is characterized by keeping the distance and by social exclusion. The base of ethnic differentiation is the existential and moral superiority of the local Hungarians. Earlier this attitude was not common in Csernely. The reason for the changing attitude is that the “socialization” deficit of the newcomer Gypsies is balanced by the revaluation of one’s own ethnicity and culture. In the changing structures the earlier, traditional patterns of living together gradually lost their validity. Currently we experience the re-drawing of ethnic boundaries, the process of which is characterized by the re-definition of the notions ‘Gypsy’ and ‘non-Gypsy’. These notions and the differentiation are the practical tools to preserve the social stability for both groups.

3. The impact of conflicts between Roma and non-Roma Hungarians on the realization of the project

The survey carried out among the population of the settlement shows us the local viewpoints concerning the project. Positive attitude toward the Biomass project can be observed in all of the groups. We have to note though that a significant number of elderly non-Roma Hungarians did not want to participate in the survey. Most of the citizens regard the Biomass project as a necessity of the renewal of the village. Despite the lack of information on the project most members of the community believe that it will have a positive impact on the lives of the citizens.

By looking at the answers regarding the current status and possibilities of the village we have to say that most of the respondents are in a state of apathy and hopelessness. The answers have similar elements: irreversible aging of the population, constant thefts and burglaries, lack of public safety, closing of the school and the local government in the state of bankruptcy. According to the respondents the desperate situation is a consequence of the “massive settlement of Gypsies” in the village. It also means that the most important factors influencing the success of the project are the conflicts between Roma and non-Roma inhabitants. Non-Roma villagers believe that the realization of the biomass project is highly endangered by the new Roma settlers. Their lifestyles and everyday practices obstruct the project. The non-Roma villagers suppose that the thefts and dilapidations committed by new Roma settlers will endanger the infrastructure of the innovative development. The strict line between non-Roma Hungarians and non-native Roma settlers is observable both in terms of everyday life and in terms of the success of the project.

The growing proportion of new settlers regarded as “troublemakers” increases the potential conflicts while also strengthens the oversimplifying general concept of Roma people as the source of all problems. The trouble is that this concept obliterates the boundaries between the integrated, native Roma community and the physically and mentally also segregated new settlers. As a consequence, the distrust between the local Roma and non-Roma community grows, significantly endangering the feasibility of the innovation.

In addition to this, the tension between the local government and the new settlers also hinders the realization of the development. The idea of development connected to renewable energy was that of the mayor. He is the main supporter of the biomass project. Unlike the former mayor he does not run from the conflicts with the new settlers. One of

the most significant aspects of his leadership is indeed the acceptance of confrontation. As a consequence, he is really unpopular among the non-native Romas. Conflicts evoke strong emotions more and more frequently with some ethno-political overtone. The non-native Gypsy community regards the mayor and anti-Roma or racist, nonetheless the mayor has a good relationship with the native Roma community. Supposedly this underlying conflict will show itself also in the reception of the project. The new Roma settlers of Csernely will stand against everything and anything coming from or connected to the local government or the mayor himself, while the integrated native Roma community will support the project.

The most serious conflicts of the local society in the present day Csernely originate from the changing of formerly functioning practices of Roma and non-Roma living together. Therefore no significant development projects can be planned or initiated without carrying out a social and cultural feasibility study.

Acknowledgement

The described work was carried out as part of the TÁMOP-4.2.1.B-10/2/KONV-2010-0001 project. The realization of this project is supported by the European Union, co-financed by the European Social Fund.

References

- [1] SZEMMELVEISZ, TAMÁSNÉ, KOVÁCS, HELGA and KOÓS, TAMÁS: The Role of Biomass in the Heat Energy Supply of Small Towns. *A Miskolci Egyetem Közleményei, Anyagmérnöki Tudományok*, Miskolc, 36/1. 2011. 131-141. (In Hungarian)
- [2] BARTH, FREDRIK: *Ethnic Groups and Boundaries: The social organization of culture difference*. Universitetsforlaget, Oslo, 1969.
- [3] FOSZTÓ, LÁSZLÓ: Distress and labelling: economic, demographical and socio-cultural dimensions of the Gypsy-Hungarian relation. In BAKÓ, BOGLÁRKA (Ed.): *Local habitats. Living together in the Carpathian basin*. MTA Társadalomkutató Központ, Budapest, 2003. 83–107. (In Hungarian)
- [4] KOTICS, JÓZSEF: Integration or Segregation of Gypsies? (Case Study from Zabola, Háromszék, Romania) *Central European Political Science Review* Volume 7, Number 26. Winter (2006) 71-84.

DETERMINATION OF ANTIMICROBIAL ACTIVITY OF ESSENTIAL OILS AS ADDITIVES TO DEVELOP BIOLOGICALLY DEGRADABLE POLYMERIC PACKAGING

ÉVA KUN

University of Miskolc, Department of Polymer Engineering,
3515 Miskolc-Egyetemváros
polkebio@uni-miskolc.hu

Biodegradability and antimicrobial properties are also favourable in the food industry and the healthcare. Poly-lactic acid plasticized with essential oil can be promising packaging material. I evaluated the antimicrobial activity of some essential oils to select the best of them. Kirby-Bauer test and macrodilution test were chosen in order to verify the applicability of the EO's. However, marjoram, clary sage, juniper and rosemary were more effective, in contrast with the ginger oil. The diffusion rate of EO's in PLA is low, approximately 10^{-15} – 10^{-18} m²/s.

Keywords: biodegradable, PLA, antimicrobial, essential oil, MIC.

Introduction

There is a growing need for biologically degradable packaging materials with similar mechanical, optical and technological properties as the polyolefins as polyethylene, polypropylene or polystyrene. PLA (Poly-Lactic Acid) is the most popular plastic for this purpose, and its price is getting closer to the materials commonly used. In the food industry, packaging has to preserve the foodstuff. Many synthetic additives applied as preservatives in and around the food, which became obnoxious for the customers in the last few years, but they accustomed to the products with long shelf life. Essential oils are natural materials, their smell can be chosen to fit to the taste of food, for example marjoram, garlic can be used for meat, and lemon or cinnamon is suitable for fruity yoghurt or cake. The concentration which is able to get in touch with the food, very low, because of the slow migration in the polymer, so toxicity and displeasingly odor is hardly possible. Key question is the efficiency of the additives, so the minimum inhibitory concentration (MIC) is useful data for comparison of different agents. There are some methods for determining MIC. My choice was a scenic method called Kirby-Bauer test or with other name as Halo-test, and a more exact process called macro-dilution test. There is a huge range of biocides to use in a polymer matrix, as organic acids (citric acid, lactic acid, benzoic acid), organic salts (Na-lactate, Na-benzoate, Na-sorbate), inorganic materials (Ag-zeolite, Zn-oxide), bacteriocins (nisine), enzymes (lysozyme) or natural plant extracts. PLA has been compounded with nisine [1, 2, 3], silver-based nanoclay [4], propolys [5], and chytosan [6], while EO's have been tried with other matrix materials, for example for polypropylene [7] or edible films [8]. Diffusivity of thyme essential oil and its components was evaluated by Colomines et al. [9]. Minimum inhibitory concentrations can be measured by detecting the inhibition zones on an agar plate sprayed with microbes, as in the case of Kirby-Bauer test, the Stokes test and the E-test, or by making a dilution test, or by counting the number of cells on a foodstuff which is in contact with the agent [10, 11].

Materials and methods

The essential oils were obtained from Aromax Zrt. with a description about their composition. The applied EO's were marjoram (*Origanum majorana*), clary sage (*Salvia sclarea*), juniper (*Juniperus communis*), ginger (*Zingiber officinale*) and rosemary (*Rosmarinus officinalis*). The main components of EO's can be seen in the following (table 1).

Marjoram	Clary sage	Juniper	Rosemary	Ginger
terpinene-4-ol	linalyl-acetate	trans-anethole	eucalyptol	β -zingiberrene
cys-sabinene-hydrate	linalool	fenchone	camphor	curcumene
p-cymol	sclareol	chavicol	α -pynene	bysabolene
γ -terpynene	myrcene	1,8-cyneole	β -pynene	ginerol

Table 1. Major components of essential oils

For the attack, I chose from 3 type of microorganisms. I used two Gram positive bacterium (*Bacillus cereus*, *Staphylococcus aureus*), two Gram negative bacterium (*Escherichia coli*, *Pseudomonas aeruginosa*) and two yeast strains (*Sacharomyces cerevisiae*, *Geotrichum candidum*). *Bacillus cereus* is a bread spoilage bacterium which can produce endospores, so has an excellent surviving ability. The used *S. aureus* strain is a meticillin resistant type, which is very dangerous, and especially grows in hospitals. *E.coli* is the main indicator microbe of the fecal contamination. Not all of the *E. coli* is pathogen, many strains are useful in the intestinal flora. *Pseudomonas aeruginosa* can be found nearly everywhere in the nature, they are the first attacker of refrigerated meat products. *S. cerevisiae* is the normal baker yeast, which is good for bier, but bad contaminant in fruit juices. *G. candidum* has real hifa and artospores, and souring dairy products.

The materials I used to keep the colonies in the right conditions, were TGY (trypton-glucose-yeast) medium (generally used as count plate nutrient), MEE (completed meat nutrient) for *Bacillus*, BA (bloody agar) for the *S. aureus*, Luria-Bertani broth for the *Escherichia coli*, and MEA (malt extract agar) for the yeast cultures. Bacteria were incubated on 30 °C, while for yeasts I used a temperature of 28 °C. The dilutions of microbe suspensions were prepared with physiological salt dilution.

As nutrient, for the Kirby-Bauer test, I used Mueller-Hinton agar plate and sterile cellulose disks with a diameter of 6 mm. For the test solvents, DMSO was used with 50v/v% concentration in distilled water, for the process I used Widal tubes and pipettes (10 μ l-1000 μ l). The concentrations were made by median dilutions from 2 to 0.0625 μ l/ml. A microbe suspension with a 0.5 McFarland (approximately 10⁴ cells/0.1 ml) was streaked by glass rod and turning three times with 60°. The colonies were leaved to relax for 2 hours in incubator, while I impregnated the solvents into the cellulose disks. After I placed the disks on the agar plates, they were incubated at 37 °C for 24 hours before reading results. If the concentration of the essential oil is enough to prevent the microbial growth, clear inhibitory zones can be seen on the agar plates around the impregnated cellulose discs. The diameter of the inhibitory zones has to be callipered. The MIC (minimum inhibitory concentration) is

the lowest concentration of an antimicrobial agent that can inhibit the visible growth of a microorganism after overnight incubation.

For the dilution test, the same dilution scale was used as in the case of the Kirby-Bauer test. I pipetted 1 ml of the essential oil solutions and 100 μ l stock solutions into Widal tubes, so each tube contained 10^6 cells/ml. After incubating overnight (24 hours) I poured agar plates from 1-1 ml of each liquid in sterile Petri dishes. I checked the number of the colony forming units in the plates after 24 and 48 hours incubation at 37 °C. There was a difference in the CFU/ml (colony forming unit / 1 ml test solution), as the samples contained enough concentration of essential oils to reduce microbial growth, produced less microbial colonies than the standard sample (without essential oil). The MIC is given in μ l/ml, where I mean the minimum inhibitory amount of essential oil (μ l) in 1 ml solution containing originally approximately 10^6 microbe cells.

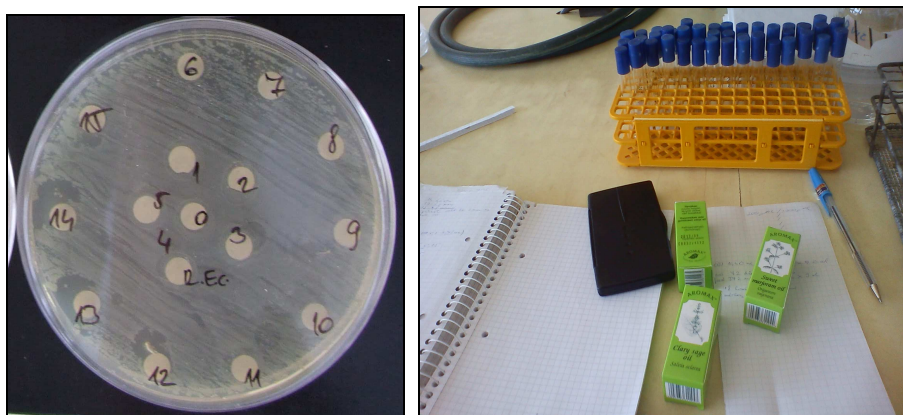


Figure 1. Kirby-Bauer test on Mueller-Hinton agar plate with *E. coli* and Rosemary oil (left), essential oils and their dilutions in Widal tubes (right)

Results

The two test gave coherent results, but the efficiency is much lower in the case of the agar-diffusion (Kirby-Bauer) test. The results of the dilution method are shown below in the Table 2.

Microorganism		Code	<i>Origanum majorana</i> (marjoram)	<i>Salvia sclarea</i> (clary sage)	<i>Zingiber officinale</i> (ginger)	<i>Juniperus communis</i> (juniper)	<i>Rosmarinus officinalis</i> (rosemary)
<i>S. aureus</i>	(Gram + bact.)	ATCC 43300	>	0,29	>	0,5	0,375
<i>Bacillus cereus</i>	(Gram + bact.)	ATCC 14579	0,375	2,0	0,375	0,375	>
<i>Escherichia coli</i>	(Gram – bact.)	ATCC 25922	0,375	0,0625	>	2,0	0,0625

Microorganism		Code	Origanum majorana (marjoram)	Salvia sclarea (clary sage)	Zingiber officinale (ginger)	Juniperus communis (juniper)	Rosmarinus officinalis (rosemary)
P. aeruginosa	(Gram – bact.)	ATCC 13880	0,75	0,5	>	0,375	0,35
Sacharomyces cerevisiae	(Yeast)	ATCC 24859	0,375	0,75	>	0,0625	0,75
Geotrichum candidum	(Yeast)	ATCC 66592	0,75	0,5	>	0,5	2

Table 2. MIC of EO's in µl/ml

The essential oils were active against the chosen microorganisms. The essential oil of ginger is weak antimicrobially, so it is not promising as an additive of a food packaging plastic material. Marjoram oil is the best one, but doesn't inhibit the growth of *S. aureus*. Rosemary oil is efficient against *E. coli* and *P. aeruginosa*.

Conclusions

Ginger essential oil is not effective enough to work with that in the future during the research work. The other 4 oils had good activity, and it would be promising to evaluate the efficiency of their main components separated. However, juniper is a very strong antimicrobial agent, possibly it will not be applied in the food industry for packaging because of its taste. The other three essential oils, marjoram, clary sage and rosemary are promising agents.

Acknowledgement

The research work is supported by TÁMOP 4.2.1.B-10/2/KONV-0001-2010.

References

- [1] Jin, Tony: Inactivation of *Listeria monocytogenes* in skim milk and liquid egg white by antimicrobial bottle coating with polylactic acid and nisin. *Journal of Food Science*, 75, (2010) p. M83-M88.
- [2] Jin, T.; Zhang, T.: Biodegradable polylactic acid polymer with nisin for use in antimicrobial food packaging. *Journal of Food Science*, 73, (2008), p. M127-M134.
- [3] Jin, T.; Zhang, H.; Boyd, G.: Incorporation of preservatives in polylactic acid films for inactivating *Escherichia coli* O157:H7 and extending microbiological shelf life of strawberry puree. *Journal of Food Protection*, 73, (2010), p. 812-818.
- [4] Busolo, M. A.; Fernandez, P.; Ocio, M. J.; Lagaron, J. M.: Novel silver-based nanoclay as an antimicrobial in polylactic acid food packaging coatings. *Food Additives and Contaminants: Part A: Chemistry, Analysis, Control, Exposure and Risk Assessment*. 27, (2010), p. 1617-1626.

-
- [5] Mascheroni, E.; Guillard, V.; Nalin, F.; Mora, L.; Piergiovanni, L.: Diffusivity of propolis compounds in Polylactic acid polymer for the development of anti-microbial packaging films. *Journal of Food Engineering*, 98, (2010), p. 294-301.
 - [6] Suyatma N. E.; Copinet, A.; Tighzert, L.; Coma, V.: Mechanical and Barrier Properties of Biodegradable Films Made from Chitosan and Poly (Lactic Acid) Blends. *Journal of Polymers and the Environment*, 12., (2004), p. 321-334.
 - [7] López, P.; Sánchez, C.; Battle, R.; Nerín, C.: Development of flexible antimicrobial films using essential oils as active agents. *Journal of Agric. and Food Chemistry*, 55, (2007), p. 8814-8824.
 - [8] Seydim, A. C.; Sarikus, G.: Antimicrobial activity of whey protein based edible films incorporated with oregano, rosemary and garlic essential oils. *Food Research International*, 38, (2006), p. 639-644.
 - [9] Colomines, G.; Domenek, S.; Ducruet, V.; Guinault, A.: Influences of the crystallisation rate on thermal and barrier properties of polylactide acid (PLA) food packaging. *International Journal of Material Forming*, 1., (2008), p. 607-610.
 - [10] Lambert, R. J. W.; Skandamis, P. N.; Coote, P. J.; Nychas, G.-J. E.: A study of the minimum inhibitory concentration and mode of action of oregano essential oil, thymol and carvacrol. *J. Appl. Microbiol.*, 91, (2001), p. 453-462.
 - [11] Tserennadmid, R.; Takó, M.; Galgóczy, L.; Papp, T.; Pesti, M.; Vágvölgyi, Cs.; Almássy, K.; Krisch, J.: Anti yeast activities of some essential oils in growth medium, fruit juices and milk. *International Journal of Microbiology*, 144, (2011), p. 480-486.

NEW FORM OF WIND ENERGY UTILIZATION

ALEX NEMES, HELGA KOVÁCS

University of Miskolc, Department of Combustion Technology and Thermal Energy
3515 Miskolc-Egyetemváros
alex.nemes@europa.com

At a time of growing concern over the rising costs and long-term environmental impacts of the use of fossil fuels and nuclear energy, wind energy has become an increasingly important sector of the electrical power industry, largely because it has been promoted as being emission-free and is supported by government subsidies and tax credits. The first wind turbines for electricity generation had already been developed at the beginning of the 20th century. The technology was improved step by step since the early 1970s. These equipments usually operate optimally only in a narrow wind speed range. The energy of the wind outside this range remain useless. Hungary is less fortunate according to wind energy utilization. The average wind speed is low, the intensity and direction of the usable winds are variable. In 2009, a Hungarian inventor Dénes Kókai, presented another way to convert the kinetic energy of the wind into mechanical energy. In this paper we examine the possibilities of the new invention according to small scale energy generation in underprivileged settlements.

Keywords: renewable energy, wind turbine, Hungarian innovation, “energy-bosun”.

Introduction

A society, which energy needs are based on local sources, is more likely sustainable than an import fuel based one, since most country prefer their own needs before export. Therefore using local energy sources should be primary interest in all terms. Among renewables, biomass is the most typical source. Beside locally grown energy plants, wind energy is also an emerging field. One should install a wind turbine in such a place where we already have done the necessary measurements e.g.: wind speed, typical wind direction and weather circumstances. These measurements usually took several months or years, or we can use weather observations on the designated area to make approximate ROI calculations.

Wind energy is non-polluting and is freely available in many areas. Wind turbines are becoming more efficient. The cost of the electricity they generate is falling. Large balancing areas and aggregation benefits of large areas help in reducing the variability and forecast errors of wind power as well as in pooling more cost effective balancing resources [1]. There are already several power systems and control areas coping with large amounts of wind power [2], like in Denmark, Germany, Spain, Portugal and Ireland that have integrated 9-20% of wind energy (of yearly electricity demand). Figure 1 shows the typical wind speeds in the European regions.

The worldwide energy demand is continuously growing and, according to the forecasts of the International Energy Agency, it is expected to rise by approx. 50% until 2030. Currently, over 80% of the primary energy demand is covered by fossil fuels [3]. Although their reserves will last for the next decades, they will not be able to cover the worldwide

energy consumption in the long run. In view of possible climatic changes due to the increase in the atmospheric CO₂-content as well as the conceivable scarcity of fossil fuels, it becomes clear that future energy supply can only be guaranteed through increased use of renewable energy sources. With energy recovery through renewable sources like sun, wind, water, tides, geothermal or biomass the global energy demand could be met many times over; currently, however, it is still inefficient and too expensive in many cases to take over significant parts of the energy supply [4]. Their further expansion is certain now that the European Union has laid down ambitious and binding targets. These state that by 2020 renewable energies are to account for as much as 20% of Europe's energy consumption. These targets focus attention not only on the electricity sector, but also on the use of renewable energy sources in heat production and in the transport sector [5]. Due to the usual adaptation reactions on the markets, it is foreseeable that prices for fossil fuels will rise, while significantly reduced prices are expected for renewable energies. Already today, wind, water and sun are economically competitive in some regions. However, to solve energy and climate problems, it is not only necessary to economically utilize renewable alternatives to fossil fuels, but also to optimize the whole value added into the chain of energy, i.e., from development and conversion, transport and storage up to the consumers' utilization [5].

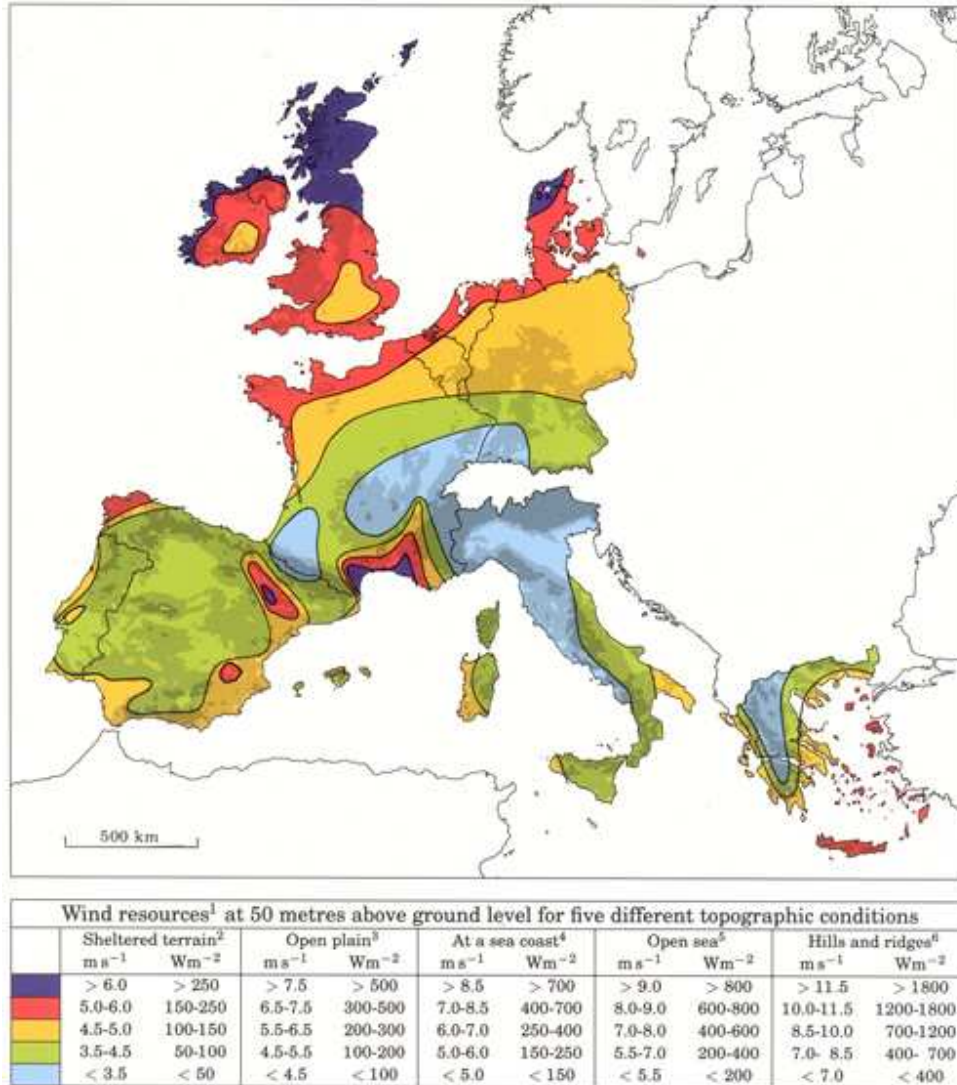


Figure 1. Wind speed in different regions of Europe [6]

As the classical definition says, the wind turbine is an equipment which convert the kinetic energy of the wind into mechanical energy by the use of vanes. This motion energy can be used to pump water, grind grain or it can be turned into electricity with a generator. The most known wind turbine type is the one called horizontal axis wind turbine (HAWT). The other kind of turbine family is the vertical axis wind turbine (VAWT), which has many different forms, such as darrieus, savonius and giromill.

GWEC's annual market update on the status of the global wind industry is the authoritative source of information on wind power markets around the world. It provides

you with a comprehensive snapshot of the global industry [7]. In 2011 the installed wind capacity reached above 40.000 MW (Figure 2.).

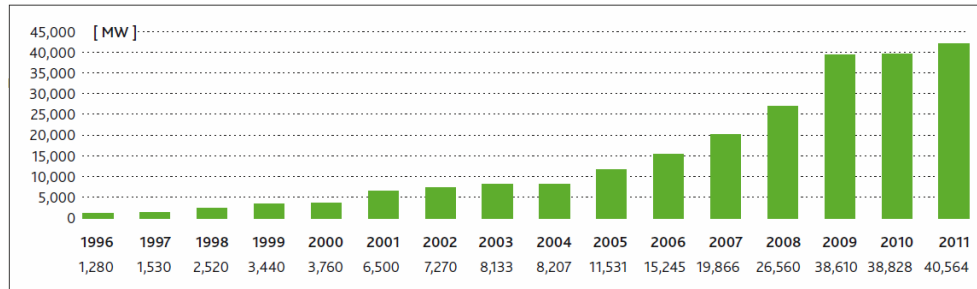


Figure 2. Global annual installed wind capacity 1996–2011
Source: Global Wind Energy Council [8]

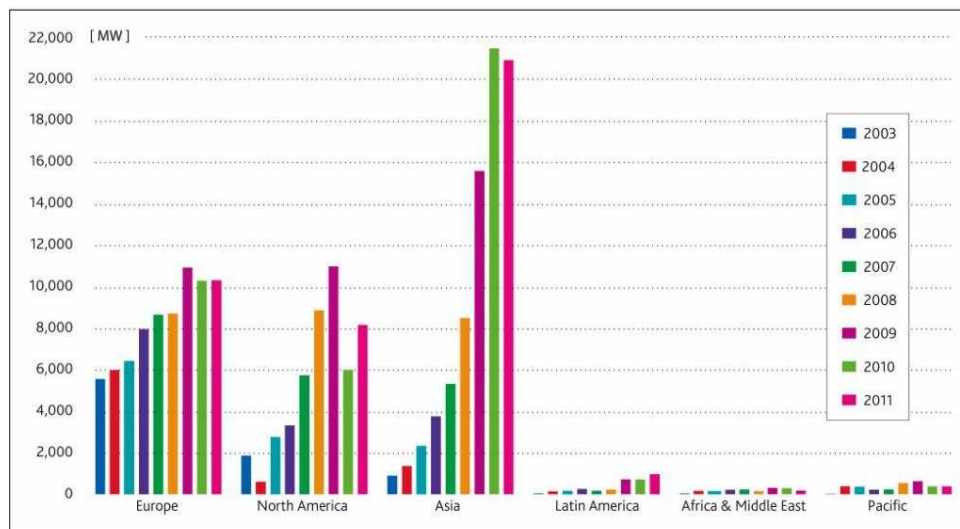


Figure 3. Annual capacity by region 1996–2011
Source: Global Wind Energy Council [8]

There is huge and growing global demand for emissions-free wind power, which can be installed quickly, theoretically everywhere in the world (Fig. 3.). China determines the energy growth of the Asian region. In 2011 wind power in the People's Republic of China accounted for 62 gigawatts (GW) of electricity generating capacity.

1. The invention

Nowadays there are many different devices which can convert the kinetic energy of the wind, to some other form of energy. These equipments usually operate optimally only in a

narrow wind speed range. The energy of the wind outside this range remain useless. Hungary is less fortunate according to wind energy utilization. The average wind speed is low, the intensity and direction of the usable winds are variable. This „usable” wind force represents a speed between 4 and 9 m/s (15-30 km/h), and its carries about 20 to 120 kWh/m² energy. Only a few percent of this energy is used by wind turbines.

So far we had two different types of wind turbines to plan with. In 2009, a Hungarian inventor Dénes Kókai, presented another way to convert the kinetic energy of the wind into mechanical energy.

The working model presented in many exhibitions has a 21x16 cm front surface. It can generate 0,24W of electric power on 18 Hz, at wind speed of 16 km/h. These numbers show its efficiency at low wind speed compared to other wind turbines.

1.1. Purpose of the new equipment

The purpose of this invention is to come up with an alternative solution beside the other wind turbines on the market. The main part of the equipment is a sail like surface, which orientation is parallel to the wind direction. The concept of operation is different from the well-known wind turbines. The vanes of a vertical or a horizontal axis wind turbine rotates clockwise or counter-clockwise, and it's driven by vectorial forces. The invention uses the wind pressure parallel to the moving surface. The motion of this surface is supply a generator which generates electricity.

The basic idea of the innovation is to force the wind through an opening, which is perpendicular to a large surface (Figure 4.). The wind pressure moves a flexible plate inside the equipment. This movement is turned into electricity by an attached generator. According to the inventor, the device can use lower wind speeds than the classical wind turbines. He presented the equipment with success, and won prices on many exhibitions, in Budapest, Zagreb, Nuremberg, Seoul in Korea.



Figure 4. The prototype of the equipment

Three main areas to cover with the new device:

- using the kinetic energy of rivers,
- an alternative for wind turbines,
- satisfy local energy needs at pipelines.

1.2. Operation principles

The prototype dimensions are: 150 by 150 cm, its surface cover 2,25 m² (see the picture above), its weight less than 15 kg. At average wind speed it produces 70-100 W of electric energy.

A large surface is needed in order to operate the equipment efficiently. A surface of these wind turbines should be made of several modules. There are two types of „energy-bosun” available (with surfaces of 2,25 m² and 4m²). According to the inventor, 5-6 modules can cover the electricity needs of an average family. The cost of this investment would be about 3300 €. (1 million HUF) Maintenance and operational costs are minimal, like in the case of the most wind turbines.

The air flow in the equipment is laminar, the flow direction is straight. The turbulent zone after the outlet of the turbine is not typical, unlike in the case of HAWTs, therefore many „energy-bosun” can be planted after each other.

The equipment stays in operation at every wind speed. The moving surface in the device opens by the wind pressure. At low wind speed the air passes through a narrow opening, and it opens further at higher wind speed.

For example, an „energy-bosun” which is optimized to a 40 km/h average wind speed, opens its air flow surface only 5% at 2 km/s wind speed. The same turbine opens 50% at wind speed of 20 km/h. The upcoming product will be installed in different sizes.

The movement is controlled by a main-valve, which is attached to a flexible plate. This plate splits the flow zone into two separated segments (Figure 5.). The speed of the air flow can be parted in three sections, these are the followings: accelerating phase, stopped stage and slowing phase. The speed of the air is increasing behind closing main-valve, and slowing behind the opening part. Since there is only one valve, which separates the zone, these flows are created in opposite sides of the moving surface. The valve closes the way of the air flow at the end position, therefore static pressure occurs on the surface of the flexible plate. This pressure forces the plate to move towards the other end point, where the wind pressure creates the same event. This alternating pressure change moves the flexible plate as a membrane.

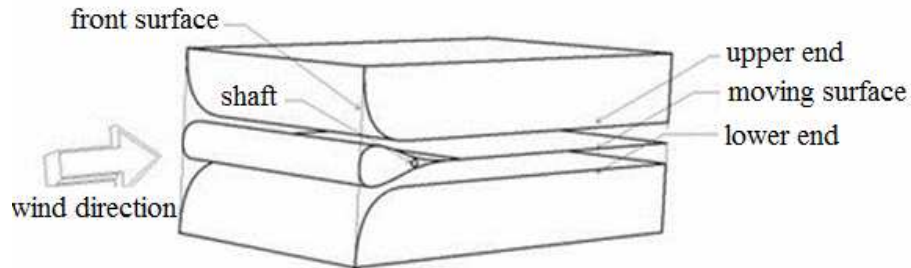


Figure 5. Structure of the invention

1.3. Advantages of the invention

The invention has many advantages compared to classical wind turbines. Horizontal axis wind turbines cannot operate close to each other in an efficient way. They needed to be parted at least 3-5 times by their diameter because the turbulent flow they generate. One can install the new devices close to each other, to cover a large surface such as a parking building or a flat-roof. The invention can also be used in big storms, which could be harmful to other kind of wind turbines.

2. Using the “energy-bosun” in underprivileged settlements

In Hungary wind energy utilization in small settlements are not prevalent. People choose solar cells or solar collectors instead of wind turbines if they want to invest in renewables. The average wind speed in Hungary is lower than the starting speed of the most wind turbines. The “energy-bosun” could be an alternative solution instead of other kind of wind turbines in domestic use. In the case of small settlements at a disadvantage, this invention could help to satisfy only the local energy needs.

Our department took part in a project, which goal was to make an alternative energy producing system for small settlements like Csernely. We began to investigate if this area is suitable for wind energy utilization as a part of this work. In order to determine the prevailing wind speeds, an anemometer (Figure 6.) had been installed at one of the highest point of the village, which area is suitable for placing wind turbines. These measures needed to forecast the energy producing ability of a wind turbine.



Figure 6. Davis Vantage Vue anemometer, and wireless data recorder

The signal sending frequency of the anemometer sensor (Figure 6.) is 2,5 seconds. The internal wireless device collects the registered wind data in half hour periods, which later can be saved to a computer via USB port.

Results

We processed data from the 23th of March, to the 19th of April in 2012. The Table 1 summarizes and the Figure 7 shows the gathered information.

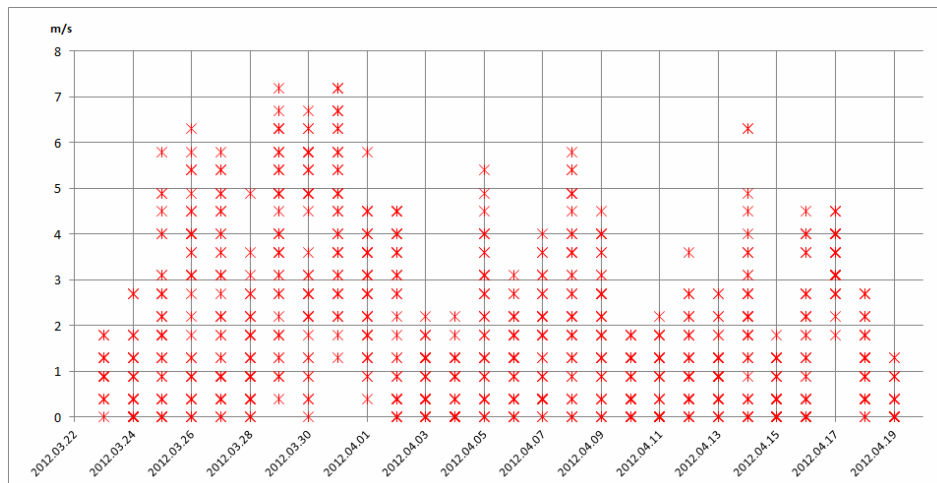


Figure 7. Distribution of wind speed (2012.03.23. – 2012.04.19.) half hour periods

The Figure 7 shows the average wind speeds during the measured interval. A red star represents the average of a half hour period that is calculated by the data register. The density of the stars shows the amount of data in the same spot.

Date	Max. temperature [°C]	Min. temperature [°C]	Average wind speed [m/s]	Biggest squall [m/s]
23/03/2012	19,5	4,7	0,97	6,3
24/03/2012	19,2	4,8	0,67	6,3
25/03/2012	20,6	2,2	1,77	12,1
26/03/2012	12,5	3,3	2,56	13,4
27/03/2012	15,4	-4	2,24	12,1
28/03/2012	17,7	0,9	1,31	11,2
29/03/2012	16	6	3,93	16,5
30/03/2012	10,9	4,2	3,66	16,1
31/03/2012	12,2	5,1	4,46	15,2
01/04/2012	8	-1,1	2,81	11,6
02/04/2012	12,2	-3,3	2,14	10,3
03/04/2012	18,8	4,3	0,76	5,8
04/04/2012	19,7	7,2	0,5	6,3
05/04/2012	19,7	5,2	1,96	9,81
06/04/2012	18,3	9	1,22	6,3
07/04/2012	15,7	4	1,45	8
08/04/2012	7,8	1,1	2,55	12,1
09/04/2012	7,8	-1,3	1,95	9,4
10/04/2012	11,6	-4,9	0,7	6,3
11/04/2012	17,1	-2,9	0,67	6,3
12/04/2012	13,4	4,9	1,02	8
13/04/2012	16,4	2,7	0,92	5,8
14/04/2012	13,8	7,4	1,95	12,5
15/04/2012	14,1	8,4	0,48	3,6
16/04/2012	15	6,1	1,45	8
17/04/2012	12,6	6	3,41	8,9
18/04/2012	10,6	4,8	1,14	6,3
19/04/2012	14	4,3	0,35	4,5

Table 1. Summarized weather data in 28 days

It can be seen in Table 1. that the biggest squalls reach 16 m/s, but the daily average wind speed is under 4,5 m/s. The average wind speed in the measured period is 1,75 m/s, therefore the energy producing capacity of a wind turbine installed would be low.

3. Conclusions

Based on the gathered data, it can be stated that the average wind speed in the surroundings of the settlement is not sufficient for installing classical wind turbines. On the other hand the new invention called the “energy-bosun” maybe suitable for energy production at these wind conditions. The anemometer is still gathering the data on the site,

so in 2-3 month time we will have sufficient amount of data to make accurate calculations for a possible investment.

Acknowledgment

The described work was carried out as part of the TÁMOP-4.2.1.B-10/2/KONV-2010-0001 project. The realization of this project is supported by the European Union, co-financed by the European Social Fund.

References

- [1] H. Holttinen, H. P. Meibom, A. G. Orths, B. Lange, M. O'Malley, J. O. Tande, A. Estanqueiro, E. Gomez, L. Söder, G. Strbac, J. C. Smith, and F. V. Hulle: Impacts of large amounts of wind power on design and operation of power systems, results of IEA collaboration. Proceeding of 14th Kassel Symposium on Energy Systems Technology, Kassel, Germany, 7-24, 2009.
- [2] L. Söder, L. Hofmann, A. G. Orths, H. Holttinen, Y. H. Wan, and A. Tuohy. Experience from wind integration in some high penetration areas. IEEE Transactions on Energy Conversion, 22(2):4-12, 2007.
- [3] Mohamed Hassan Ahmed Mohamed: Design Optimization of Savonius and Wells Turbines, Dissertation zur Erlangung des akademischen Grades, Otto-von-Guericke-Universität Magdeburg, 2011.
- [4] MESA+ Institute for nanotechnology – University of Twente, <http://www.utwente.nl/mesaplus/nme/Introduction/>
- [5] M. V. Mark and W. Dürschmidt. Electricity from renewable energy sources. Federal Ministry for the Environment, Nature Conservation and Nuclear Safety (BMU), Berlin – Germany April, 2009.
- [6] European Wind Atlas. Copyright © 1989 by Risø National Laboratory, Roskilde, Denmark
- [7] Global Wind Report 2011, GWEC's Annual Market Update launched at EWEA 2012, Copenhagen
- [8] Global Wind Energy Council: Global wind report, annual market update, 2011. http://www.gwec.net/fileadmin/documents/NewsDocuments/Annual_report_2011_lowres.pdf

ANNEALING HEAT TREATMENT OF 17% Cr FERRITIC CAST STEEL

**JÓZSEF PARTI, VALÉRIA MERTINGER, MÁRTON BENKE,
DÁVID CSEH**

University of Miskolc, Institute of Materials Science
3515 Miskolc-Egyetemváros
femvali@uni-miskolc.hu

Automotive castings are predominantly produced of ductile irons and compacted graphite irons. These materials satisfy the requirements of the automotive companies for a long time. The evolving environmental requirements tend to decrease the pollutant emission and to decrease the petrol consumption demand changes in the applied materials as well. The present examination is dealing with the heat treatment of a Cr alloyed ferritic stainless steel developed for die casting. The aim of the heat treatment is to decrease the hardness of the as-cast semi-product according to the requirements of the subsequent machining. The effect of the heat treatments with different times and temperatures were examined through structure examinations and hardness measurements.

Keywords: cast ferritic stainless steel.

Introduction

High Cr and Ni content steels are widely used in many manufacturing processes in the chemical and petrochemical industry. The automotive industry has also recognized the necessity of heat resistant alloys for a long time, for example, to apply them to exhaust systems to endure thermal loading and oxidation during the operation of engines. Various heat resistant alloys such as cast irons, stainless steels, and Ni-base superalloys have been considered as candidate materials of automotive exhaust systems [12]. Among those candidates, ferritic stainless steels attracted a lot of attention due to their favorable mechanical strength and corrosion resistant properties. Currently they are the leading engineering materials in several fields of applications that require resistance to wear, corrosion [1, 2], creep or thermal fatigue [7]. The high corrosion resistance of these steels is due to alloying elements such as Cr, Ni and Mo. Chromium is the basic alloying element added to iron to obtain passivity and does so when it is added in the amount of or greater than 17% (w/w%). The addition of a low Ni content (max 3 %) seems to be an important alternative to improve the mechanical properties. The presence of the low amount of Ni in the ferritic microstructure is beneficial to increase the notch-toughness [3, 4] and to decrease the ductile-to-brittle temperatures and yield strength of the ferritic matrix. The ferritic stainless steels cannot be hardened by heating and quenching such as the austenitic stainless steels. If the ferritic stainless steels are alloyed with strong carbide-forming elements, such as Mo, Ti, V and Nb, hard phases, MC carbides can be obtained in the soft ferrite phase [5, 6]. The improvement of the properties of Fe–Cr–Ni cast steels is directly related to the development of the microstructure, which mainly consists of a ferritic matrix and carbides and/or dispersed intermetallics [8]. The improvement is not always the

hardening. The hardness is usually limited by the casting and the subsequent machining, so an annealing process is inserted.

Annealing heat treatments for different cast structures were performed to get the proper structure and hardness after the casting and before the machining.

Experimental

The examined alloy contains W as well compared to the standard quality 1.4740 W (Table 1.). The alloying elements are mainly ferrite and carbide forming elements. The role of the Ni is to increase the corrosion resistance. The heat treatments were performed on samples with dimensions 15x15x15 mm machined from the cast semi-products, so the effect of inhomogeneity of the microstructure was also possible to examine. 3 or 4 samples were taken from different locations of one cast semi-product. The cast structures were always examined before the heat treatments.

C	Si	Cr	W	Ni	Mn	Mo	Nb
0.3-0.45	1.0-1.7	17-20	1.5-2	Max 0.9	Max 0.8	Max 0.5	Max 0.6

Table 1. The composition of alloy 1.4740, w/w%

The temperatures of the annealing heat treatments were determined based on the intersection of the Fe-Cr-C ternary phase diagram at C = 0.4%; considering to modify only the carbide phase and to avoid any allotropic transformation of the matrix during the annealing. The Cr content of the alloy and the selected isotherms (800, 850, 900 °C) are shown in Fig. 1. The lengths of the heat treatments were 0.5 and 2 hrs. for every sample.

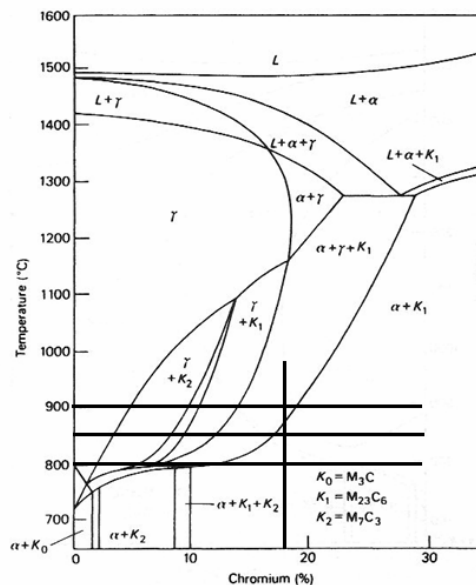


Figure 1. The intersection of the Fe-Cr-C phase diagram at C = 0.4 % [9]

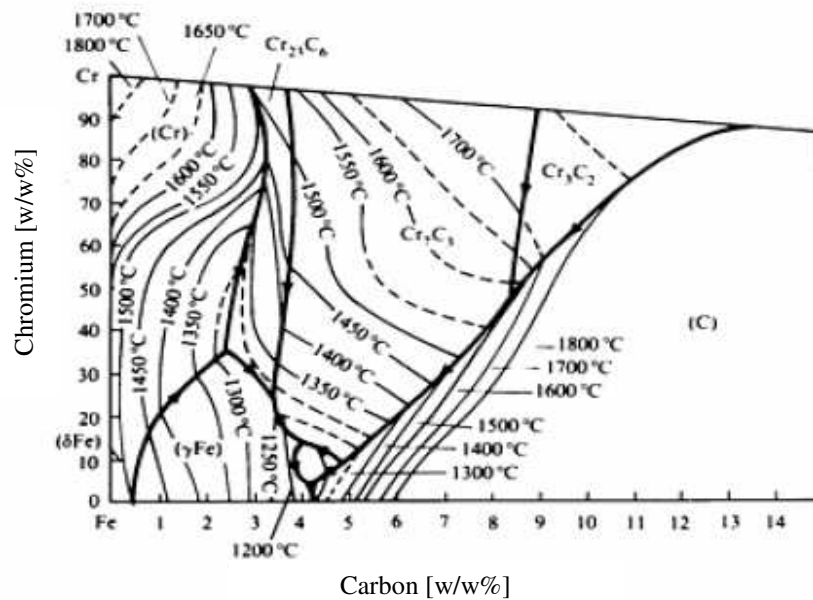


Figure 2. The liquidus surface of the Fe-Cr-C phase diagram [11]

The heat treatments were carried out in an electric heating laboratory furnace. The coolings were performed in furnace or on air to avoid thermal stresses [10]. The evaluation of the heat treatment experiments were based on the results of the hardness measurements (HB) and the observation of the changes in the microstructure, comparing the effects of the length and temperature of the heat treatments. Optical microscopy, scanning electron microscopy, energy dispersive microprobe and X-ray diffraction were used for the structure examinations. The sample preparation consisted of mechanical polishing and chemical etching.

Results and discussion

Characterization of the cast structure

The cast structure exhibited a large scatter considering the hardness and composition. The results of the hardness measurements are summarized in Figure 3. The maximal values notably exceed the ordered value (HB 280). The quantity of the second phase increases from the edge to the inner regions of the sample. Its morphology also changes. There is a 100 μm wide carbide free region at the edge of the cast; followed by a 300 μm wide region where finely dispersed carbides are found, which is followed by the carbide net characteristic for the inner regions, furthermore, enriched clusters are also present (Figure 4). The quantity and the morphology of the carbides strongly differ from the previous structures in Figure 5. The quantity of the carbide is smaller; the net is dashed (Figure 6). Inclusions and cavities can also be observed. Figure 7. shows two different microstructures of the typical two phases on backscattered image with higher magnification. The phase

marked with 2 appears in a net at the grain boundaries or in a regular lamellar form. On the lamellar structure it can be stated that it possess higher Cr content than the matrix (Table 2).

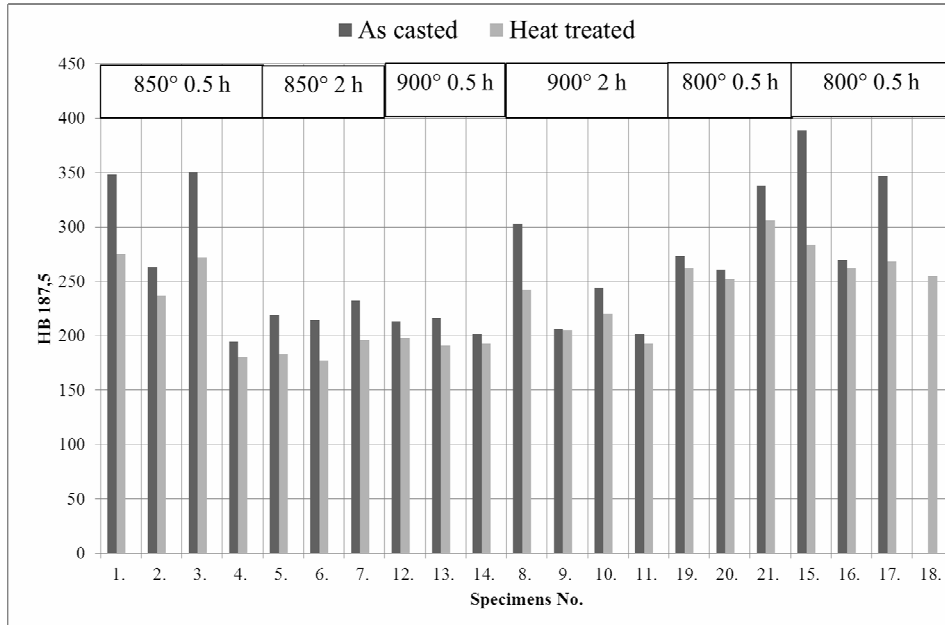


Figure 3. The results of the hardness measurements

On the contrary, three phases can be distinguished in Figure 8. marked with 1-2-3. The grain boundary net (area 3) and the lamellar structure (area 4) also appear. The dendritic morphology of phase 1 suggests that it solidified from the liquid, being the matrix. Phase 2 is the phase between the carbide lamellae, its composition is similar to the matrix but with lower Cr content. Phase 3 is the carbide net based on its morphology and composition being rich in Cr and W. It appears to be a reaction product. Area 4 has similar composition being also rich in Cr and W, but its lamellar morphology differs from area 3.

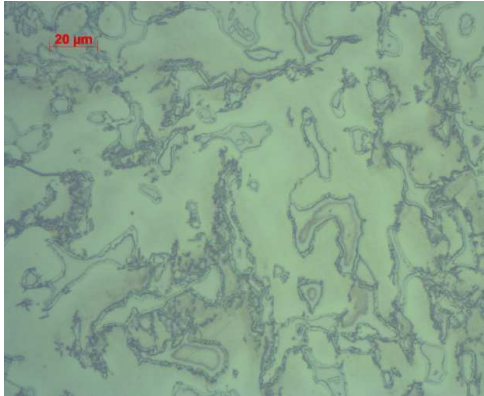


Figure 4. As-cast, 348 HB

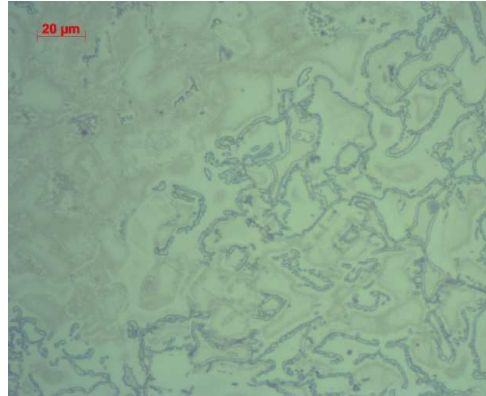


Figure 5. As- cast 218 HB

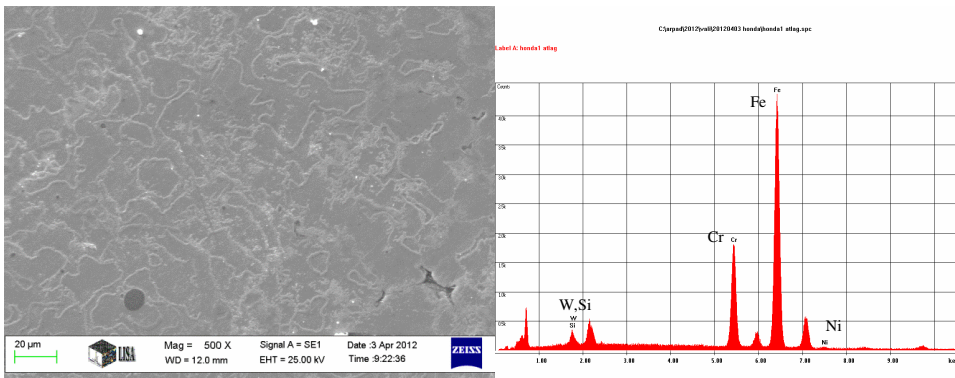


Figure 6. SE image and areal composition of the cast structure

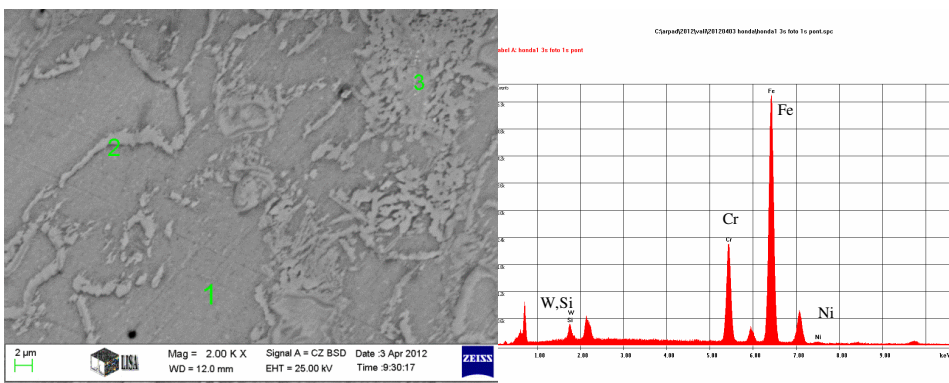


Figure 7. Backscattered electron image (BSD) and areal composition of the cast structure

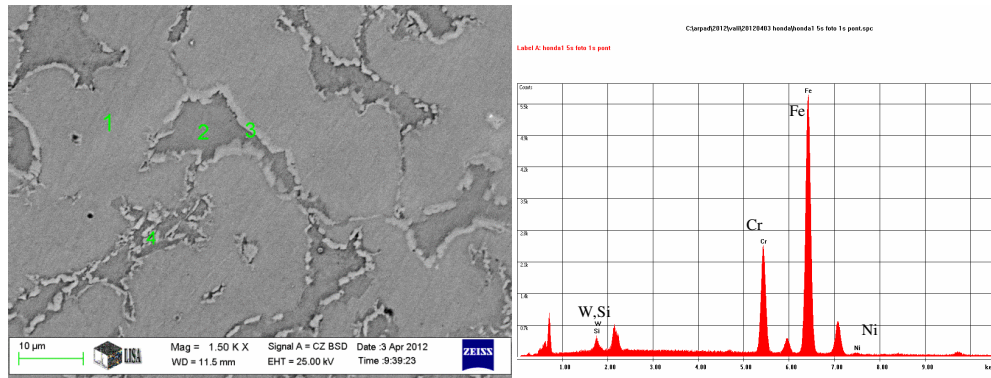


Figure 8. Backscattered electron image 2 (BSD) and areal composition of the cast structure

Examined point	Measured element [w/w %]				
	Fe	Cr	W	Si	Ni
Fig. 6. areal average	75.7	18.67	3.47	1.83	0.33
Fig. 7.					
area 1.	76.12	17.78	3.44	2.14	0.52
area 2.	76.72	17.16	3.44	2.17	0.51
area 3.	50.93	40.19	7.5	1.09	0.29
Fig. 8.					
area 1.	75.93	18.41	3.03	1.98	0.64
area 2.	81.01	12.64	3.29	2.67	0.39
area 3.	52.9	37.47	8.56	0.85	0.22
area 4.	69.67	22.6	5.6	1.76	0.38

Table 2. The measured compositions by EDAX

The reaction product formed in a peritectic reaction according to the liquidus surface (Figure 2) and probably transformed subsequently. After the examination of the morphology and the composition of the phases found in the microstructure, the aim of the annealing heat treatment can be determined as being to fragment and spheroidize the net of the carbide phase

The result of the heat treatment

The measured hardness results of the heat treated samples reveal that the hardness did not drop below the required value of 280 HB due to the heat treatment at 800 °C. The hardness was measured to be 306 HB after the 30 min annealing (sample marked with 21).

The hardness approached the ordered 280 HB after 2 hours (sample marked with 15), it was 280 HB. After annealing at 850 °C the hardness decreased to 275 HB even after the 30 min annealing (sample marked 1). According to this the temperature and the duration of this heat treatment are both appropriate. Not surprisingly, during the experiment at 900 °C the desired value was reached independently on the annealing time. The microstructure

examinations gave the following results: Only minor changes were observed in the carbide lamellae in the sample treated at 800 °C (Figure 9). It can be seen on the figures of the annealed sample that the fragmentation of the carbide net is actuated but its continuity does not change dominantly. The size and distribution of the carbides does not change notably confirming the measured hardness values.

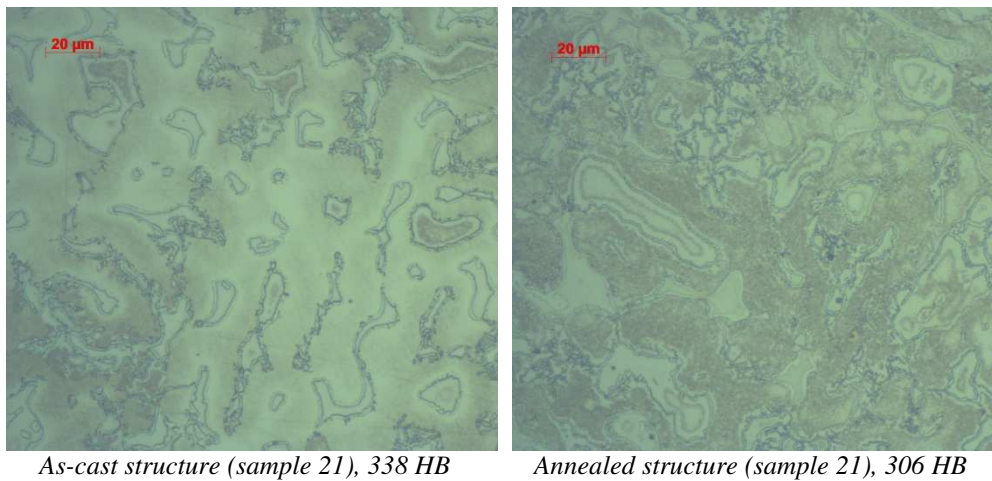


Figure 9. The effect of 800 °C 0.5 hrs

The fragmentation of the carbide lamellae can be observed in the case of heat treating at 850 °C, the continuous net turns into elongated, semi-spheroidic carbides. Continuous lamellae can still be observed causing the hardness value to be close to the desired value. The distribution of the carbides is still familiar to the structure of the as-cast structure.

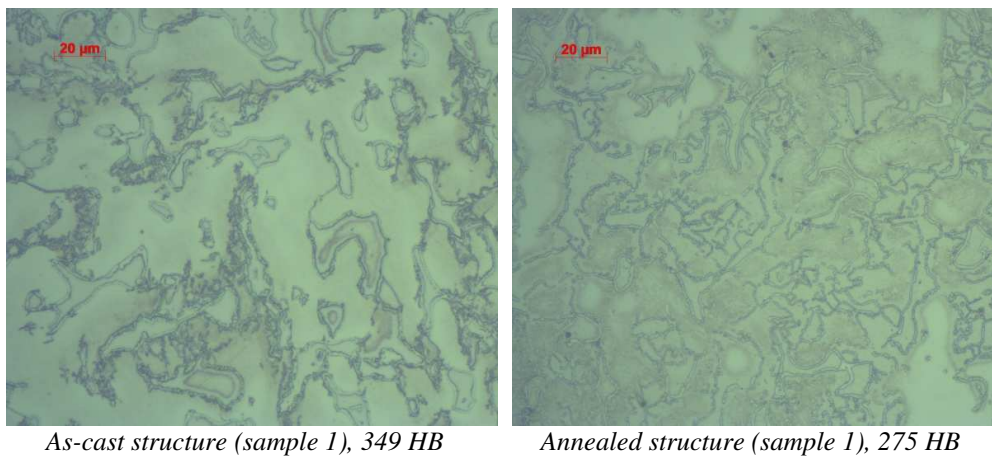


Figure 10. The effect of 850 °C 0.5 hrs

Not only the fragmentation of the carbide lamellae, but their spheroidic morphology and disperse distribution are also evident on the images of the sample annealed at 900 °C compared to the as-cast structure. The duration of the heat treatment also causes differences in the structure, but it emphasizes the temperature of the heat treatment. The effect of the annealing at 800 °C for 2 hours is less than the effect of the annealing at 850 °C for 30 minutes. This difference holds notably information to be considered by the selection of the applied annealing temperature. To emphasize this, Figure 12 shows the structure after annealing at 850 °C for 2 hrs.

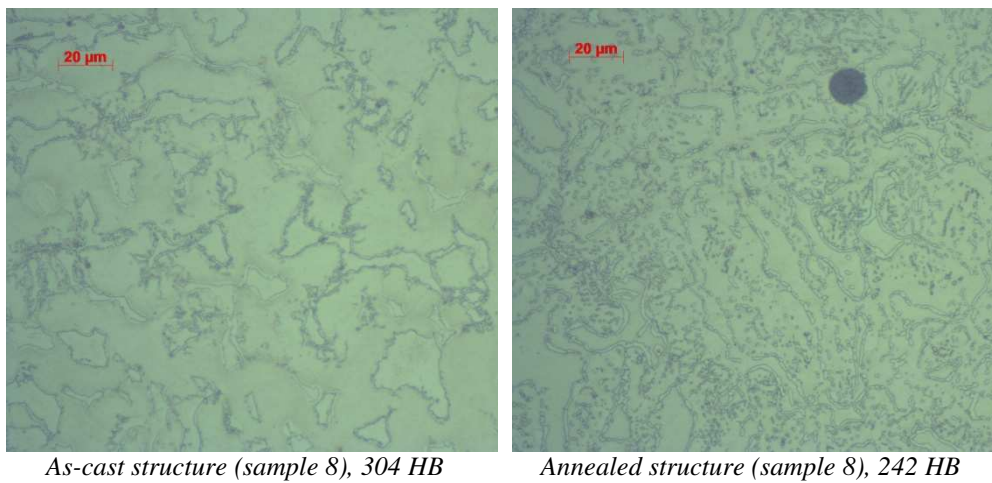


Figure 11. The effect of 900 °C 0.5 hrs

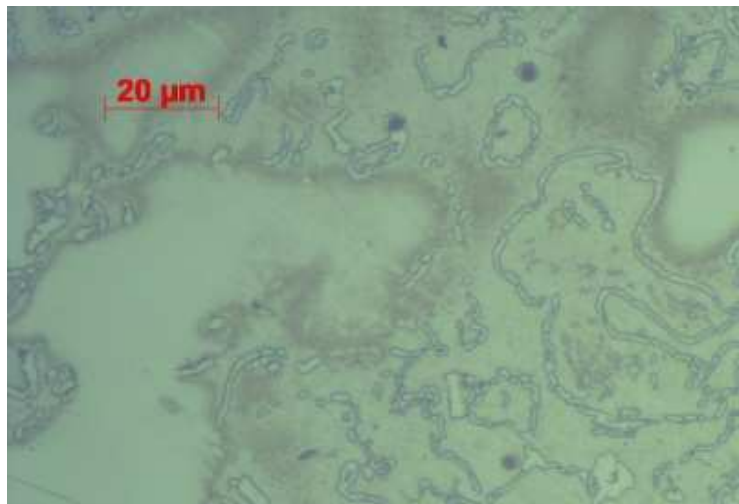


Figure 12. The effect of 850 °C 2 hrs, (sample 7)

X-ray diffraction measurements were performed on sample 8 to identify the phases. The as-cast and the 2 hours heat treated sample were examined. Figure 13 shows the diffractogram of the as-cast sample. The high intensity peaks evidently derive from the (110), the (200) and the (211) reflections of the ferrite phase. However, small intensity peaks of the austenite phase also appear. The quantity of the austenite is very small, around 1-2%. The difference between the peaks of the as-cast and the heat treated sample is in the shape, that is, the half value breadth and the integral breadth of the peaks (Figure 14). These values of the as-cast sample are larger, i.e. the peaks of this sample are wider. The integral intensity of the (220) peak (the area below the peak) of the heat treated sample (57 Cpsx°) is somewhat larger than that of the as-cast sample (40 Cpsx°). The reason of that was probably the difference between the size of the surfaces of the samples (the examined samples did not have the same size), not a microstructural difference. The annealing heat treatment does not cause a notable change in the cell parameter (consequently, the lattice distance- d). The reason of that is that the heat treatment does not change the composition, and/or the change in the Cr content does not change the cell parameter notably, since the atomic radii of the Fe and Cr are very close to each other. The difference between the breadth of the peaks of the as-cast and the annealed sample results from the presence of two solid solutions with different compositions in the as-cast sample (Figure 8 areas 1 and 2).

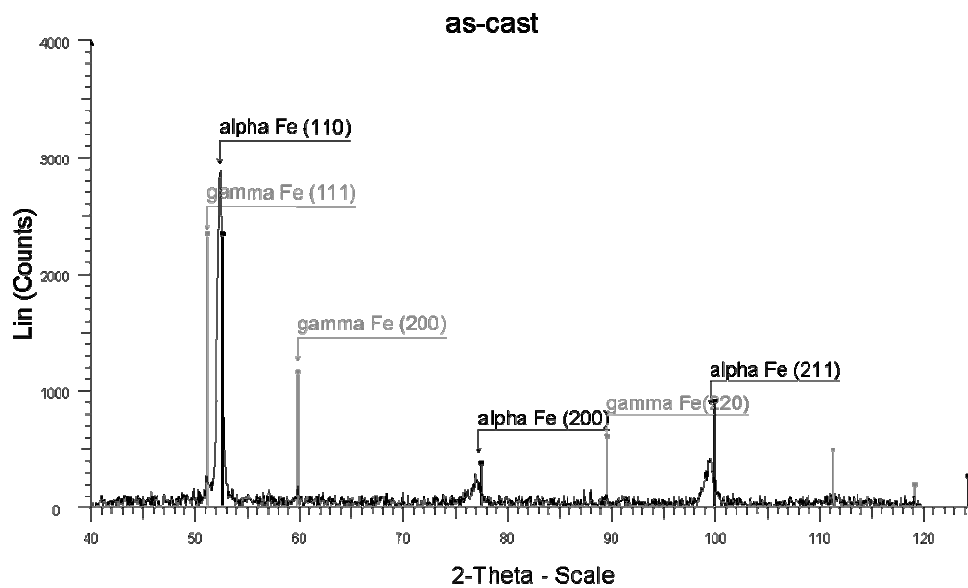


Figure 13. As-cast sample, marked 8

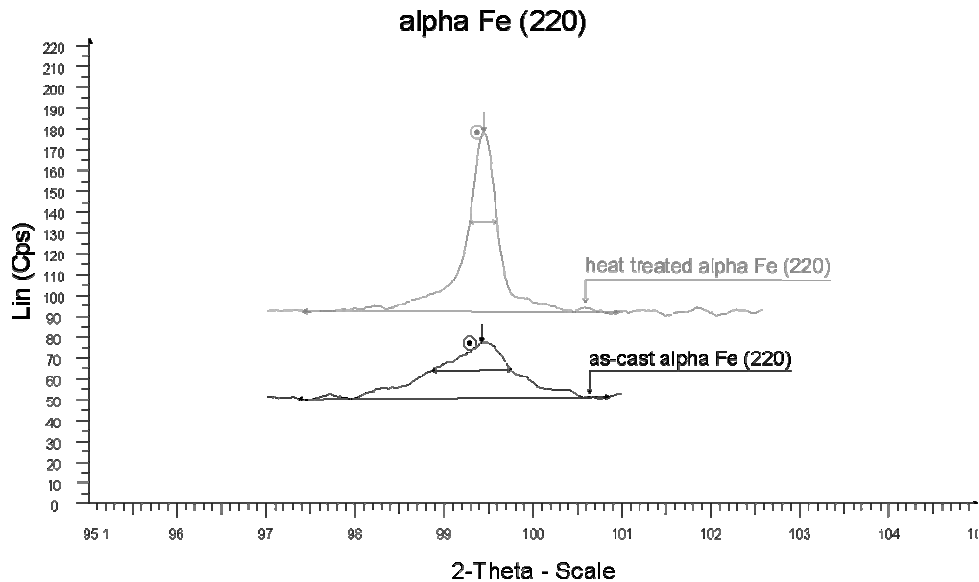


Figure 14. As-cast (marked 8), and the heat treated samples

Summary

The decrease of hardness of the as-cast ferritic stainless steel castings is required to reach the demanded mechanical properties through an annealing heat treatment. The optical and scanning electron microscope examinations explain the reason of the high hardness of the cast semi products. Their microstructure consists of two phases, characteristic on the cast structures. A notable amount of a second phase, dominantly chromium carbide is present in the form of lamellae or carbide net increasing the hardness. The aim of the annealing heat treatment is the fragmentation and the disperse distribution of the carbides. The experiments revealed that the increase of the annealing temperature strongly affects the resulting microstructure. Applying 800°C the continuity of the net is not affected notably, while applying 850°C the net becomes fragmented and the carbides start to form spheroidic shapes. Notably changes can be reached applying 900°C where the net disappears and the carbides become spheroidic and disperse. The annealing time has a similar effect. The changes in the microstructure increases using longer annealing duration on the same temperature. The hardness was decreased below 280 HB annealing the examined stainless steel containing 17% Cr at 850°C for 30 minutes.

Acknowledgement

The authors say thank you to Árpád Kovács for the scanning electron microscope examinations. The present research was supported by the TÁMOP-4.2.1.B-10/2/KONV-2010-0001 project in the framework of the New Hungarian Development Plant. The realization of this project is supported by the European Union, co-financed by the European Social Found.

References

- [1] R. K. Melekhov, O.I.Radkevych, H. V. Chumalo, and R. M. Yurkevych, Corrosion cracking of cast Cr-Ni-Mo ferritic- austenitic steels, *Materials Science*, Vol. 41, No. 5, (2005)
- [2] Saban Bülbül, Yavuz Sun, Corrosion behaviours of high Cr–Ni cast steels in the HCl solution, *Journal of Alloys and Compounds* 498 (2010) 143–147.
- [3] I. Dlouhy , Z. Chlup, V. Kozak, Constraint effects at brittle fracture initiation in a cast ferritic steel, *Engineering Fracture Mechanics* 71 (2004) 873–883.
- [4] M. Vardavoulias, G. Papadimitriou, Effect of Ni addition on the fracture behaviour of a cast ferritic stainless steel, *Materials Letters* 27 (1996) 349-353.
- [5] Y. Sun, H. Ahlatci, E. Ozdogru, H. Cimenoglu, Dry sliding wear behaviour of Fe–0.4C–25Cr–XNi cast steels, *Wear* 261 (2006) 338–346.
- [6] V. Kuzucu, M. Aksoy, M. H. Korkut, The effect of strong carbide-forming elements such as Mo, Ti, V and Nb on the microstructure of ferritic stainless steel, *Journal of Materials Processing Technology* 82 (1998) 165–171.
- [7] I. M. Moustafa, M. A. Moustafa, A. A.Nofal, Carbide formation mechanism during solidification and annealing of 17% Cr-ferritic steel, *Materials Letters* 42 _2000. 371–379.
- [8] Se Jin Ko, Yoon-Jun Kim, High temperature fatigue behaviors of a cast ferritic stainless steel, *Materials Science and Engineering A* 534 (2012) 7–12.
- [9] H. K. D. H. Bhadeshia: *Steels Microstructure and properties*, Elsevier, (2006)
- [10] Zorkóczy Béla: *A hőkezelés technológiája*. Nehézipari könyv- és folyóiratkiadó Vállalat. 1952.
- [11] *ASM Metals Handbook Volume 3. Alloy Phase diagram*, ASM International (1991)
- [12] *ASM Specialty Handbook Heat Resistant Materials*, ASM International (1999)

DIRECT CATHODIC DEPOSITION OF COPPER ON STEEL WIRES FROM PYROPHOSPHATE BATHS¹

TAMÁS I. TÖRÖK¹, VIKTOR OROSZ², ZOLTÁN FEKETE³,
GEORGINA SZIRMAI⁴

^{1,2,4}Institute of Metallurgy and Foundry Engineering
Department of Chemical Metallurgy and Surface Techniques

University of Miskolc, 3515 Miskolc-Egyetemváros,

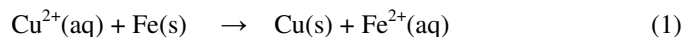
³ArcelorMittal Szentgotthárd Co.Ltd. 9970 Szentgotthárd
fektt@uni-miskolc.hu

There is a rather different art compared to the common batch type processes within the domain of continuous cathodic deposition of metals on wires. In the case of direct electroplating of copper onto the cylindrical surface of a drawn steel wire running with high speed it is not at all an easy task to control all the deposition parameters satisfactorily in order to ensure good adhesion and all the other properties required for further processing. In this respect, the relatively newly introduced copper pyrophosphate baths brought about also new challenges which were among our primary motivations in launching a research project in cooperation with a company in Hungary where copper and zinc plated steel core wires are produced. While aiming at studying the effects of the major parameters influencing the properties of copper layers formed by cathodic deposition, several sets of experiments were performed in a laboratory Hull cell under varied circumstances. The thin copper layers so deposited were then characterised by using highly sophisticated techniques, like scanning electron microscopy (SEM), radio frequency powered glow discharge optical emission spectroscopy (GD OES) for elementary depth profiling to detect and follow the consequences of the changing plating parameters and the possible contaminating effects.

Keywords: cathodic deposition, pyrophosphate solution, copper electroplating.

Introduction

The well known and widely used simple sulphuric acid copper sulphate electroplating baths cannot be used for direct cathodic deposition of copper onto the bare and active surface of steels as it is almost impossible to counteract the initial contact chemical reduction (so-called cementation [1]) of copper by the solid surface of iron due to the significantly lower standard electrode potential of Fe²⁺/Fe than that of Cu²⁺/Cu:



And, as a result of such a surface catalyzed chemical reduction reaction (*Eq. 1*) the adherence and structure of the first thin copper deposit will not be good enough to build up a thick, compact and sound copper surface layer afterwards. In the past, this problem was

¹ Part of this publication was presented at the XXVI. microCAD International Conference in Miskolc, 30 March, 2012

avoided by using copper (I) cyanide electroplating baths in which the copper ions (Cu^+) form strong anionic complexes with CN^- anions, which will efficiently hinder the direct chemical reduction of copper via shifting the reduction potential to more negative values. Otherwise, the cathodic deposition of copper from such cyanide baths was often utilized only for developing a very thin primary copper layer (so-called copper strike), then the further amounts of copper could be deposited, for example, from a cheaper acid copper sulphate type electrolytes. In this respect the choice of AMSC Ltd.Co. in Szentgotthárd was different as they are applying a non-cyanide copper plating bath first, which is a relatively new remedy for the given problem.

Though the copper pyrophosphate electrolytes are known for some time, and what is also very important, they are much more benign to the environment than the highly toxic cyanide baths, their introduction and implementation in continuous steel wire plating technologies are still relatively rare. Also, there are only a few engineering companies which design and build such continuous plating lines. Anyhow, the heart of such plating lines is the cells which normally have a much different shape and size compared to the geometry of the mostly rectangular tanks used in the batch type electroplating. The set of parallel cells used in Szentgotthárd are shown in Figure 1 where the long troughs made of highly corrosion resistant chromium-nickel steel are connected to the positive pole of the direct current source and are in physical and electrical contact with the high purity copper anode rods placed on the bottom of the cells. The running steel wires are connected to the negative terminal of the DC power source via sliding contacts at both ends of the long cells. The permanent and vigorous circulation of the electrolyte is a very important factor of the whole design because of the high rate of electrochemical deposition.

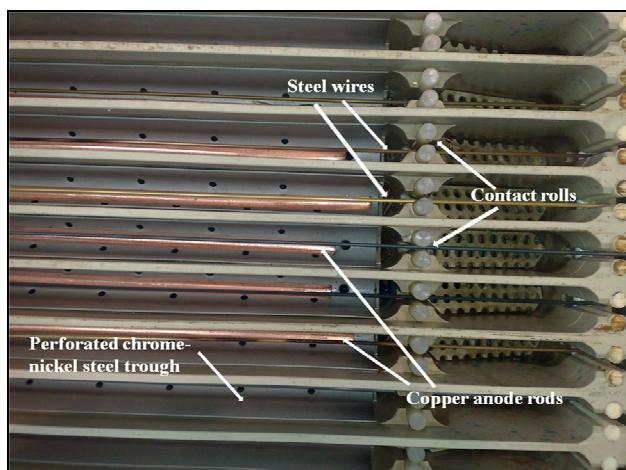


Figure 1. Photograph taken from above of a continuous wire electroplating line without the aqueous electrolyte solution filled in

Such modern continuous electroplating cells are used all along the plating line by AMSC Ltd.Co. in Szentgotthárd, where the high strength steel core wires are first coated with a thin layer of copper from the pyrophosphate baths (copper strike), after which they

use an acid copper sulphate plating bath to thicken the copper deposit. They also electroplate zinc on the top in order to build up finally a double layer of copper and zinc in proper proportion. The mass ratio of Cu and Zn in the deposits is indeed a very important factor in view of the composition and microstructure of the brass to be developed during the subsequent heat treatment. However, as one of the most crucial points of the continuous multi-step electroplating is the first deposition step, we have concentrated our laboratory scale experimental investigations on it.

The major types of the copper pyrophosphate electroplating baths invented and tested decades ago can be found, for example, in the book by Pinner [2] written about copper and copper alloy plating. As the art and science of electroplating has been long established, it is not much of a surprise that Pinner has already described five different pyrophosphate copper baths. The pyrophosphate copper baths still in use today often fall into the composition and concentration ranges summarized in Table 1. They are, otherwise, gaining more ground in practice also in microelectronics to coat the inner surfaces of throughholes on printed circuit boards.

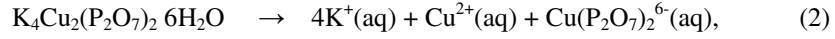
Component		Concentration	
		g/dm ³	mol/dm ³
Copper	Cu ²⁺	20 – 40	0.32 – 0.63
Potassium or sodium	K ⁺ /Na ⁺	~ 250 / 150	~ 4 – 8
Pyrophosphate	P ₂ O ₇ ⁴⁻	100 – 300	0.57 – 1.72
Nitrate	NO ₃ ⁻	5 – 10	0.08 – 0.16
Ammonia	NH ₃	1 – 3	0.06 – 0.18
Orthophosphate	HPO ₄ ²⁻	< 120	< 1.2
Organic additive(s)	brightening, etc.	as required	

Table 1. Major components and their concentration ranges of pyrophosphate copper baths in use today

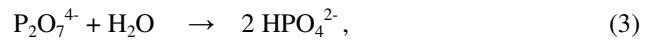
The copper pyrophosphate baths can be prepared from simple non-toxic salts like the double potassium or sodium salts of copper pyrophosphate, K₄Cu₂(P₂O₇)₂·6H₂O or Na₄Cu₂(P₂O₇)₂·6H₂O, to which some more pyrophosphate salts (e.g. K₄P₂O₇) must be added in excess in order to increase the complexing power of the pyrophosphate anions. In the plating baths the role of ammonia and KNO₃ is also important as they help control the anodic dissolution of copper and the depolarisation of the cathode, respectively. KNO₃ also increases advantageously the electrical conductivity of the aqueous electrolyte solution.

Looking at the basics of the rather complex aqueous chemistry of such mixtures of water soluble pyrophosphate salts, let us consider first only K₄Cu₂(P₂O₇)₂·6H₂O dissolved in water at a concentration of the pyrophosphate about 0.4 mol·dm⁻³ (not far from the range given for Cu²⁺ in Table 1). In such an aqueous solution there will be about 0.4 mol Cu, 0.8

mol P and also 0.8 mol K per liter and we can suppose the formation of the following ionic species:



where (aq) refers to the water soluble simple and complex ionic species formed after dissolving the given potassium copper pyrophosphate salt in water. With changing pH and/or redox potential, however, the pyrophosphate anions can hydrolyse to the orthophosphate:



and form colloidal hydroxide precipitates, e.g. $\text{Cu}(\text{OH})_2$ above $\text{pH} > 11$ or pyrophosphate precipitates with copper, e.g. $\text{CuH}_2\text{P}_2\text{O}_7$ or $\text{Cu}_2\text{P}_2\text{O}_7$ at $\text{pH} < 7$. The results of such equilibrium processes can also be predicted from thermodynamic calculations, for example, by using the HSC Chemistry data base and software [3]. As an example, the most stable phosphorus containing aqueous ionic species are depicted in Figure 2 in the form of the so-called Pourbaix diagram.

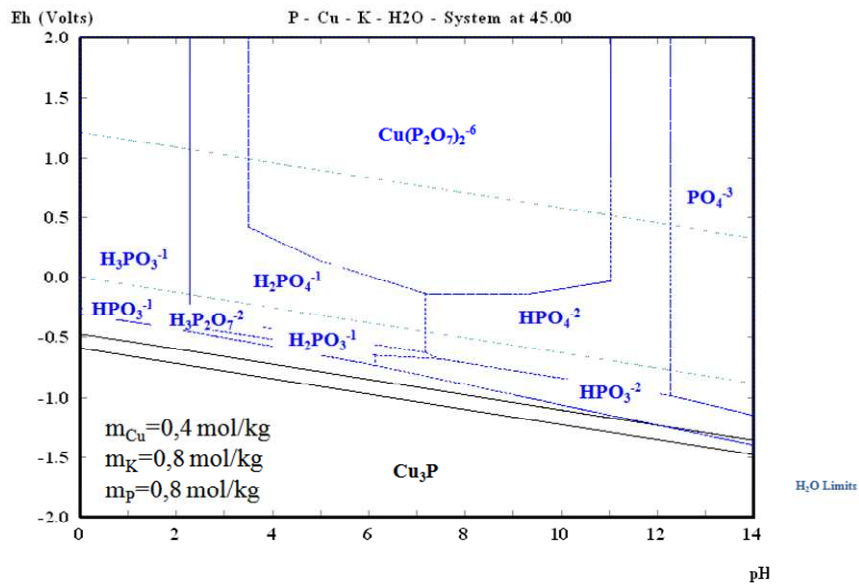


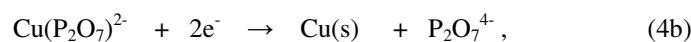
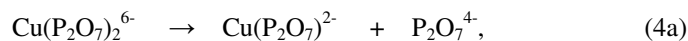
Figure 2. The most probable phosphorus containing aqueous ionic species in the function of pH and Eh redox potential at 45 °C for the given molalities of Cu, K, and P

It is seen also from Eq. 2 that after the complete dissociation and complex formation of the potassium-copper pyrophosphate salt $\text{K}_4\text{Cu}_2(\text{P}_2\text{O}_7)_2$, there are not enough “free” $\text{P}_2\text{O}_7^{4-}$ anions to complex all the copper ions after dissolution. Therefore, in the course of the preparation of the copper pyrophosphate electroplating baths some excess $\text{P}_2\text{O}_7^{4-}$ anions are

added to the solutions often in the form of its potassium salt, instead of the cheaper sodium pyrophosphate, as the $K_4P_2O_7$ is more soluble and has a higher electrical conductivity.

Higher degree of the complexation of the dissolved copper cations and the presence of excess $P_2O_7^{4-}$ anions in the solution are very important factors from the point of view of the initial cathodic deposition when the copper plating solution first wet the surface of iron (i.e. the steel wires) because the cementation reaction (Eq. 1) must be hindered/inhibited at this stage of the electrochemical deposition. Such advantageous surface effect of the $P_2O_7^{4-}$ anions has recently been proved by K. Johannsen et al. [4], who confirmed the earlier proposition of Konno and Nagayama [5], namely that the pyrophosphate ions are adsorbed on the electrode surface prior to copper electrodeposition.

For the actual cathodic reduction of copper Konno and Nagayama [5] proposed the following scheme:



but also suggested that at high concentration of $P_2O_7^{4-}$ in the solution copper would be reduced directly from the complex anions $Cu(P_2O_7)_2^{6-}$ to solid $Cu(s)$ deposit.

Anyhow, all the above mentioned considerations and previous theoretical and experimental results reflect the high complexity of the solution chemistry of such aqueous systems. Therefore, such pyrophosphate copper plating baths must be controlled with a highly sophisticated manner and any additional observation in this context should be valuable also for the given industrial practice.

Experimental procedure

From the technological point of view, there is another very important factor, which has not been mentioned yet, it is the cathodic current density, which also affects the quality of the initial copper deposit. The current density is normally quite high in the continuous plating lines (around $10 \text{ A}\cdot\text{dm}^{-2}$ in the case of AMSC Co.Ltd) in order to facilitate the throughput of production. This technological parameter can be comfortably investigated in a special laboratory plating cell commonly known as the Hull cell, which has been used to study the major circumstances of the direct cathodic deposition of copper. Our Hull cell was a home-made device equipped with all the necessary measuring and controlling accessories (Figure 1).



Figure 3. Photograph of the thermostated laboratory Hull cell assembly equipped also with a mechanical stirrer

The electrolyte solutions used in the laboratory experiments were obtained from the AMSC Co.Ltd. and their actual composition fell in the concentration ranges given in Table 1. This industrial copper pyrophosphate solution contained quite much “free” pyrophosphate corresponding to a factor of $7.5 = 200/26.5$, which factor shows the ratio of the relevant concentrations of P_2O_7 compared to that of Cu expressed in g/dm^3 . The solution samples received from the factory also contained some lead contamination as the steel wires are normally drawn through a hot molten lead bath as well, that is used for tempering prior to their arrival to the electroplating cells. Consequently, some lead used to adhere to the surface, getting carried over even to the aqueous processing tanks where it might contaminate the aqueous cleaning (degreasing, pickling, rinsing) solutions and the subsequent first electroplating bath as well which is filled up with the given copper pyrophosphate electrolyte solution. Therefore, our laboratory Hull cell experiments, in addition to investigating, first of all, the effects of the cathodic current density and solution stirring, were also extended to checking the effect of the possible lead contamination. The latter parameter was even raised excessively in a few laboratory experiments by adding water soluble lead acetate to the technological solutions to highlight its influence on the quality of the copper deposit. Surface morphology and in depth elemental composition of the so deposited copper layers were then examined by scanning electron microscopy (SEM) and radio frequency glow discharge optical emission spectroscopy (GD OES) [6].

Experimental results and discussion

The copper deposit obtained at the slanted surface of the steel cathode plate of the experimental Hull cell is shown in Figure 4.

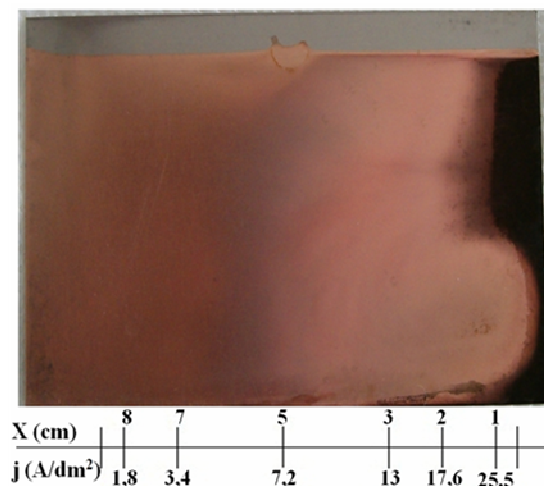


Figure 4. Photograph of the electroplated copper deposit obtained on a steel cathode plate in the stirred laboratory Hull cell filled up with pyrophosphate copper solution and operated for 30 s. Local current densities (j) are also shown along the length (X) of the cathode plate

It is clearly seen in Figure 4 that there is a relatively bright and sound copper deposit obtained at around $10 \text{ A}\cdot\text{dm}^{-2}$ and below, and sound copper layer was deposited even at somewhat higher current densities (up to about $25 \text{ A}\cdot\text{dm}^{-2}$) if the solution was vigorously stirred (i.e. in the lower region of the sample plate). This observation is in full agreement with the characteristic cathodic deposition phenomena known for the diffusion controlled regions in the function of current densities and stirring rates [7-9].

Thickness of the copper deposits obtained from the pyrophosphate bath on the drawn and heat treated steel wires in the electroplating lines of AMSC Co.Ltd. is lower than $1 \mu\text{m}$, the surface coverage of which was tested via the feroxyl test [10]. The two photographs in Figure 5 reveal the regions, as well as the corresponding current density ranges, where the thin copper layers cover the steel plate relatively well, i.e. in the middle section ($\sim 3\text{...}14 \text{ A}\cdot\text{dm}^{-2}$), extending somewhat further to the right towards higher current densities where the mechanical stirring was more intensive. The X and j scales and the deposition parameters were the same as given in Figure 4.

Surface morphology of the electroplated deposit also depends on the current density [7-9], therefore it was examined with high magnification by scanning electron microscopy. One example of the SEM images is shown in Figure 5(b) for the case when the copper deposit was obtained at a current density of about $10 \text{ A}\cdot\text{dm}^{-2}$. The quite fine globular structure is clearly seen.

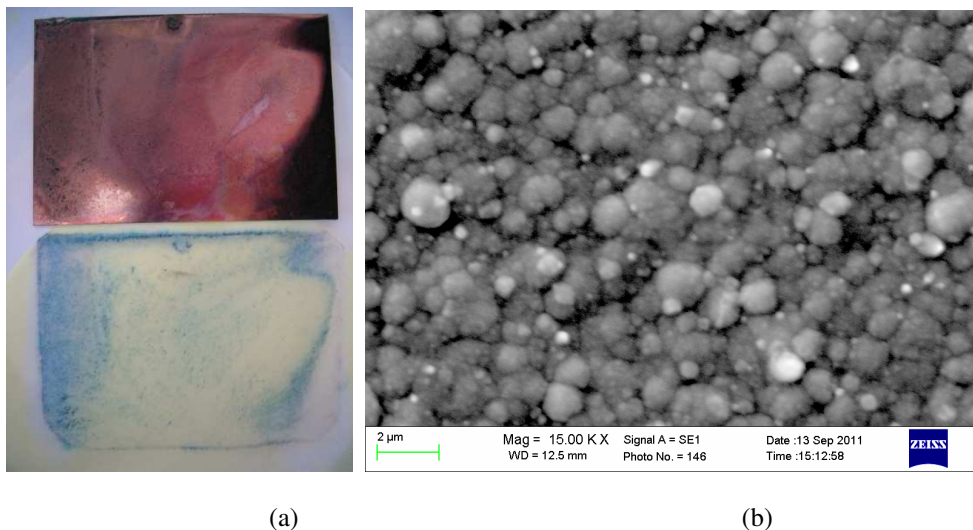


Figure 5. Photographs of the deposited very thin ($< 1\ \mu\text{m}$) copper and its print (a) obtained on a filter paper previously immersed in a feroxyl test solution. The blue spots refer to porosities reaching down to the steel substrate.

The SEM image (b) shows the surface morphology of the electroplated copper obtained at $10\ \text{A}\cdot\text{dm}^{-2}$.



Figure 6. Photograph of copper electroplated steel plate from lead contaminated ($0.15\ \text{g}/\text{dm}^3\ \text{Pb}$) solution



Figure 7. Photograph of copper electroplated steel plate from lead contaminated ($0.3\ \text{g}/\text{dm}^3\ \text{Pb}$) solution



Figure 8. Photograph of copper electroplated steel plate from lead contaminated ($1.5 \text{ g/dm}^3 \text{ Pb}$) solution

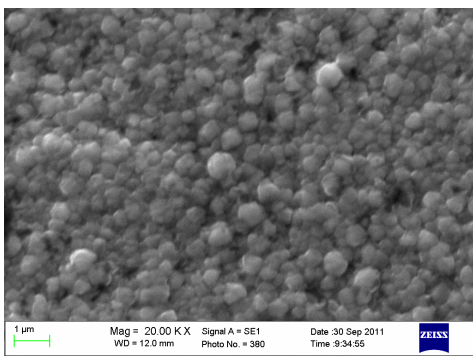


Figure 9. SEM image of copper electroplated steel plate from lead contaminated ($0.15 \text{ g/dm}^3 \text{ Pb}$) solution

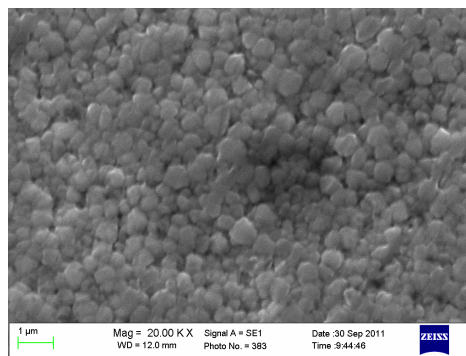


Figure 10. SEM image of copper electroplated steel plate from lead contaminated ($0.3 \text{ g/dm}^3 \text{ Pb}$) solution

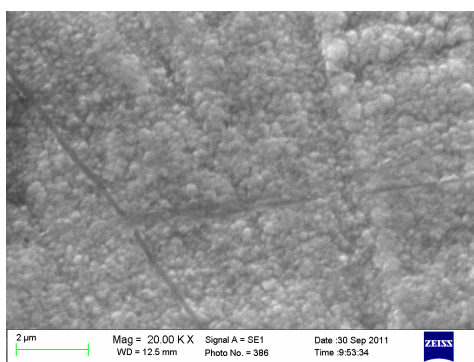


Figure 11. SEM image of copper electroplated steel plate ($1.5 \text{ g/dm}^3 \text{ Pb}$)

Electroplated metal layers might incorporate also some other components (additives, contaminating elements, etc.) from the plating baths. To detect the presence and distribution of such elements in depth of the thin copper deposit, the technical capabilities of our GD OES equipment (GD Profiler2) could be utilized here. It allowed us to detect several elements adsorbed onto the surface of the deposit and/or incorporated in the copper layer deposited during the Hull cell experiments. The interfacial appearance of phosphorus (marked in Figure 12 with an arrow), for example, must be the consequence of the partial and parallel reduction of phosphorus from the selectively adsorbed pyrophosphate anions at the very beginning of the copper electrodeposition when the highly complexed aqueous solution starts wetting the bare surface of the steel sample plate under the imposed cathode potential. The detected intensities of P then are decreasing with the thickening copper layer which shows the changing deposition characteristics as the copper deposit is covering more fully the iron substrate with time. Contrary to the distribution of P in depth of the copper deposit, two other contaminating elements (K and O), shown as well in Figure 12, do not quite follow the passage of P, though a very small convexity can be observed on the curve of O coinciding with that of P at the interface. Some incorporation of K is also obvious from the in depth spectra shown in Figures 12 and 13. In one of the experiments run with deliberately contaminating the tested copper pyrophosphate solutions with lead, the concentration of dissolved Pb was increased quite considerably (by adding soluble lead salt to the plating solution), then the copper layer so deposited was also analysed down to the steel substrate and even somewhat below (as the Fe intensity is reaching a plateau), shown in Figure 13.

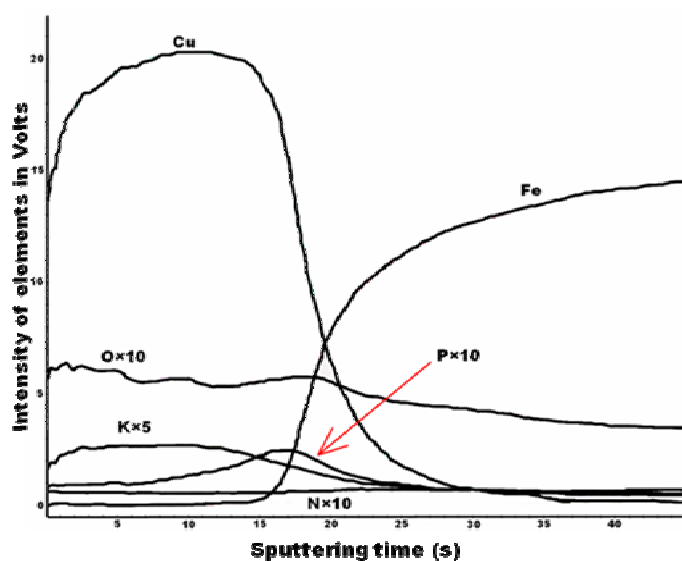


Figure 12. Intensities (some multiplied by 5 or 10) of some elements detected in the copper layer in the function of sputtering time, which is proportional to the depth down and into the steel substrate

The GD depth profile presented in Figure 13 shows that the lead ions got reduced (Pb intensities are multiplied by 10) together with copper onto the steel cathode plate. Its effect on the surface appearance of the copper deposit (Figures 6-8) as well as on the surface morphologies are slight but still apprehensible (Figures 9-11). The slight but unambiguous accumulation of phosphorus (intensities also multiplied by 10) due to the preferential adsorption of the pyrophosphate anions at the beginning of electrodeposition from such copper plating baths could be detected in all of the GD in depth profiles, confirming the proposal of Konno and Nagayama [5]. And, this latter phenomenon should contribute much to the inhibition of the direct surface reduction (cementation) of Cu^{2+} ions by the highly electronegative and active surface iron atoms. Consequently, it will be the mechanism of electrocrystallization, which should primarily govern the reduction of copper cations from the pyrophosphate anion complexes as well as the following crystallization (i.e. the arrangement of the surface copper adatoms into the developing and growing solid deposit/structure). In this way there is a better chance for the build-up of a sound and well adhering electrodeposited copper film on the iron sample plates or even on the steel wires during the core wire production on the continuous wire drawing and electroplating lines.

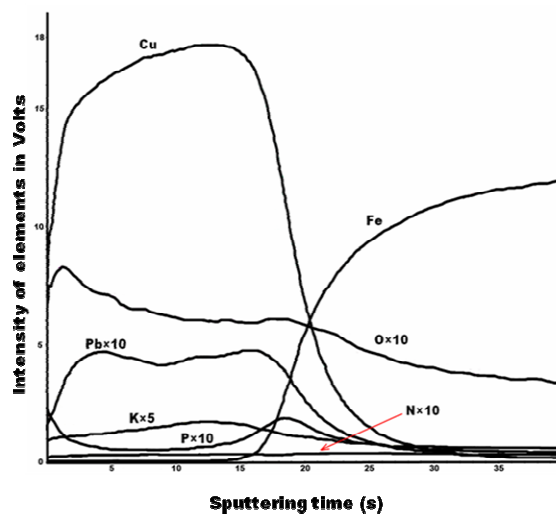


Figure 13. Intensities (some multiplied by 5 or 10) also of the contaminating elements like Pb, K, P, and O detected in the copper layer in the function of sputtering time (the GD excitation parameters were the same as with Figure 12)

Conclusions

The adherence and overall good quality of copper electrodeposits does depend on the initial steps of the cathodic reduction of copper ions being complexed in the pyrophosphate type copper electroplating solutions studied in this research work with reference to the industrial production of thin brass layers on drawn steel wires in AMSC Co.Ltd. The choice

and application of the Hull cell for our laboratory investigations in order to reveal some further important details of copper electrodeposition within and also outside the working range of the given technological parameters at AMSE was proved to be indeed an appropriate one to the task. The thin copper deposits so obtained could then be further examined by means of some available and sophisticated testing techniques like SEM and GD OES. In this way we have pointed out the workable ranges of the main electrolysis parameters. We have detected some increased and well incorporated amounts of phosphorus (and oxygen) at the interface of the copper deposit and that of the steel substrate by means of the GD OES in depth profile analysis. This new observation can also be considered as an additional experimental evidence of the assumed cementation inhibiting effect of the surface adsorbed pyrophosphate anions at the beginning of direct copper electrodeposition onto bare steel surface. Due to that primary pyrophosphate surface adsorption effect the industrial use of such pyrophosphate copper electroplating baths are not only environmentally more benign than the formerly used cyanide baths, but they can also lead to the formation of cathodic copper deposits with sound structural characteristics even at relatively high current densities, as it was proved well by our laboratory experiments.

Acknowledgements

This work was carried out as part of the TÁMOP-4.2.1.B-10/2/KONV-2010-0001 project in the framework of the New Hungarian Development Plan. The realization of this project is supported by the European Union, co-financed by the European Social Fund. The authors are grateful to Ms Szabina Szabó and Ms Viktória Veréb for performing the Hull cell experiments as well as to Mr Árpád Kovács and Mr Tibor Kulcsár for the SEM and GD OES investigations, respectively.

References

- [1] Oldright G. L, Keyes H. E, Miller V, and Sloan WA: Precipitation of lead and copper from solution on sponge iron Bulletin 281 Dept.of Commerce, Government Printing Office, Washington, 1928
- [2] Pinner R: Copper and Copper Alloy Plating, C.D.A. Publication No. 62. London, 1962.
- [3] HSC Chemistry 5.1 October 31, 2002, Roine A, Outokumpu Research Oy
- [4] Johansen K, Page D, Roy S Electrochimica Acta 2000, 45, 3691-3702
- [5] Konno H, Nagayama M, Electrochimica Acta 1978, 1001
- [6] Bouchacourt M, Schwoehrer F: Grimm Source, book chapter 2.2. (pp. 55-61) R. Payling, D. G. Jones, A. Bengtson (Eds.): Glow Discharge Optical Emission Spectrometry, John Wiley & Sons, Chichester, 1997.
- [7] T. I. Török (Ed.): Modern Surface Techniques and Methods of Waste Utilization in Metals Processing (in Hungarian), University of Miskolc, Phare 2004.
- [8] Kékesi T.: Evolution, characteristics, and suggestibility of polarization during copper electrorefining (in Hungarian) Sci. Qual. Comm. HAS, 1992, Budapest
- [9] Raub E, Müller K: Fundamentals of Metal Deposition, Elsevier, Amsterdam, 1967.
- [10] ASTM B 733 – 04 Section 9.6.1

University of Miskolc, Department of Research Management and International Relations
Responsible Publisher: Prof. Dr. Mihály Dobróka prorector
Published by the Miskolc University Press under leadership of Erzsébet Burmeister
Responsible for duplication: Erzsébet Pásztor
Miskolc-Egyetemváros, 2012
Copies: 200
TU – 339 – 2012 – ME